Ophiolites in accretionary complexes along the Early Cretaceous margin of NE Asia: age, composition, and geodynamic diversity

S. D. SOKOLOV[1], M. V. LUCHITSKAYA[1], S. A. SILANTYEV[2], O. L. MOROZOV[1], A. V. GANELIN[1], B. A. BAZYLEV[2], A. B. OSIPENKO[3], S. A. PALANDZHYAN[4] & I. R. KRAVCHENKO-BEREZHNOY[1]

[1]*Geological Institute of the Russian Academy of Sciences, 7 Pyzhevsky per., Moscow, 109017, Russia (e-mail: sokolov@geo.tv-sign.ru)*

[2]*Vernadsky Institute of Geochemistry and Analytical Chemistry, 19 Kosygina St., 119991, Moscow, Russia*

[3]*Vernadsky State Geological Museum, 11/2 Mokhovaya St., Moscow, 103009, Russia*

[4]*Institute of the Lithosphere of Marginal and Inland Seas, Russian Academy of Sciences, 22 Staromonetny per., Moscow, 109180, Russia*

Abstract: The existing published data, combined with our own new field, petrographic, and geochemical observations and data show that ophiolites of the West Koryak fold system originated in a variety of tectonic environments. This fold system stretches along the boundary shared by two of NE Asia's largest tectonic units, the Verkhoyansk–Chukotka and Koryak–Kamchatka foldbelts. The fold system abounds in Palaeozoic and Mesozoic ophiolites and sedimentary and volcanic island-arc assemblages. The ophiolites are Palaeozoic and Mesozoic in age. The variety of geological and geochemical signatures implies ophiolite origin in diverse tectonic settings. The Early Palaeozoic ophiolites of the Ganychalan accreted terrane and Devonian(?) ophiolites of the Ust–Belaya accreted terrane are fragments of the Panthalassan oceanic lithosphere. Serpentinite mélange in the Ust–Belaya terrane contains some blocks of island-arc provenance. They are probably Late Palaeozoic–Early Mesozoic in age as determined by K–Ar measurements, which require validation by other techniques. Mesozoic, chiefly Late Jurassic–Early Cretaceous ophiolites of the Beregovoi and Kuyul accreted terranes, originated in a suprasubduction-zone (SSZ) setting (ensimatic island arc and back-arc basin). Among the Mesozoic ophiolites, one finds blocks of oceanic assemblages in serpentinite mélanges as well. Basalt and chert blocks of clearly oceanic derivation are viewed as detached fragments of the upper part of the oceanic lithosphere. The ophiolites have experienced a variety of accretionary scenarios. Palaeozoic ophiolites docked onto the Koni–Taigonos island arc (of Late Palaeozoic–Early Mesozoic age), probably in the Late Palaeozoic or Early Mesozoic, whereas Mesozoic ophiolites accreted onto the Uda–Murgal island arc (of Late Jurassic–Early Cretaceous age) in the terminal Early Cretaceous. Sedimentary deposits, whose base is late Albian in age, make a post-accretionary sequence. These island arcs portray the overall history of the convergent boundary between the North Asian continent and NW Pacific. Ophiolites of the Ganychalan and Ust–Belaya terranes consist of thrust sheets and, jointly with Yelistratov Peninsula ophiolites, make up the basement to the forearc of the Uda–Murgal island arc, ophiolites of Cape Povorotny and Kuyul terrane being incorporated in accretionary prisms of the same arc. Ophiolites and associated metamorphic, volcanic, and sedimentary rocks of Palaeozoic–Early Cretaceous age underwent three deformation phases, each reflecting a different stage in the evolution of the NE Asian continental margin and readily correlative with principal tectonic events in the northern Circum-Pacific region.

In NE Asia, ophiolites have been reported from the Verkhoyansk–Chukotka and Koryak–Kamchatka foldbelts (Fig. 1). The ophiolites span a broad Early Palaeozoic to Mesozoic age interval. The Verkhoyansk–Chukotka belt, except for the Kolyma loop (Fig. 1), displays a structural grain dominated by northwesterly trends resulting from collisional processes (Pushcharovsky *et al.* 1992; Bogdanov & Tilman 1992; Parfenov *et al.* 1993). Accreted terranes found in the belt represent fragments of microcontinents, such as Chukotka, Omolon, Okhotsk, etc. Ophiolites occur sporadically within collisional piles of the Chersky Range and South Anyui suture, where they make up

From: DILEK, Y. & ROBINSON P. T. (eds) 2003. *Ophiolites in Earth History.* Geological Society, London, Special Publications, **218**, 619–664. 0305-8719/03/$15

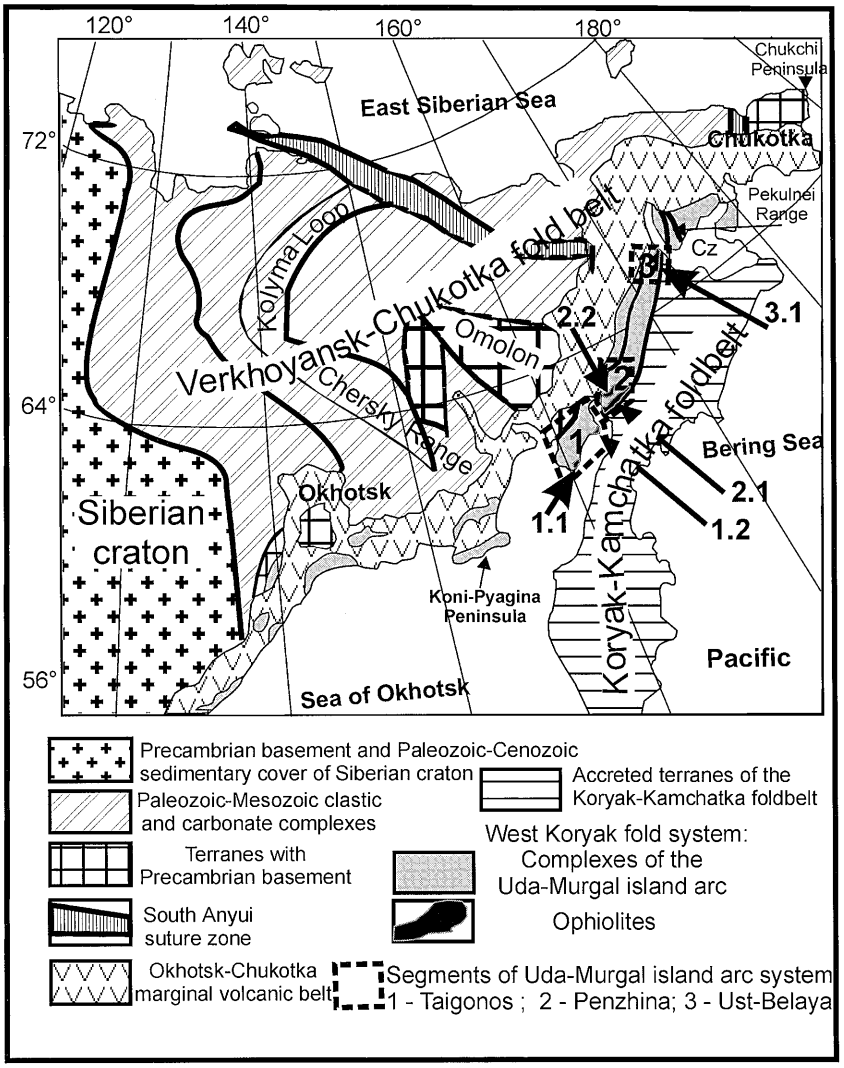

Fig. 1. Tectonic map of NE Asia (by S. D. Sokolov and G. Ye. Bondarenko). Black areas are ophiolites: 1.1, Cape Povorotny; 1.2, Yelistratov Peninsula; 2.1, Kuyul terrane; 2.2, Ganychalan terrane; 3.1, Ust–Belaya terrane.

small, undeformed slices associated with greenschist- and amphibolite-facies metamorphic rocks (Parfenov *et al.* 1993; Nokleberg *et al.* 1994; Oxman *et al.* 1995).

The Koryak–Kamchatka foldbelt is located east of the Okhotsk–Chukotka Volcanic Belt and stretches north–south to NE–SW (Fig. 1). It is a typical example of an accretionary continental margin formed through successive docking onto the Asian continent of outboard terranes having a variety of ages and geodynamic settings and arriving from the Pacific (Zonenshain *et al.* 1990; Bogdanov & Til'man 1992; Pushcharovsky *et al.* 1992; Sokolov 1992; Parfenov *et al.* 1993; Nokleberg *et al.* 1994). The terranes are of the following types: island arc, ophiolite, back-arc and turbidite basins, oceanic crust, and accretionary prism. Ophiolites are widespread, making up major bodies and entire terranes (Markov *et al.* 1982; Peyve 1984; Palandzhyan 1992; Sokolov 1992; Nokleberg *et al.* 1994).

No consensus exists regarding the age, composition, or provenance of NE Asian ophiolites. Some workers (e.g. Fujita & Newberry 1982; Parfenov 1984; Zonenshain *et al.* 1990) view the ophiolites as fragments of a large oceanic basin, a

former constituent of the Palaeo-Pacific. Others believe them to be relics of minor oceanic basins or rifts (Lychagin *et al.* 1991; Bogdanov & Til'man 1992; Oxman *et al.* 1995), and still others suggest that both Palaeo-Pacific and back-arc basin fragments come into play (Peyve 1984; Sokolov 1992; Nokleberg *et al.* 2001). This controversy is due primarily to poor knowledge of the ophiolite assemblages; hence the critical importance of the new structural and compositional data presented here. Dating the ophiolites is crucial to unravelling their history. According to earlier workers (e.g. Coleman 1984; Ishiwatari 1994; Dilek *et al.* 1999; Searle & Cox 1999; Shervais 2001), ophiolites originate from a variety of tectonic environments, that obviates any palaeotectonic reconstructions or formative scenarios for the NE Asian margins without first identifying geodynamic affinities of the ophiolites. In addition, there are virtually no English-language publications on NE Asian ophiolites; hence, one more objective of this paper is to fill in this informational gap.

The ophiolites discussed in this paper occur in the West Koryak fold system, which is located at the junction of the Verkhoyansk–Chukotka and Koryak–Kamchatka foldbelts (Fig. 1). In recent years, we have acquired new data on field relationships and evolution of this major tectonic unit, which incorporates accreted ophiolitic assemblages of various ages (Sokolov *et al.* 1999; Silantyev *et al.* 2000). The paper focuses on new data and issues related to the tectonic setting, inner structure, composition, and age of the ophiolites.

Geological framework

In NE Asia, four major tectonic units (Fig. 1) with distinctive structural grains and geological histories are recognized: (1) the Siberian craton; (2) the Verkhoyansk–Chukotka foldbelt; (3) the Koryak–Kamchatka foldbelt; (4) the Okhotsk–Chukotka continental-margin volcanic belt (OCVB) (Fig. 1). These units represent continuous, albeit discrete, accretion onto the Siberian craton of geodynamically diverse terranes and microcontinents (Fig. 2).

The West Koryak fold system lies along the boundary between the Koryak–Kamchatka and Verkhoyansk–Chukotka foldbelts. Most of the West Koryak fold system is overlain by OCVB volcanic and sedimentary rocks, and the latter also unconformably overlap the Verkhoyansk–Chukotka foldbelt. The OCVB is a Late Cretaceous Andean-type continental-margin volcanic belt. It was initiated after a major mid-Cretaceous (Aptian–Albian) phase of accretion (Fig. 2) onto the Asian continent (Sokolov 1992).

The West Koryak fold system incorporates numerous island-arc assemblages and ophiolites that were brought together at the end of the Early

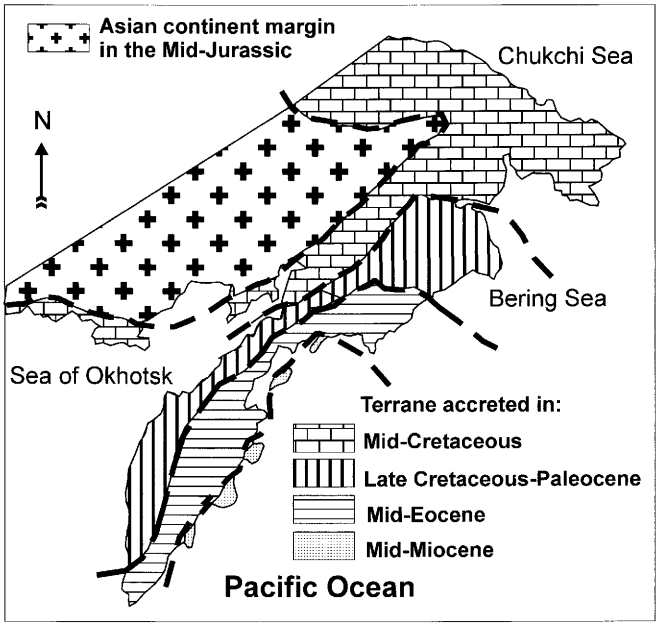

Fig. 2. Reconstruction showing continental growth of NE Asia (after S. D. Sokolov 1992).

Cretaceous (Markov *et al.* 1982; Parfenov 1984; Zonenshain *et al.* 1990; Sokolov 1992; Parfenov *et al.* 1993).

The island-arc volcanic and sedimentary assemblages are of calc-alkaline affinity and range in age from Carboniferous to Early Cretaceous. Parfenov (1984) attributed these rocks to a continuous Late Palaeozoic to Mesozoic Koni–Murgal island arc. However, Filatova (1988) viewed the Late Jurassic to Early Cretaceous volcanic and sedimentary sequences as part of the Uda–Murgal island arc. Zonenshain *et al.* (1990) identified the Koni–Murgal volcanic belt as a separate system, which they interpreted as an agglomeration of island-arc assemblages of various ages that were joined together in Mid-Cretaceous time. According to those workers, the original position of these assemblages is unknown, although they are believed to have been formed a considerable distance away from Siberia's continental margin (Zonenshain *et al.* 1990). These considerations drew on the pioneering palaeomagnetic data pinpointing the Omolon terrane in the Late Palaeozoic and Early Mesozoic at more southerly latitudes. These data, however, were at odds with palaeobiogeographical conclusions on the boreal faunas and Angara floras (Shapiro & Ganelin 1988). Sokolov (1992) postulated two convergent boundaries of contrasting ages in the region; one of Late Palaeozoic to Early Mesozoic age, during which the Koni–Taigonos island arc existed, and the other of Late Jurassic to Early Cretaceous age, composed of the Uda–Murgal island-arc system (Fig. 1).

The volcanic and sedimentary assemblages of the Koni–Taigonos island arc are best exposed and most thoroughly studied in the Koni–Pyagina and Taigonos peninsulas (Nekrasov 1976; Zaborovskaya 1978). These areas provide a stage for reconstructing, in Permian to Mid-Jurassic times, the volcanic arc proper and the North Taigonos back-arc basin. These assemblages are also present in the Penzhina District (Khudoley & Sokolov 1998), in the Pekulnei Range, and in Chukotka (Morozov 2001). In the Penzhina segment, Carboniferous island-arc assemblages are exposed in the Kharitonya terrane and in thrust sheets within the Upupkin terrane; in this locality, they consist of coarse andesitic pyroclastic rocks and tuffaceous epiclastic rocks of Permian and Triassic ages (Khudoley & Sokolov 1998; Sokolov *et al.* 1999). In the Pekulnei Range and in Chukotka, the Late Palaeozoic to Early Cretaceous island-arc sequence includes metavolcanic and metasedimentary rocks, layered gabbros, and Early Mesozoic granitic rocks (Morozov 2001).

Unfortunately, numerous aspects of the Koni–Taigonos island arc are still unclear. These include both the arc's polarity and basement composition, as well as the origin of its various segments. Faunal and floral data point to rock formation at high latitudes (Shapiro & Ganelin 1988; Sokolov 1992), which, in combination with structural data (Sokolov *et al.* 1999) and spatial position, suggest that the arc originated along a convergent boundary between the Asian continent and the NW Pacific. Various outboard terranes that arrived from the Palaeo-Pacific were accreted onto the arc (Zonenshain *et al.* 1990; Parfenov *et al.* 1993). These terranes are best exposed in the Penzhina segment, where they include the Ganychalan composite terrane and metamorphic rocks of the Upupkin terrane. Fragments of these assemblages have also been reported from the pre-arc basement of the Taigonos segment of the Uda–Murgal arc and as Ordovician deposits and ophiolites (Fig. 1; see also Fig. 15, below).

Upper Jurassic to Lower Cretaceous volcanic and sedimentary rocks of the Uda–Murgal island-arc system are traceable for about 3000 km, from the Mongolia–Okhotsk foldbelt in the south along the Sea of Okhotsk coastline (via the Koni, Pyagina, and Taigonos peninsulas) as far northeastward as the Chukchi Peninsula (Fig. 1). The volcanic and sedimentary lithologies and the character and age of basement vary from place to place along the arc. In the southern segment, the only identifiable features are the volcanic portion of the island-arc system and some constituents of its associated back-arc basin. Island-arc assemblages rest on heterogeneous basement that includes fragments of the Asian continent (Siberian craton, Verkhoyansk complex, Okhotsk microcontinent), and the Koni–Taigonos Late Palaeozoic to Early Mesozoic island arc. Hence, the Late Jurassic to Early Cretaceous convergent boundary was located at an angle to the pre-existing structural grain. Throughout the study area, volcanic arc assemblages were located along the continental margin, strongly suggesting the existence of a continental-margin belt.

The Taigonos and Penzhina segments provide evidence for reconstructing a lateral succession: volcanic arc–forearc–accretionary prism–trench–oceanic plate (Fig. 3). Basement to the island arc was provided by the pre-existing Koni–Taigonos arc with its accreted terranes, including the Early Palaeozoic ophiolites of the Ganychalan terrane. Within these segments, island-arc deposits were also formed in a continental margin setting. Further NE, however, the back-arc region was the locus of marine deposition, and the continental-margin belt gave way to an ensialic arc (Sokolov *et al.* 1999).

In the Pekulnei segment, island-arc assemblages rest on heterogeneous basement that incorporates

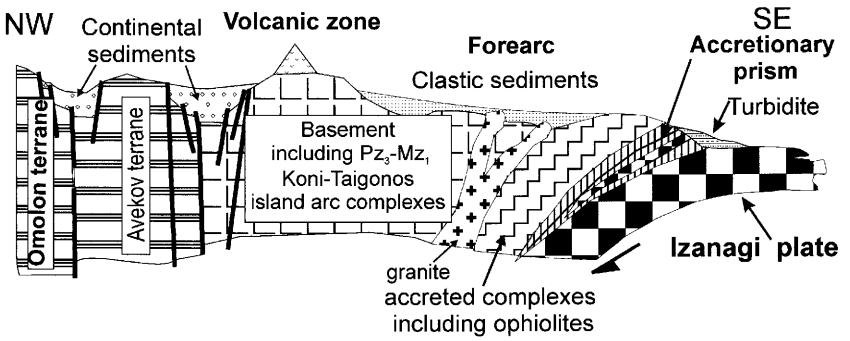

Fig. 3. Taigonos segment of the Uda–Murgal island arc (Late Jurassic–Early Cretaceous).

fragments of both lower continental crust and oceanic lithosphere (Sokolov *et al.* 1999; Morozov 2001). A back-arc basin floored with oceanic crust was situated behind the arc and was probably linked to the Anyui palaeo-ocean.

The northeastern Chukotka branch (Fig. 1) of the convergent boundary had heterogeneous basement that incorporated, among other things, ancient sialic crust. Consumption of oceanic crust along the Chukotka branch was not extensive, probably because of the strike-slip nature of plate interaction within this segment (Morozov 2001).

Ophiolites of the West Koryak fold system (Fig. 1) occur either in forearc basement (type 1) or within accretionary prisms of the Uda–Murgal island arc (Fig. 1) (type 2). Type 1 ophiolites were accreted in the Late Palaeozoic–Early Mesozoic (Parfenov 1984; Sokolov *et al.* 1999) onto the Koni–Taigonos island arc. Type 2 ophiolites were accreted in Late Jurassic and, mainly, in Early Cretaceous times onto the frontal part of the Uda–Murgal island-arc system (Parfenov 1984; Khanchuk *et al.* 1990; Sokolov *et al.* 1999). Ophiolites have been reported from the Taigonos, Penzhina, and Ust–Belaya segments of the island arc.

Ophiolites are well exposed along the SE coast of the Taigonos Peninsula (Fig. 1). The largest ophiolitic outcrops occur within the accretionary pile exposed at Cape Povorotny and in pre-arc basement on the Yelistratov Peninsula (Belyi & Akinin 1985; Ishiwatari *et al.* 1998). In the Penzhina segment, two large ophiolitic terranes, the Ganychalan and Kuyul terranes, are well documented (Markov *et al.* 1982; Palandzhyan 1992; Ganelin & Peyve 2001; Nekrasov *et al.* 2001).

Analytical techniques

Major and trace element analyses were carried out in various laboratories using a range of methods.

Mineral compositions from Cape Povorotny rocks were measured in polished sections on an automated CAMEBAX-Microbeam four-channel wavelength-dispersive electron probe at the Vernadsky Institute (GEOKHI). Whole-rock major element analyses from peridotites and gabbros were performed by X-ray fluorescence (XRF) on a Philips PW-1600 XRF automated multichannel spectrometer, and REE contents were determined by instrumental neutron activation analysis (INAA) at GEOKHI. All analytical investigations of the volcanic rocks were carried out at the Analytical Centre of the Geological Institute, Russian Academy of Sciences (GIN RAS) by INAA and inductively coupled plasma mass spectrometry (ICP-MS).

Mineral chemistry of Yelistratov Peninsula ophiolitic peridotites and Ganychalan terrane plutonic rocks was analysed by N. N. Kononkova on a CAMECA CAMEBAX electron microprobe at GEOKHI at an accelerating voltage of 15 kV and beam current of 35 nA. Natural and synthetic minerals were used as standards. Rock chemistry was analysed on a PLASMA QUAD PQZ+Turbo (VG Instruments) mass spectrometer at the Institute of Mine Geology, Petrography, Mineralogy, and Geochemistry, Moscow. Routine sample preparation included dissolution in concentrated HF + $HClO_4$ mixture, followed by precipitation using HNO_3. Analytical reproducibility was controlled using certified F, W, rare earth element (REE) + 25 ppb standard solutions and AGV-1 standard.

Major, trace, and REE analyses on plagiogranites from blocks in the Main Mélange unit of Cape Povorotny, Ganychalan terrane, and Kuyul terrane ophiolites, as well as ultramafic and mafic rocks of Ganychalan ophiolites were performed at the GIN RAS Analytical Centre. Major elements were measured by wet chemistry, and trace elements by XRF on a Russian-made ARF-6 quantographer in the concentration range 0.0001% to *n*%. REE were analysed by INAA in the range 0.000001% to *n*%.

Ion microprobe measurements on minerals from Ust–Belaya peridotites were performed at the Northeastern Interdisciplinary Research Institute,

Far East Division of the Russian Academy of Sciences (SVKNII DVO RAN), Magadan, on a CAMEBAX instrument (analysts E. M. Goryacheva and G.A. Merkulov). Major elements in ultramafic and mafic rocks were analysed at the X-ray Spectral Analysis Laboratory (SVKNII) and by gravimetric analysis at the Central Laboratory, Geological Survey, Magadan. Whole-rock K–Ar measurements were carried out by A. D. Lyuskin, at the Laboratory of Isotope Geochronology, SVKNII.

REE in clinopyroxenes from the Ganychalan terrane plutonic rocks were measured on a Cameca IMS 4f ion microprobe, at the Institute of Microelectronics (IMAN), Russian Academy of Sciences, Yaroslavl.

Major elements and V, Cr, Co, Ni, Cu, and Ba from Kuyul terrane peridotites were determined by wavelength-dispersive XRF using routine techniques at the Karpinsky Geological Institute (St. Petersburg, Russia). Other trace elements, including REE, were analysed by ICP-MS at the Institute of Geochemistry (Irkutsk, Russia). Mounts of 0.1 ± 0.001 g were digested with HF and HNO_3 mixture in Teflon bombs for 24 h, evaporated until dry, taken up in HNO_3, and once again evaporated until dry. Further HCl was added and the product again evaporated until dry to assure quantitative removal of HF and chlorides. The samples were redissolved with deionized water. No undissolved spinels were detected in the Teflon bombs, and the fact that Cr values were comparable with those obtained by XRF suggests that all of the spinels went into solution. The samples were run on a VG Elemental Plasmaquad with long peak dwell times (320 ms per mass unit). Calibration was carried out using a set of high-Mg laboratory standards. Estimated precision is less than 10% for all of the determined elements.

Microprobe analyses of minerals from Kuyul terrane peridotites were carried out at the Institute of Volcanology (Petropavlovsk-Kamchatsky, Russia) using a CAMECA CAMEBAX system equipped with a KEVEX energy-dispersive spectrometer with an accelerating voltage of 15 kV and a sample current of 15 nA (counting time 100 s). Precision is estimated to be better than about 2% for all main components.

Radiometric ages are taken from a number of publications, where their interpretation is provided as well.

Ophiolites in the Cape Povorotny accretionary complex

Geological setting

Five tectonic units are recognized in the Taigonos Peninsula (Fig. 4): (1) the Avekov terrane, which is composed of Precambrian and Lower Palaeozoic metamorphic sequences; (2) the Pylgin suture zone, which incorporates metamorphosed Mesozoic volcanic and sedimentary rocks; (3) the Central Taigonos terrane, made up of Upper Permian–Lower Cretaceous island-arc strata; (4) the East Taigonos granite–metamorphic belt; (5) the Beregovoi terrane, which is composed of prearc complexes and the accretionary prism of the Uda–Murgal volcanic arc (Sokolov *et al.* 1999; Silantyev *et al.* 2000).

A broad spectrum of igneous and metamorphic rocks are hosted by serpentinite mélange in the Cape Povorotny accretionary complex and make up the following succession of tectonic units, from south to north (Fig. 5): (1) the Povorotny serpentinite mélange with blocks of sheeted dykes, ultramafic rocks, and gabbro; (2) the Median serpentinite mélange, with small blocks and fragments of ultramafic rock, gabbro, volcanic and terrigenous rocks, and chert; (3) the Main Mélange unit, a serpentinite mélange with blocks of peridotite, garnet-free and garnet-bearing amphibolites, greenschists, island-arc volcanic and sedimentary rocks, oceanic basalts and chert, and gabbro–diabase with plagiogranite veins (Fig. 6).

Petrography and geochemistry of metamorphic and igneous rocks

Amphibolites occur as disrupted blocks in serpentinite mélanges exposed on Cape Povorotny (Fig. 5). They consist of: (1) massive melanocratic rocks composed almost wholly of hornblende and minor plagioclase or garnet–hornblende rocks; (2) albite–hornblende schists. Judging by the characteristic mineral assemblages and mineral and bulk-rock compositions, the protoliths were made dominantly of plutonic rocks and subordinate volcanic rocks (Silantyev *et al.* 2000). Geochemical signatures of high-grade amphibolites have been detailed by Silantyev *et al.* (2000), indicating that volcanic protoliths of these rocks ranged in affinity from within-plate basalt (WPB) or enriched mid-ocean ridge basalt (E-MORB) to normal MORB (N-MORB).

Mafic plutonic rocks are widespread as tectonic blocks in the Povorotny and Median mélanges. Gabbros typically occur as isolated boudins and small tectonic slices in the serpentinite matrix. Plutonic rock compositions from the Cape Povorotny ophiolite mélange have a wide range, implying the existence of different gabbroic series of several geochemical types. Silantyev *et al.* (2000) presented chemical data indicating that gabbros chemically similar to boninite plutonic suites are abundant in the Cape Povorotny serpentinite mél-

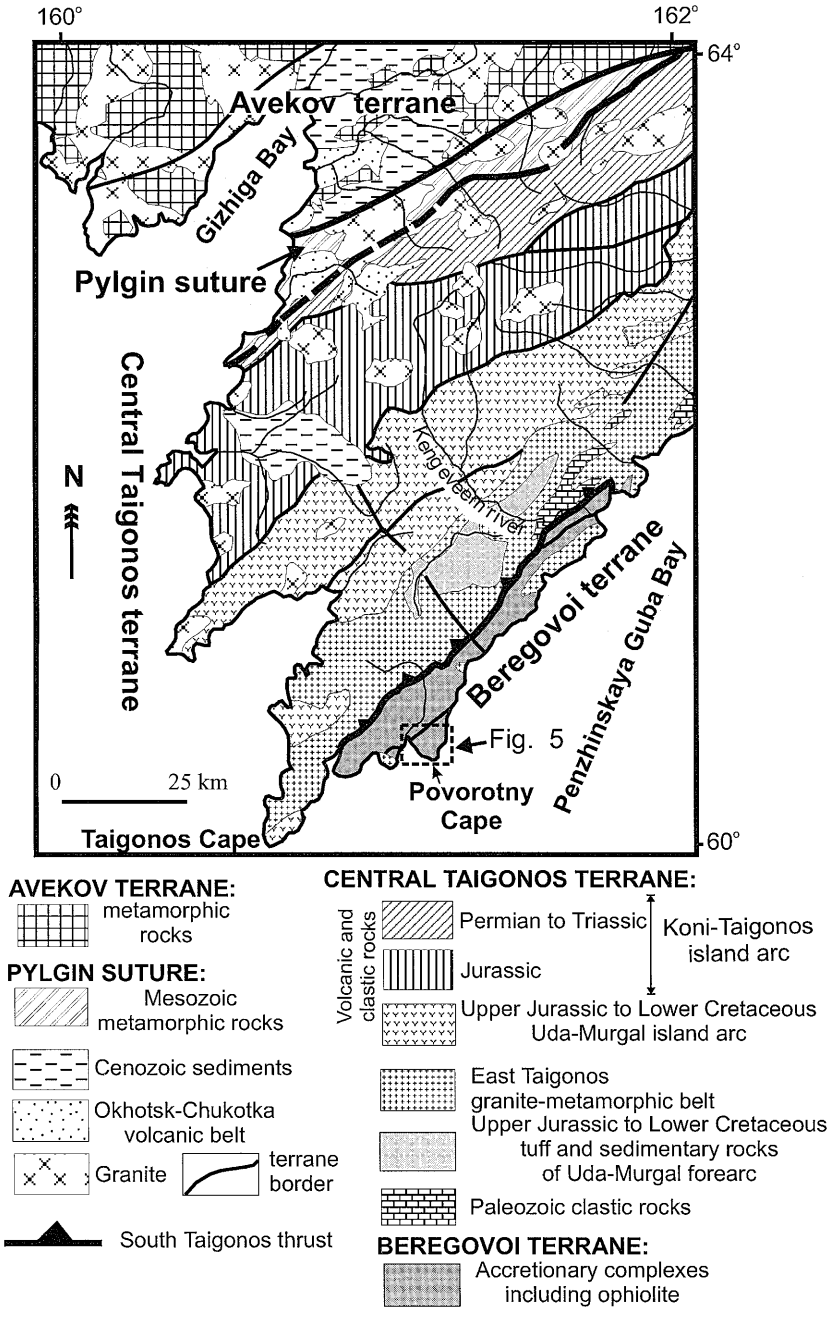

Fig. 4. Tectonic map of the Taigonos Peninsula (after Sokolov *et al.* 1999).

anges. These boninite-like gabbros are low in TiO_2, their REE patterns being typical of boninites and their plutonic equivalents (low total REE contents, concave chondrite-normalized REE patterns, and considerable light REE (LREE) variations). The Cape Povorotny boninite gabbros are associated with N-MORB and within-plate or E-MORB gabbros and dolerites. This group of plutonic rocks, including hornblende-bearing gabbro, is moderate to relatively high in TiO_2, FeO, and P_2O_5 at

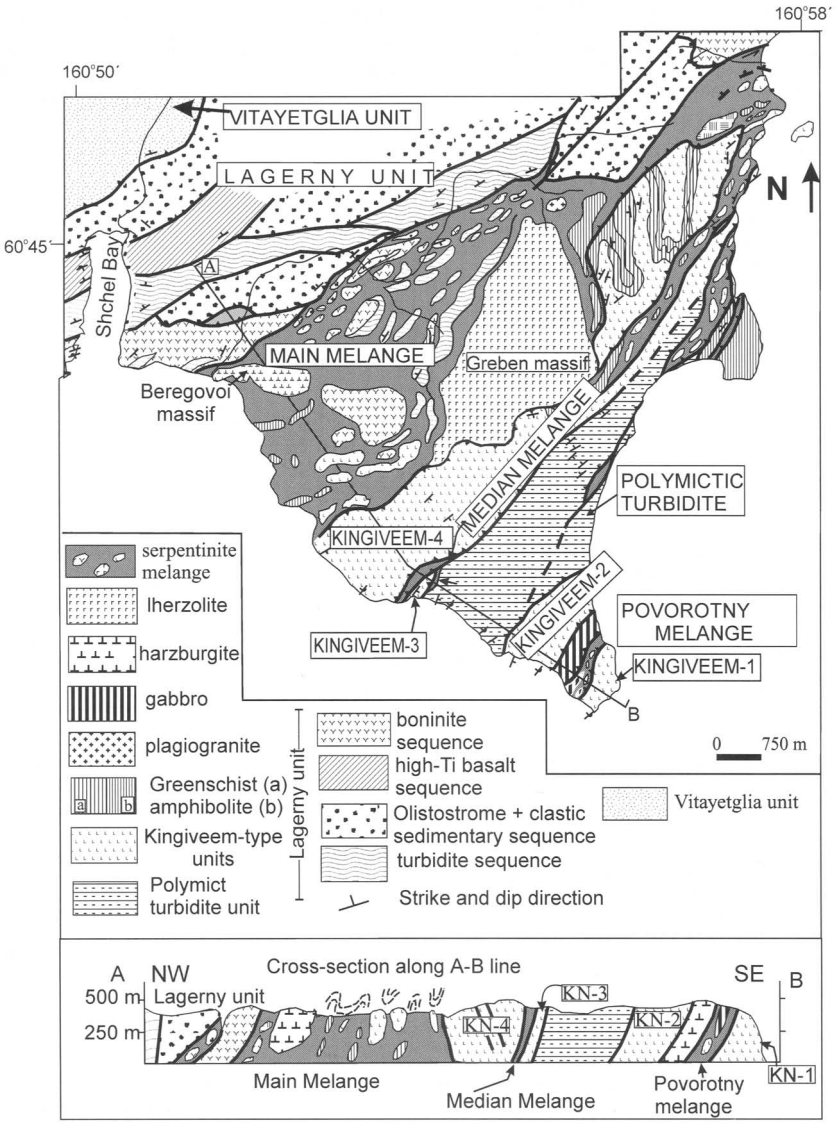

Fig. 5. Map showing tectonic units of the Cape Povorotny accretionary complex (after Sokolov *et al.* 1999).

moderately high REE totals (analytical data have been presented by Silantyev *et al.* (2000)).

Felsic veins in gabbro–diabase from blocks in the Main Mélange unit (Fig. 6) are composed of plagiogranite and, sporadically, tonalite. The plagiogranites have magmatic textures with euhedral plagioclase crystals partly intergrown with quartz–albite granophyre, suggestive of crystallization at shallow depths. The plagiogranites are composed of quartz, saussuritized plagioclase, epidote, chlorite, and magnetite. The tonalites differ from the plagiogranites in having smaller amounts of quartz, and in that they contain light green amphibole and andesine plagioclase is andesine.

The plagiogranites and tonalites have low Al_2O_3 (11.12–13.7%), K_2O (0.03–0.06%) and K/Rb ratios (0.01–0.03), and relatively high Y (37–44 ppm) (Table 1). Rb (7 ppm) and Zr (120, 160 ppm) contents of the plagiogranites (Table 1) are similar to those of the average Mid-Atlantic Ridge plagiogranites at latitude 2–3°N (Rikhter 1997).

Chondrite-normalized REE patterns of the plagiogranites are nearly flat to slightly LREE en-

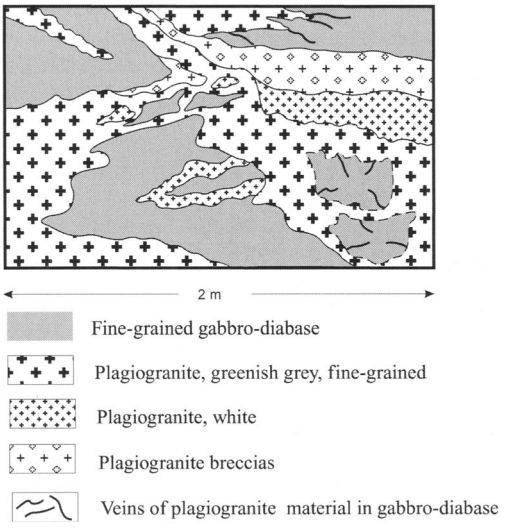

Fig. 6. Network of plagiogranite veins in gabbro–diabase from blocks in the Main Mélange zone.

riched ($La_n/Yb_n = 1.01–1.95$) and show distinct negative Eu anomalies ($Eu_n/Eu^* = 0.49–0.63$, Fig. 7). The increase in total REE content from gabbro–diabase to plagiogranite and similarity of the REE patterns suggest that the rocks are cogenetic (Fig. 7).

Comparison between the Cape Povorotny plagiogranites and those from the Bay of Islands ophiolites, Newfoundland (Elthon 1991), shows that both have negative Ta and Ti anomalies (Fig. 8) indicative of suprasubduction zone origin (Pearce & Norry 1979; Saunders *et al.* 1980; Shervais 1982; Elthon 1991). Negative Ta and Nb anomalies are also shown by the Cape Povorotny plagiogranites when plotted on the ocean-ridge granite (ORG)-normalized (Pearce *et al.* 1984) patterns (Fig. 9). Chondrite-normalized REE patterns of plagiogranites and trondhjemites from the Maqsad ophiolite, Oman, considered by Amri *et al.* (1996) to have formed at a mid-ocean ridge, differ from those of Cape Povorotny plagiogranites in having lower REE totals and REE patterns with both negative and positive Eu anomalies (Fig. 10). It should be noted that Cox *et al.* (1999) and Searle & Cox (1999) assumed that Oman ophiolitic crust and its plagiogranite were generated above an intra-oceanic subduction zone.

Basalts are the dominant volcanic rocks in the Main and Median mélanges of the Cape Povorotny accretionary complex (Fig. 5). Basalts make up isolated tectonic blocks and flow units within terrigenous–tuffaceous sequences. Based on petrographic and geochemical evidence, these rocks are divided into the following groups (Sokolov *et al.* 1999; Silantyev *et al.* 2000): (1) boninites with low TiO_2, extremely low middle REE (MREE) and heavy REE (HREE), and high MgO contents; (2) aphyric and phyric calc-alkaline basalts and low-K tholeiitic basalts; (3) pillowed and massive tholeiitic basalts with marked N- and E-MORB geochemical features.

Cape Povorotny peridotites (Bazyler *et al.* 2000) occur in dismembered ophiolite sequences at various localities confined to NE-trending tectonic units. From SE to NW, these units crop out in the Povorotny, Median, and Main (including Greben and Beregovoi massifs) serpentinite mélanges (Fig. 5).

The central zone of the Greben massif is composed of spinel lherzolite. The outer zone of the Greben massif, the Beregovoi massif, and small peridotite blocks of the Main and Median mélanges are composed of harzburgite proper and Cpx-bearing harzburgite. Peridotites from the Povorotny mélange are also harzburgites, but more depleted, judging from spinel compositions (Table 2). Compositions of other mineral phases have been given by Bazylev *et al.* (2001). The Median mélange is dominated by cumulate peridotites, including pyroxene-bearing dunites, chromitites, wehrlites, and plagioclase harzburgites, which are also found in the Main Mélange.

Spinels from residual peridotites (lherzolites and harzburgites) have Cr number (Cr/(Cr + Al)) ranges as wide as 0.18–0.70 (Bazylev *et al.* 2001), suggesting SSZ provenance for at least some of these rocks (Dick & Bullen 1984). Representative spinel compositions from the peridotites are given in Table 2. The Mg number (100Mg/(Mg + Fe)) of olivines and orthopyroxenes from the residual spinel peridotites does not correlate with the spinel Cr number (varying in the range 89.6–91.7), indicating their origin by open-system melting or melt–rock interaction, rather than by simple partial melting (Bazylev *et al.* 2001). Silicate mineral compositions from peridotites have been reported by Bazylev *et al.* (2001). Spinel compositions from the cumulate peridotites have high Cr number (0.30–0.79), elevated iron oxidation degrees, and low Ti contents, further supporting an SSZ rather than a MOR affinity for these rocks (Arai 1992).

REE patterns from all the peridotite varieties including wehrlites are also LREE enriched, some of the spectra being U-shaped. They also have significant negative Nb and Zr anomalies, some samples also having negative Ti anomalies (Fig. 11). The data on rock geochemistry have been given by Bazylev *et al.* (2001). These features were explained by Bazylev *et al.* as resulting from open-system melting (Ozawa & Shimizu 1995) of mantle material accompanied by melt influx.

Table 1. *Major (wt%) and trace (ppm) element contents of gabbro–diabases and plagiogranites in blocks from the Main Mélange zone*

Sample	c-2415	c-2340	c-2415/1	c-2340/2	c-2340/4	c-2340/1	c-2340/3
SiO_2	51.53	51.8	53.71	63.84	73.04	75.51	77.03
TiO_2	0.76	0.94	1.03	0.60	0.69	0.43	0.53
Al_2O_3	13.12	14.68	14.07	13.7	12.22	12.56	11.12
Fe_2O_3	3.84	2.60	4.91	1.59	0.53	1.34	1.37
FeO	6.52	4.60	6.60	2.93	0.50	0.58	0.65
CaO	8.96	12.94	5.97	6.22	3.77	1.61	3.50
MgO	7.35	5.91	5.05	3.20	1.30	1.03	0.20
MnO	0.08	0.06	0.09	0.04	0.02	<0.01	0
Na_2O	4.07	3.98	4.68	5.83	5.66	6.15	5.47
K_2O	0.04	0.35	0.32	0.10	0.30	0.20	0.06
P_2O_5	0.07	0.02	0.11	0.01	0.09	0.02	0.02
LOI	3.30	2.46	3.01	2.31	1.02	0.84	0.40
Total	99.64	100.34	99.56	100.36	99.74	100.33	100.35
Th	–	–	–	0.9	–	1.5	–
Zr	–	–	–	120	–	160	–
Hf	–	–	–	4.4	–	5.9	–
Nb	–	–	–	2.7	–	3.9	–
Ta	–	–	–	0.06	–	0.10	–
Y	–	–	–	44	–	37	–
Rb	–	–	–	7	–	7	–
Sr	–	–	–	21	–	130	–
Ba	–	–	–	–	–	–	–
Cs	–	–	–	0.3	–	0.3	–
Sc	–	–	–	20	–	13	–
Co	–	–	–	2.2	–	1.2	–
La	–	1.70	4.60	11.00	11.00	5.60	14.00
Ce	–	5.30	11.00	28.00	26.00	17.00	31.00
Nd	–	4.90	9.50	19.00	18.00	11.00	19.00
Sm	–	1.80	3.40	6.00	5.60	3.20	5.70
Eu	–	0.35	0.95	1.10	1.40	0.93	1.40
Tb	–	0.51	0.83	1.20	1.30	0.92	1.30
Yb	–	2.00	3.20	4.60	4.60	3.70	4.80
Lu	–	0.32	0.50	0.71	0.73	0.65	0.82
La_n/Yb_n	–	0.57	0.96	1.60	1.60	1.01	1.95
La_n/Sm_n	–	0.84	1.1	1.03	1.11	0.87	1.19
Eu_n/Eu^*	–	0.63	0.89	0.49	0.63	0.63	0.56

c-2415 to c-2415/1, gabbro–diabase; c-2340/2 to c-2340/3, tonalites and plagiogranites. Major elements were measured by wet chemistry, trace elements by XRF, and REE by INAA.

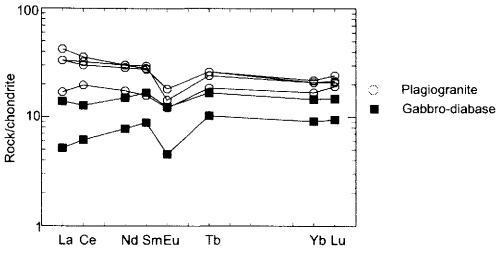

Fig. 7. Chondrite-normalized (Sun & McDonough 1989) REE patterns for gabbro–diabase and plagiogranites from blocks in Main Mélange zone.

As the data reported above and by Bazylev *et al.* (2001) preclude a mid-oceanic ridge origin for the Cape Povorotny lherzolites, the earlier geodynamic interpretation of these rocks (Palandzhyan & Dmitrenko 1999; Silantyev *et al.* 2000) should be revised.

Origin of igneous and metamorphic rocks

The available geochemical data collectively suggest the principal rock assemblages that make up the ophiolite mélange in the Cape Povorotny accretionary pile to be (Silantyev *et al.* 2000):

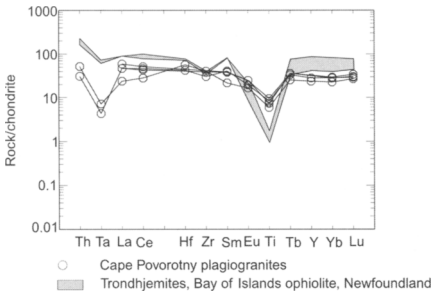

Fig. 8. Chondrite-normalized (Sun & McDonough 1989) REE patterns for plagiogranites from Cape Povorotny, Taigonos Peninsula, and Bay of Islands (Newfoundland).

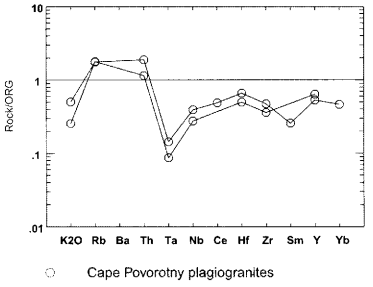

Fig. 9. ORG-normalized (Pearce *et al.* 1984) patterns for plagiogranites from Cape Povorotny, Taigonos Peninsula.

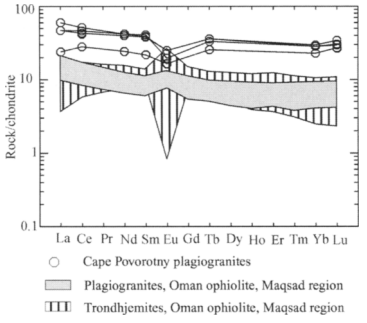

Fig. 10. Chondrite-normalized (Sun & McDonough 1989) REE patterns for plagiogranites from Cape Povorotny, Taigonos Peninsula, and trondhjemites and plagiogranites from Oman ophiolite, Maqsad region.

(1) high-grade amphibolites derived from plutonic and, rarely, volcanic rocks of N- and E-MORB affinities; (2) plutonic rocks including boninitic and normal gabbro and diabase with N-MORB and within-plate or E-MORB affinities, and plagiogranites; (3) MORB-like basalt, WPB, and various products of SSZ magmatism, including boninite; (4) peridotites, including spinel lherzolite, spinel harzburgite, dunite, and wehrlite of SSZ affinity. Thus, the Cape Povorotny ophiolite sequence probably contains lithospheric fragments of two types.

Type 1 consists of spinel lherzolite, spinel harzburgite, dunite, and wehrlite. Spinel lherzolites and harzburgites originated through various degrees of mantle melting above a subduction zone. Judging by data reported by Silantyev *et al.* (2000), the low-Ti volcanic rocks of island-arc affinity (low in TiO_2, Cr, Nb, and with high Mg number) from the Main Mélange and the Cape Povorotny spinel harzburgites might be cogenetic, both representing products of subduction magmatism. The compositions of spinel from the cumulate peridotites, particularly elevated degrees of iron oxidation and low Ti contents, confirm an SSZ rather than oceanic-basin origin for these rocks (Arai 1992). Plutonic rocks of boninite affinity, as well as boninites and calc-alkaline volcanic rocks and low-K basalts, occur in the same lithospheric fragments (Silantyev *et al.* 2000).

The plagiogranites may have originated through anatexis of a gabbroic parent or as interstitial melt crystallized during mafic magma fractionation. The similarity of chondrite-normalized REE patterns for the gabbro–diabase and plagiogranite supports the latter interpretation. Negative Ta, Nb, and Ti anomalies in the plagiogranites point to their origin in an SSZ setting (Figs 8 and 9) (Pearce & Norry 1979; Saunders *et al.* 1980; Shervais 1982; Elthon 1991; Saunders *et al.* 1991; Pearce 1992).

Type 2 lithospheric fragments in the Cape Povorotny ophiolitic mélange have oceanic geochemical and mineralogical signatures. These fragments are observed in the Main Mélange (Fig. 5) and are represented by protoliths of the high-grade amphibolites, gabbros, and dolerites, which show N-MORB and within-plate (or E-MORB) affinities, as well as MORB and WPB volcanic rocks.

According to Shervais (2001), Type 1 magmatic and metamorphic assemblages can be interpreted as products of a complete life cycle of SSZ ophiolites that includes (1) birth: low-K tholeiites, basaltic andesite, and spinel harzburgites; (2) youth: boninites (volcanic and plutonic) and cumulate peridotites; (3) maturity: basaltic andesite, andesite, hornblende gabbro, and plagiogranite; (4) death: formation of high-T metamorphic soles (amphibolite and garnet amphibolite).

P–T estimates for metamorphic rocks suggest two principal types of metamorphism for Cape Povorotny ophiolites (Silantyev *et al.* 2000). Type 1 reflects relatively high-P (8 kbar) and medium-T (500–700 °C) conditions and is unique to the high-grade amphibolites, and type 2, which post-

Table 2. *Spinel composition (wt%) from Cape Povorotny peridotites, Taigonos Peninsula*

No.:	1	2	3	4	5	6	7	8	9	10	11	12	13
Sample:	T40/1	T41/1	C2312	C2356	C2362/1	T4/2	C94011	C94011	T49/1	C2352/1	C9413/6	C9413/6	C2314
Rock:	LH	LH	LH	LH/H2	H1	H1	H1	H1	H1	H1	H1	H1	H1
Phase:	Spl1	Spl1	Spl1	Spl1	Spl1	Spl1	Spl1	FCR	Spl1	Spl1	Spl1	FCR	Spl1
Points:	3	4	8	4	1	3	4	2	2	2	4	2	2
SiO_2	0.02	0.01	0.09	0.12	0.01	n.a.	0.25	3.35	n.a.	0.05	0.10	4.30	0.06
TiO_2	0.02	0.01	0.07	0.12	0.08	0	0.03	0.03	0	0.10	0.06	0.17	0.05
Al_2O_3	50.60	47.54	50.20	47.50	40.61	39.06	33.97	2.94	30.89	29.84	28.95	2.60	27.92
FeO	13.91	15.39	14.04	14.63	14.80	15.60	17.55	55.30	19.63	16.73	18.84	51.39	18.49
MnO	0.07	0.07	0.12	0.09	0.17	0.19	0.25	3.61	0.34	0.17	0.22	3.06	0.19
MgO	17.92	18.01	18.16	18.07	16.79	16.08	14.81	4.75	12.98	14.99	13.70	5.87	13.33
Cr_2O_3	18.18	20.13	17.13	19.29	27.44	29.07	31.86	26.46	35.56	37.40	37.18	28.98	39.09
NiO	0.22	0.25	n.a.	n.a.	n.a.	0.15	0.16	0	0.07	n.a.	0.11	0.05	n.a.
V_2O_3	n.a.	n.a.	n.a.	n.a.	n.a.	n.a.	0.13	0.15	n.a.	n.a.	0.24	0.16	n.a.
ZnO	n.a.	n.a.	0.11	n.a.	0.26	n.a.	0.37	0.42	n.a.	0.12	0.21	0.74	0.15
Total	100.94	101.41	99.93	99.80	100.15	100.15	99.38	97.01	99.47	99.39	99.60	97.33	99.29

No.:	14	15	16	17	18	19	20	21	22	23	24	25	26
Sample:	C9413/4	C9413/4	C2492/2	C2492/2	C2492/2	C2492/2	C2501/1	C9425/8	C9425/8	C2315	C2501/14	T19/5	C2330/4
Rock:	H1	H1	CP1	CP1	CP1	CP1	CD1	CP1	CP1	CD1	CWH1	H2	H2
Phase:	Spl1	FCR	Spl1*	Spl2	Spl2	Spl2	Spl1	Spl1	FCR	Spl1	Spl1	Spl1	Spl1
Points:	2	3	1	1	3	2	2	7	2	4	9	2	2
SiO_2	0.25	5.36	0.12	0.24	0.07	0.06	0.06	0.11	2.40	0.07	0.16	n.a.	0.07
TiO_2	0.05	0.11	0.20	0.33	0.36	0.09	0.21	0.29	0.22	0.13	0.15	0	0.03
Al_2O_3	33.08	1.66	30.67	25.10	16.13	11.15	28.33	25.45	0.61	25.10	23.29	22.27	22.12
FeO	16.46	54.55	26.09	35.42	38.76	39.05	19.50	26.41	67.28	18.18	24.16	22.97	19.80
MnO	0.20	2.94	0.22	0.56	0.52	0.42	0.25	0.26	0.51	0.21	0.24	0.26	0.24
MgO	15.46	6.25	12.72	10.54	8.38	6.93	14.24	12.38	2.20	13.28	11.21	11.50	11.47
Cr_2O_3	33.43	27.56	29.63	27.39	35.12	40.56	36.45	34.13	20.59	41.83	40.46	43.27	44.67
NiO	0.15	0.11	n.a.	n.a.	n.a.	n.a.	n.a.	0.20	0.08	n.a.	0.12	0.01	n.a.
V_2O_3	0.26	0.15	n.a.	n.a.	n.a.	n.a.	n.a.	0.18	0.08	n.a.	0.25	n.a.	n.a.
ZnO	0.34	0.38	n.a.	n.a.	n.a.	0.28	0.07	0.19	0.07	0.12	0.25	n.a.	0.26
Total	99.69	99.06	99.60	99.58	99.33	98.54	99.11	99.60	94.04	98.92	100.28	100.28	98.68

No.:	27	28	29	30	31	32	33	34	35	36	37
Sample:	T1/2	C2356/1	T19/3	T20/4	C2493	C2493	C2493	C2493	C2493/1	C2493/1	C2493/1
Rock:	H2	H2	CD2	CO2	H2?	H2?	H2?	H2?	H2?	H2?	H2?
Phase:	Spl1	Spl1	Spl1	Spl1	Spl2	Spl2	Spl2	FCR	Spl2	Spl2	Spl2
Points:	3	8	2	2	1	1	1	1	4	1	3
SiO_2	n.a.	0.11	n.a.	n.a.	0	0.40	0.56	0.27	0.11	0.06	0.16
TiO_2	0	0.10	0.02	0.11	0.02	0.10	0	0.01	0.04	0.03	0.06
Al_2O_3	19.16	14.42	11.75	10.32	10.55	7.64	4.74	1.96	12.66	10.42	5.46
FeO	21.80	26.00	23.99	24.89	39.80	49.78	48.67	68.10	43.03	49.97	64.45
MnO	0.31	0.28	0.43	0.43	0.66	0.41	0.53	0.44	0.44	0.52	0.38
MgO	10.85	8.52	9.84	7.81	6.80	6.06	5.29	3.17	7.97	7.01	5.21
Cr_2O_3	47.16	50.02	52.85	56.10	42.35	35.36	39.50	24.04	34.13	30.67	22.62
NiO	0.06	n.a.	0.04	0.02	n.a.	n.a.	n.a.	n.a.	0.72	0.69	0.91
V_2O_3	n.a.	n.a.	n.a.	n.a.	n.a.	n.a.	n.a.	n.a.	0.21	0.21	0.19
ZnO	n.a.	0.21	n.a.	n.a.	n.a.	n.a.	n.a.	n.a.	0.25	0.19	0.13
Total	99.34	99.65	98.92	99.68	100.18	99.75	99.29	97.99	99.55	99.75	99.57

Total iron as FeO; n.a., not analysed. Rocks: LH, spinel lherzolites; H, spinel harzburgites; C, cumulate peridotites (WH, wehrlite; D, dunite; P, peridotites with identified pyroxene; O, orthopyroxenite). Rocks 1 and 2 belong to the moderately and strongly depleted rock groups, respectively. Minerals: Spl1, primary spinel; Spl2, secondary high-*T* metamorphic spinel; FCR, secondary medium-*T* metamorphic spinel. The spinel was analysed on a CAMEBAX microprobe at Vernadsky Institute using natural and synthetic mineral standards. Spot microprobe analyses were obtained at 15–20 kV accelerating voltage and 35 mA beam current.
*Primary spinel, partly recrystallized during high-*T* metamorphism.

dates type 1, is associated with low-*T* recrystallization of all igneous and metamorphic rocks, including the pre-existing high-grade amphibolites, under greenschist- and zeolite-facies conditions (350–380 °C and <2 kbar) (Silantyev *et al.* 2000). Silantyev *et al.* (2000) proposed that discrete blocks of high-grade amphibolite from Cape Povorotny ophiolites reflect dismemberment of an inverted subduction-related metamorphic aureole. Judging by the *P–T* path of different metamorphic events recorded in the amphibolites, Cape Povorotny high-grade amphibolites were exhumed from a depth of *c.* 20 km (Silantyev *et al.* 2000).

The available geochemical and petrological data suggest that the Cape Povorotny ophiolite developed as follows: (1) generation of MORB-like and within-plate magmatic assemblages (gabbro, diabases, and volcanic rocks) in an oceanic basin; (2) partial subduction of these rocks into a relatively shallow, warm, and young subduction zone with partial detachment of the subducting oceanic lithosphere and its tectonic incorporation into the SSZ pile; (3) formation of an SSZ magmatic complex, including spinel lherzolite and harzburgite, cumulate peridotites, and plagiogranite; (4) exhumation of high-grade amphibolites and residual peridotites followed by their tectonic incorporation into the SSZ pile.

Ophiolites in the Yelistratov Peninsula

Geological setting

In the Yelistratov Peninsula, ophiolites make up forearc basement to the Uda–Murgal island arc (Sokolov *et al.* 1999) and are unconformably overlain by Lower Cretaceous clastic deposits (Parfenov 1984; Filatova 1988). A preliminary geological description of the ophiolite was given by Belyi & Akinin (1985).

Our study shows that ophiolitic rocks occur in a number of tectonic slices (Fig. 12). On the north of the peninsula, the serpentinite mélange dips steeply NW, under the Jurassic–Lower Cretaceous sequence of calc-alkaline volcanic rocks of the Uda–Murgal island arc (Fig. 12). In the southern part, the mélange is overlain by slices of cumulate gabbro and Berriasian to Hauterivian (Rosenkrantz 1986) tuffaceous and terrigenous deposits (Belyi & Akinin 1985; Ishiwatari *et al.* 1998). The mélange contains harzburgite and dunite blocks of various sizes showing different degrees of serpentinization, and sheeted dykes, metabasalt, and radiolarite. The gabbro sheet forms a gentle synform and, in the south, is underlain by a slice of harzburgite slice. The sheeted dyke complex is

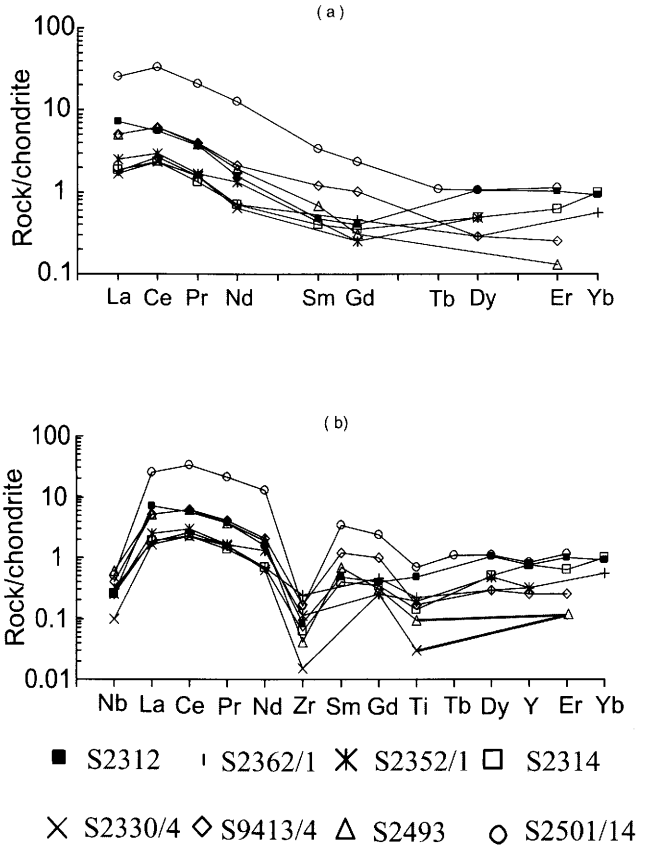

Fig. 11. Chondrite-normalized (Anders & Grevesse 1989) concentrations of REE (**a**) and other trace elements (**b**) in peridotites from Cape Povorotny. Analytical data have been given by Bazylev *et al.* (2001).

composed of a differentiated series from basalt to dacite.

The age of the ophiolite is uncertain, but microfossils from radiolarites encountered in the Northern mélange zone range from Mid- to Late Jurassic (Belyi & Akinin 1985).

Relevant mineralogical data were recently published and discussed by Ishiwatari *et al.* (1998), Palandzhyan & Dmitrenko (1999) and Saito *et al.* (1999). This review draws generally on these papers, as well as on our own mineralogical and chemical data, partly presented below.

Petrography and geochemistry of mafic and ultramafic rocks

The rock suite of the Yelistrarov Peninsula ophiolite assemblage includes both residual and cumulate peridotites, cumulate plagioclase lherzolite, pyroxenite and gabbronorite, gabbroic screens between the diabase dykes, and discrete blocks of foliated metabasalt.

Mantle peridotites are dominated by spinel harzburgites with subordinate pyroxene-bearing dunites. Overall, their serpentinization degree ranges from 85 to 100%. Primary, low-Ti spinels in the residual peridotites are moderately to highly chromian with Cr numbers ranging from 0.41 to 0.66 (Table 3). Those in dunites have Cr numbers up to 0.75. Saito *et al.* (1999) reported an even wider range of spinel Cr number in the peridotites (0.29–0.72). The oxidation degree ($Fe^{3+}/(Cr + Al + Fe^{3+})$) of spinels in harzburgite ranges from 0.021 to 0.044, and in dunites it is up to 0.087 (Table 3). Olivines in these peridotites are high-magnesian with Mg numbers in the range of 90.6–91.9 and have elevated nickel contents as compared with other ultramafic lithologies (0.36–0.40 wt% NiO) (Table 4). Residual peridotites exhibit a negative correlation between spinel Cr number and olivine Mg number, such that rocks

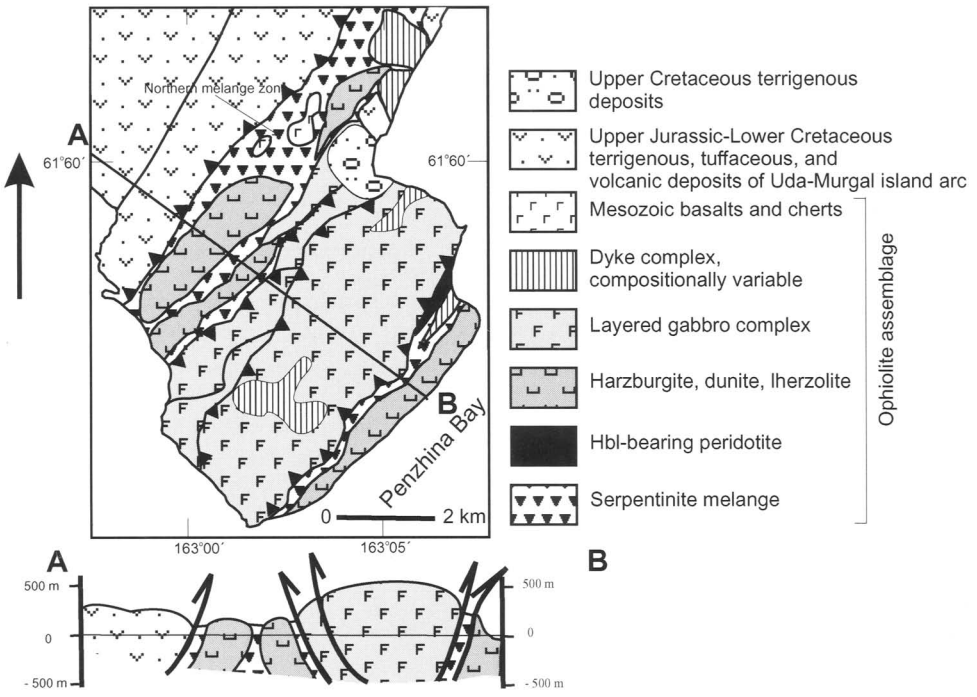

Fig. 12. Map showing schematic geological structure of the Yelistratov Peninsula.

Table 3. *Representative spinel compositions from the peridotites of the Yelistratov Peninsula ophiolite complex*

Sample:	C2518/1	C2529/4	C2524/1	C2524/3	C2524/2	C2526	C2520/5	C2524/4	C2518/7
Rock:	Hz	Hz	Hz	Hz	D	O	OC	PW	PL
Points:	3	5	3	4	3	5	3	3	8
SiO_2	0.05	0.21	0.09	0.07	0.08	0.08	0.17	0.17	0.11
TiO_2	0.07	0.02	0.07	0.08	0.10	0.48	0.34	0.97	0.72
Al_2O_3	34.03	26.97	22.63	17.85	11.67	16.43	17.53	18.34	15.00
FeO	14.14	17.65	18.54	19.86	24.37	31.33	39.16	44.31	49.94
MnO	0.14	0.21	0.18	0.22	0.30	0.32	0.44	0.37	0.38
MgO	16.64	13.54	12.74	12.22	10.36	8.44	6.57	6.26	5.48
Cr_2O_3	34.71	41.57	45.60	50.76	53.05	42.55	34.13	29.07	27.40
NiO	0.22	0.14	0.09	0.10	0.07	0.17	0.11	0.26	0.17
V_2O_3	0.21	0.20	0.35	0.19	0.20	0.28	0.35	0.61	0.65
ZnO	0.12	0.22	0.10	0.09	0.11	0.28	0.37	0.07	0.18
Total	100.32	100.72	100.39	101.43	100.32	100.35	99.17	100.43	100.03
Cr no.	0.406	0.508	0.575	0.656	0.753	0.635	0.566	0.515	0.551
Mg no.	0.716	0.607	0.585	0.569	0.507	0.408	0.324	0.298	0.269
Fe no.	0.028	0.026	0.031	0.044	0.087	0.130	0.205	0.253	0.332

Rock types: Hz, spinel harzburgite; D, dunite; O, orthopyroxenite; OC, olivine clinopyroxenite; PW, plagioclase websterite; PL, plagioclase lherzolite. All Fe is in the form FeO. Cr number = $Cr/(Cr + Al)$; Mg number = $Mg/(Mg + Fe^{2+})$; Fe number = $Fe^{3+}/(Cr + Al + Fe^{3+})$, where Fe^{3+} is calculated from stoichiometry.

Table 4. *Representative olivine composition from the peridotites of the Yelistratov Peninsula ophiolite complex*

Rock:	Hz	Hz	Hz	Hz	O	OC	PW	PL
Sample:	C2518/1	C2529/4	C2524/1	C2524/3	C2526	C2520/5	C2524/4	C2518/7
Points:	4	5	5	4	5	4	4	4
SiO_2	40.80	41.87	41.02	41.46	40.20	40.11	39.81	39.73
FeO	7.92	8.40	9.14	8.88	12.62	13.54	16.13	16.79
MnO	0.12	0.13	0.13	0.15	0.19	0.18	0.24	0.26
MgO	50.63	50.25	49.63	50.20	47.85	46.41	44.81	44.34
CaO	0.05	0.04	0.04	0.05	0.05	0.05	0.06	0.05
NiO	0.38	0.39	0.38	0.37	0.28	0.14	0.24	0.18
Total	99.89	101.08	100.34	101.10	101.18	100.44	101.29	101.34
Mg no.	91.9	91.4	90.6	91.0	87.1	85.9	83.2	82.5

Rock types: Hz, spinel harzburgite; O, orthopyroxenite; OC, olivine clinopyroxenite; PW, plagioclase websterite; PL, plagioclase lherzolite. All Fe is in the form FeO. Mg number = 100Mg/(Mg + Fe)

with the least chromian spinels contain the most magnesian (91.4–91.9) olivines.

The cumulate rock suite includes Ol-bearing and Ol-free gabbronorite and hornblende gabbronorite (Saito *et al.* 1999), as well as wehrlite, olivine orthopyroxenite, clinopyroxenite, olivine websterite, and plagioclase-bearing pyroxenite and lherzolite. A few isolated bodies of hornblende-bearing plagioclase peridotite are also present. The degree of serpentinization in ultramafic rocks of the cumulate sequence ranges from 15 to 50%, being significantly higher only in olivine-rich lithologies.

The cumulate peridotites are distinctly less magnesian than the residual peridotites and have olivines with Mg numbers of 79.4–87.1 and reduced NiO contents of 0.14–0.28 wt% (Table 4). Primary spinel is present in most of the cumulate peridotites, except for some plagioclase lherzolites with the least magnesian silicates. The spinel has moderate titanium contents (0.34–0.97 wt% TiO_2), moderate Cr numbers (0.45–0.65), and high oxidation indices (0.130–0.330) (Table 3). Clinopyroxenes from the cumulate peridotites are relatively low in aluminium (1.8–2.9 wt% Al_2O_3) and titanium (0.10–0.24 wt% TiO_2) but show somewhat elevated sodium contents (0.16–0.27 wt% Na_2O) as compared with mantle peridotites, whose clinopyroxenes have 0.05–0.23 wt% Na_2O. In the cumulate peridotites, plagioclase is An_{92-93} anorthite.

Compositions of spinel harzburgites and orthopyroxene dunites from the northern and southern outcrops are similar and have U-shaped REE patterns with chondrite-normalized contents of Ce 0.13–1.8, Tb 0.03–0.41, and Yb 0.06–0.57 (Table 5, Fig. 13). Such patterns for peridotites (as well as for clinopyroxenes from these rocks) are widely accepted as being typical of SSZ magmatism (Parkinson & Pearce 1998; Batanova & Sobolev 2000; Bizimis *et al.* 2000).

Mafic screens between dykes consist of amphibole gabbro, Cpx-bearing amphibole gabbro, and amphibole gabbronorite. Mafic rocks of the sheeted dyke complex include both aphyric and porphyritic diabases, commonly with an aphanitic groundmass. These rocks consist of variable proportions of mostly albitized plagioclase, amphibole, clinopyroxene, orthopyroxene, and sporadic olivine.

Small blocks of foliated metabasalts occur in the Northern zone mélange (Fig. 12). They typically lack primary minerals and consist of carbonate, actinolite, chlorite, epidote, and albite.

The most mafic rocks of the sheeted dyke complex are strongly depleted and fractionated low-K tholeiites with island-arc signatures, such as characteristic REE patterns, high field strength element (HFSE) depletion, and relatively elevated contents of large ion lithophile elements (LILE), including La (Fig. 14, Table 6). Metabasalts from the Northern mélange zone and lavas from a breccia of Berriasian to Valanginian age have similar chemical signatures (Fig. 14, Table 6). The sheeted dyke complex contains some rocks (Table 4) closely resembling high-Ca boninites.

Origin of mafic and ultramafic rocks

A number of mineralogical and chemical indicators can be used to elucidate the geodynamic setting of peridotites. The ranges of Cr number in residual spinels from the Yelistratov peridotites are typical of SSZ settings rather than mid-ocean ridges, whose typical ranges are 0.2–0.6 (Arai 1994). High iron oxidation degrees in cumulate spinels coupled with the moderate titanium contents indicate an island-arc setting for magmatism (Arai 1992). The decrease of olivine Mg number with increasing Cr number in spinel (Tables 3 and 4) suggests extensive melt–rock interaction during a magmatic process and is inconsistent with a

Table 5. *Rare earth element contents of peridotites of the Yelistratov Peninsula*

Sample:	M-97-26/1	M-97-26/2	M-97-26/3	M-97-38/1	M-97-38/2	M-97-38/3	C-2518/1	C-2524/1	C-2524/3	C-2520/4	C-2518/6	C-2518/7	C-2520/6
Rock:	Harz	Dun	Dun	Harz	Harz	Harz	Harz	Harz	Harz	Dun	Pl-Lherz	Pl-Lherz	Ol-Web
La	0.26	0.055	0.55	0.21	0.47	0.2	0.039	0.035	b.d.l.	b.d.l.	0.048	0.293	b.d.l.
Ce	0.36	0.078	1.1	0.16	0.92	0.26	0.074	0.111	0.221	0.225	0.255	0.519	0.16
Pr	n.a.	n.a.	n.a.	n.a.	n.a.	n.a.	b.d.l.	b.d.l.	0.038	0.023	0.049	0.089	0.029
Nd	n.a.	n.a.	n.a.	n.a.	n.a.	n.a.	0.07	0.055	0.196	b.d.l.	0.382	0.623	0.112
Sm	0.048	0.009	0.007	0.006	0.006	0.013	b.d.l.	b.d.l.	b.d.l.	b.d.l.	0.157	0.183	0.13
Eu	0.027	0.009	0.005	0.002	0.006	0.004	0.011	b.d.l.	b.d.l.	b.d.l.	0.085	0.103	0.038
Gd	n.a.	n.a.	n.a.	n.a.	n.a.	n.a.	0.054	b.d.l.	0.024	0.03	0.312	b.d.l.	0.158
Tb	0.007	0.003	0.001	0.004	0.003	0.003	b.d.l.	b.d.l.	b.d.l.	b.d.l.	b.d.l.	b.d.l.	0.036
Dy	n.a.	n.a.	n.a.	n.a.	n.a.	n.a.	b.d.l.	0.016	0.028	0.049	0.362	0.53	0.36
Er	n.a.	n.a.	n.a.	n.a.	n.a.	n.a.	0.036	0.018	0.014	0.046	0.179	0.325	0.184
Yb	0.092	0.021	0.01	0.018	0.019	0.055	0.055	0.032	b.d.l.	0.07	0.129	0.258	0.233
Lu	0.018	0.005	0.002	0.0043	0.0053	0.013	b.d.l.	b.d.l.	b.d.l.	b.d.l.	0.029	0.045	0.032

n.a., not analysed; n.d., not determined; b.d.l., below detection limit; Harz, harzburgite; Dun, dunite; Pl-Lherz, plagioclase-bearing lherzolite; Ol-Web, olivine websterite. Rare earth element contents were determined by ICP-MS.

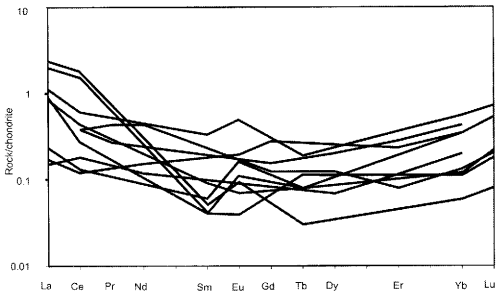

Fig. 13. Chondrite-normalized REE patterns for peridotites, Yelistratov ophiolite. U-shaped patterns for residual peridotites suggest suprasubduction-zone setting for magmatism.

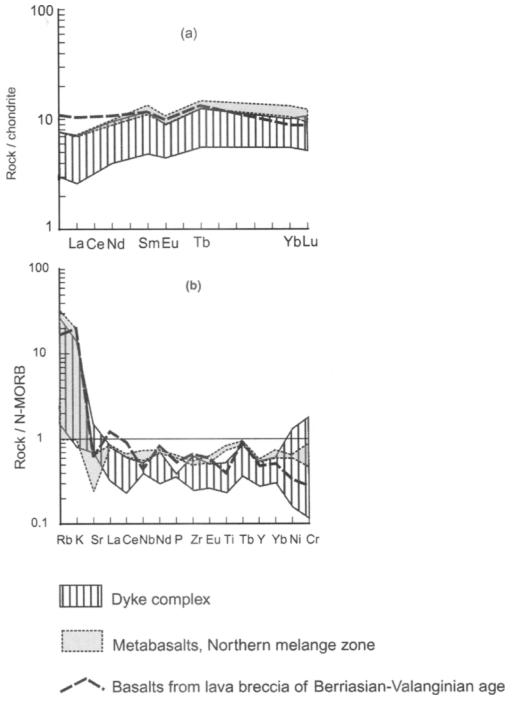

Fig. 14. Chondrite-normalized (Sun & McDonough 1989) (**a**) and N-MORB-normalized (Saunders & Tarney 1984) (**b**) patterns for basic rocks of dyke and lava complexes from the Yelistratov Peninsula.

simple partial melting of mantle (Jaques & Green 1980). The olivine–spinel compositional relationships of this type were described from mantle peridotites of SSZ origin (Bazylev *et al.* 1993, 2001; Sobolev & Batanova 1995), but they do not appear in the mid-ocean ridge mantle peridotites (Dick & Bullen 1984; Arai 1994).

Table 6. *Major (wt%) and trace element (ppm) contents in dykes and lavas of the Yelistratov Peninsula ophiolite*

Sample:	M-97-37/3	C-2505/2	C-2505/6	C-2533/3	C-2533/7	C-2516/4	C-2527/3	M-97-23/1
SiO_2	51.35	55.38	51.33	45.71	54.2	53.03	48.39	41.24
TiO_2	0.43	0.72	0.46	0.33	0.37	0.55	1.12	1.01
Al_2O_3	13.22	15.2	14.22	13.78	13.45	16.15	13.49	10.82
Fe_2O_3	3.41	5.42	4.86	4.99	3.73	3.94	6.14	4.55
FeO	6.48	4.22	5.03	8.77	4.87	4.26	5.72	8.31
MnO	0.16	0.07	0.27	0.09	0.08	0.16	0.52	0.2
MgO	10.09	5.33	10.9	14.25	8.42	9.81	10.09	7.91
CaO	9.01	6.28	4.84	4.26	7.16	2.2	5.59	20.79
Na_2O	3.17	4.95	2.61	1.88	2.91	3.78	2.75	0.2
K_2O	0.18	0.08	1.42	0.25	0.91	2.06	2.01	0.01
P_2O_5	0.05	0.05	0.05	0.05	0.05	0.07	0.08	0.08
LOI	1.76	2.1	3.88	5.57	3.82	3.65	3.98	4.24
Total	99.31	99.8	99.87	99.93	99.97	99.66	99.88	99.36
Cr	513	33.3	52.1	359	65.1	81.3	259	135
Co	–	22.2	29.8	69.5	34.3	30.5	51.9	–
Ni	–	21.6	46.3	181	40.7	45.8	86.7	–
V	248	383	274	265	298	201	282	281
Sc	–	38.5	37.9	42	38.2	26	47.3	–
Nb	1.3	1	1	1	1	1.1	1.8	1.4
Rb	1.52	2.6	27	2.4	7.6	17	33	1
Sr	123.7	200	150	95	200	82	87	32
Zr	26.3	55	29	22	33	58	47	44
Y	15.08	19	12	9.8	13	17	19	19
La	1.3	2.5	2	1	1.5	3.6	2.5	2.5
Ce	2.3	6.2	4.6	2.6	4.3	9.1	6.3	6.2
Nd	2.5	5.6	3.7	2.4	3.9	6.5	5.4	5.8
Sm	0.96	2.1	1.2	0.87	1.4	2.1	2	2.4
Eu	0.36	0.61	0.43	0.31	0.47	0.7	0.63	0.74
Tb	0.3	0.58	0.38	0.26	0.48	0.64	0.6	0.68
Yb	1.5	2	1.3	1.1	1.7	1.8	2.1	2.6
Lu	0.24	0.36	0.19	0.18	0.26	0.3	0.32	0.41

1–6, rocks of dyke complex; basalt from volcanic breccias K1b-v; 8 and 9, metabasalts from Northern mélange zone. Major elements were determined by wet chemistry, trace elements by XRF, and REE by INAA.

The subdivision of Yelistratov residual peridotites by Ishiwatari *et al.* (1998) and Saito *et al.* (1999) into the Northern ultramafic body (with more depleted peridotites showing spinel Cr number (0.39–0.72) of presumable SSZ origin) and the Southern ultramafic body (with less depleted peridotites showing spinel Cr number (0.29–0.49) of presumable mid-ocean ridge origin) is highly questionable in view of the following. The residual spinel Cr number of 0.49 is out of the ranges typical for slow-spreading mid-ocean ridges (Dick 1989), and the spinel Cr number of 0.29 is out of ranges typical both for fast-spreading mid-ocean ridges and for geochemically anomalous segments of slow-spreading ridges (Dick & Natland 1996; Bazylev & Silantyev 2000). Therefore, the ranges of residual spinel Cr number of 0.29–0.49 are not consistent with any particular mid-ocean ridge setting. Additionally, the large difference between the minimum and maximum values of the residual spinel Cr number found within a body implies a large difference in the mantle partial melting degrees (e.g. Jaques & Green 1980) between neighbouring parts of this body. Such a difference cannot be achieved by a decompression mechanism of mantle melting below a mid-oceanic ridge (Langmuir *et al.* 1992), but invokes another mantle melting mechanism and another geodynamic setting for the magmatic process.

The reported trace element data for the residual peridotites are consistent more with the conclusion of Palandzhyan & Dmitrenko (1999) that all the harzburgites of the Yelistratov complex, as well as the ultramafic–mafic cumulate rocks, are of SSZ origin. It can also be concluded that the volcanic rocks and sheeted dykes were generated in an ensimatic island arc.

Ophiolites of the Ganychalan terrane

Geological setting

The Ganychalan terrane is situated within the Penzhina segment of the Uda–Murgal island arc (Fig. 15).

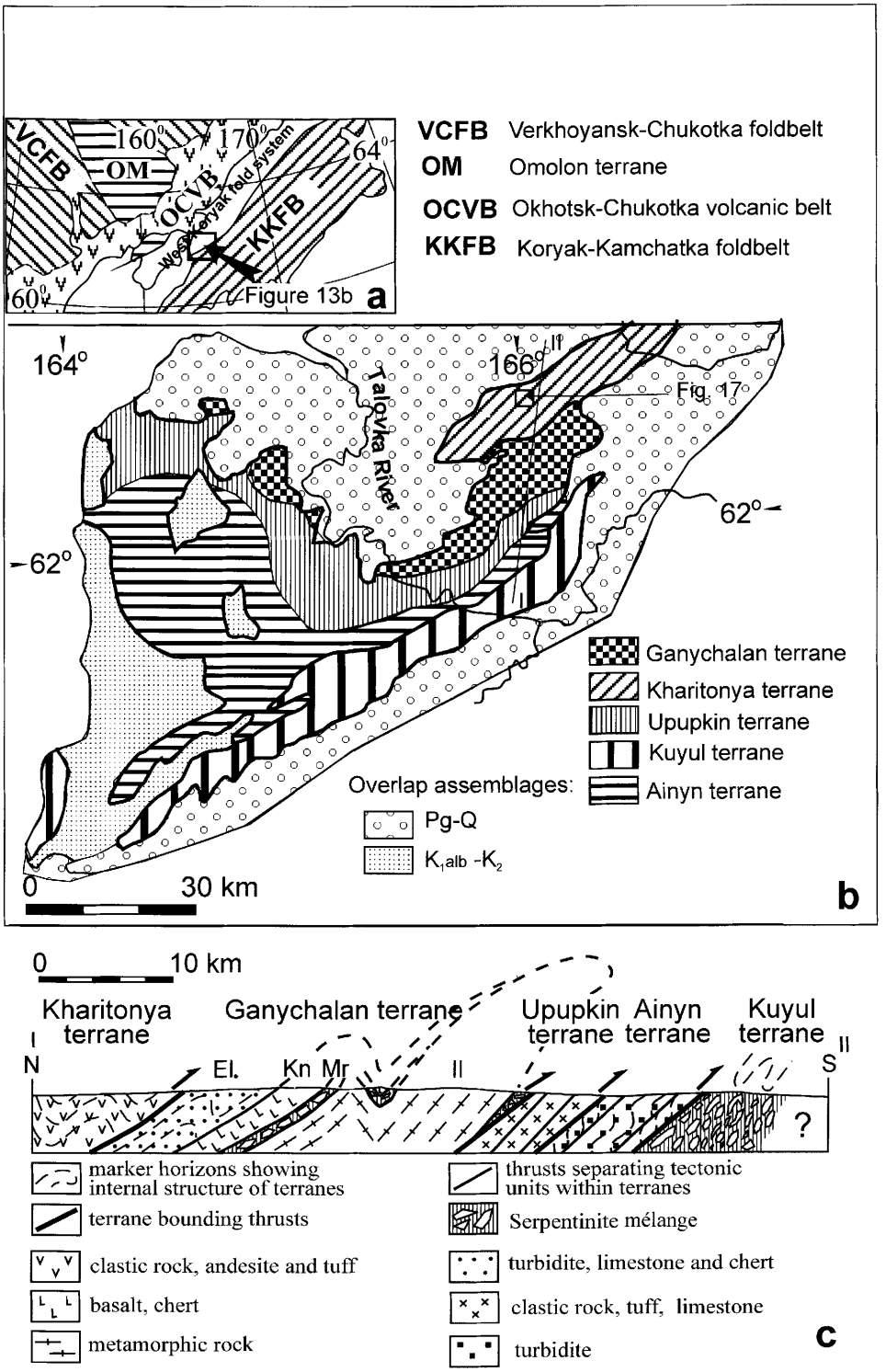

Fig. 15. Geological map of the Penzhina segment (after Sokolov *et al.* 1996).

On the NW, it is separated from the Kharitonya terrane by a high-angle normal fault boundary. The Kharitonya terrane is a fragment of the Koni–Taigonos volcanic arc and consists of an Early Carboniferous terrigenous assemblage intercalated with intermediate volcanic rocks in its lower part and with carbonaceous shales and coal beds in the upper (Khanchuk *et al.* 1992; Sokolov 1992). On the SE, the Ganychalan terrane rests techtonically over the Upupkin thrust pile along a thrust plane dipping from 30° to 80°.

The internal structure of the Ganychalan terrane is a large closed or tight antiform of complicated shape with a thick normal NW limb and tectonically reduced overturned SE limb (Fig. 15c). The Ganychalan terrane consists, from bottom upward, of four tectonic slices: Ilpenei, Mrachnaya, Khinantynup, and Elgeminai (Fig. 16) (Khudoley & Sokolov 1998; Ganelin & Peyve 2001). The Ilpenei slice is composed of basalt, tuff, shale, chert, limestone, and quartzite, all affected by metamorphism of greenschist and glaucophane schist facies (Dobretsov 1974; Silantyev *et al.* 1994; Vinogradov *et al.* 1995). Metabasalts in this slice are MORB- and ocean island basalt (OIB)-like (Khanchuk *et al.* 1992; Silantyev *et al.* 1994). The cherts yielded deformed unidentifiable radiolarians, but sporadic finds of poorly preserved conodonts suggest a Palaeozoic age (V. A. Aristov, pers. comm.). The radiometric age of greenschist metamorphism is 327 ± 5 Ma (whole-rock Rb/Sr determination,Vinogradov *et al.* 1995). The metamorphic rocks are viewed as a subduction complex associated with the Koni–Taigonos island arc.

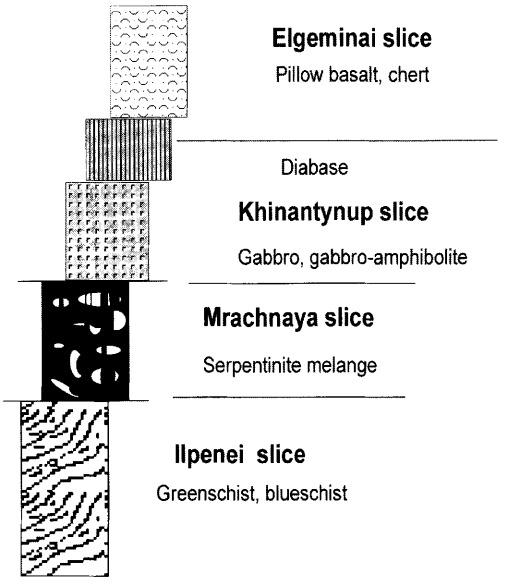

Fig. 16. Tectonostratigraphic units of the Ganychalan terrane.

The Mrachnaya, Khinantynup, and Elgeminai slices (Figs 16 and 17) exhibit ultramafic–mafic

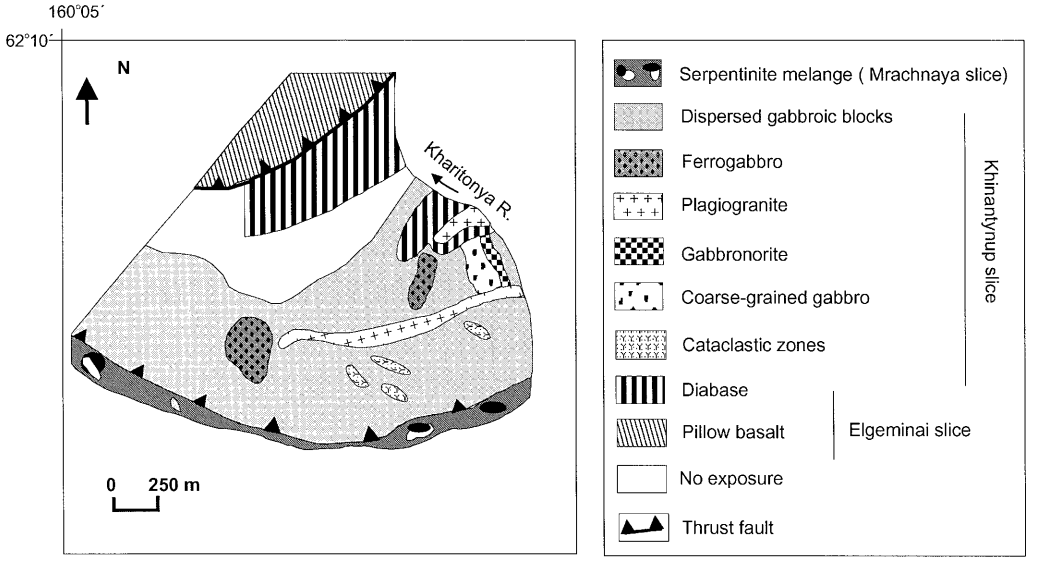

Fig. 17. Geological map of the central Ganychalan terrane (by V. G. Batanova & A. V. Ganelin).

magmatic assemblages that comprise a dismembered ophiolite suite of Early Palaeozoic age, constrained by radiometric and palaeontological data (Markov *et al.* 1982; Khanchuk *et al.* 1992; Ganelin & Peyve 2001; Nekrasov *et al.* 2001).

The Mrachnaya slice is composed of a serpentinite mélange consisting of chaotically oriented blocks of ultramafic and gabbroic rocks. The most widespread lithologies are plagioclase wehrlite, pyroxenite, troctolite, and olivine gabbro associated with minor olivine-free normal gabbro and plagiogranite. Dunite and harzburgite are extremely rare and are totally serpentinized.

The Khinantynup slice is a plutonic assemblage dominated by mafic lithologies, including leucocratic medium-grained layered gabbro, coarse-grained isotropic gabbro, gabbronorite, and ferrogabbro. Felsic rocks include a gneissosed tonalite–plagiogranite body, 50–70 m thick, which is concordant with textures in gabbroic host rocks, and small concordant (0.1–0.5 m) lenses and veins of quartz diorite, tonalite, and plagiogranite. The base of the gabbroic section contains layers of zoisite-bearing amphibolite and quartz–garnet–amphibole schists (Markov *et al.* 1982). A hornblende Ar/Ar age of the gabbroic rocks is Early Ordovician (559 Ma; Khanchuk *et al.* 1992). Toward the top of the slice, gabbro gives way to gabbro–diabase and diabase, which are chilled against the host gabbro. Gabbro–diabases are crosscut by a 20–30 m thick tonalite–plagiogranite body. Felsic rocks contain abundant gabbro–diabase xenoliths. Irregular zones of pegmatitic gabbro are found along the contact of gabbro–diabases and tonalite–plagiogranite body. This disrupted dyke system can be viewed as a deformed sheeted dyke complex that occurs along the tectonic contact with volcanic and sedimentary rocks of the Elgeminai slice. These rocks include albitized basalts, spilites, amygdaloid pillowed basalts, and subordinate intercalations of chert and siliceous tuff. These are interpreted as the upper portion of the ophiolite assemblage, overlain by terrigenous and carbonate strata. Basalts yield whole-rock K–Ar ages of 490–480 Ma (Dobretsov 1974). Cherts contain conodonts of Arenig to Llanvirn age (485–464 Ma).

Petrography and geochemistry of the plutonic and volcanic rocks

In serpentinized peridotites, the only surviving primary mineral is chrome-spinel. The rocks have high Mg number of 88.6–90.2, but are rather low in Cr (850–1600 ppm) and Ni (900–1300 ppm). Their high Cr number of 65.6–87.4 and relatively high-Mg spinels (Mg number 36.4–57.4) suggest that they are ultramafic cumulates (Nekrasov *et al.* 2001).

Plagioclase wehrlite, troctolite, and olivine gabbro of the Mrachnaya slice are fragments of a cumulate complex. They show variable proportions of mafic minerals and plagioclase with ensuing broad variations in major element oxides, especially CaO, Al_2O_3, and MgO (Table 7). This group is the lowest in TiO_2, Zr, Y, and REE among Ganychalan ophiolite plutonic rocks. The rocks have REE (La + Sm + Yb) in the range 0.14–0.87 ppm and sawtooth REE patterns (Fig. 18), some of which show positive Eu anomalies. They contain high-Mg, high-Cr clinopyroxenes (Mg number 87.3–88.4; 0.53–1.15 wt% Cr_2O_3), which are low in TiO_2 and REE (Table 8).

Petrographically and geochemically, the gabbroic rocks of the Khinantynup slice fall into several varieties. Leucocratic gabbro is high in Al_2O_3 (22.7–24.8 wt%) and low in TiO_2 and other

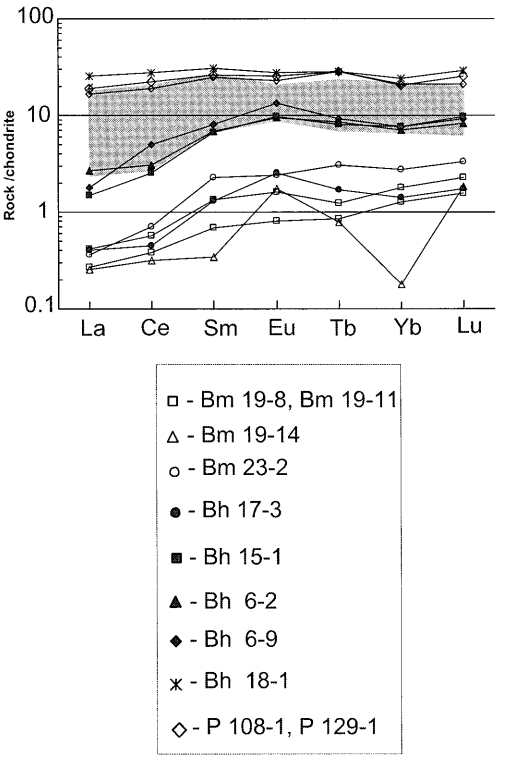

Fig. 18. Chondrite-normalized (Sun & McDonough 1989) REE patterns of mafic plutonic rocks from the Ganychalan terrane. Grey field indicates gabbro from Ocean Drilling Program Site (ODP) 894, Hess Deep (Pedersen *et al.* 1996).

Table 7. *Major (wt%) and trace (ppm) element contents of magmatic rocks of the Ganychalan terrane*

Sample:	1 Bm 19-8	2 Bm 19-11	3 Bm 19-14	4 Bm 23-2	5 Bm 17-3	6 Bh 3-3	7 Bh 15-1	8 Bh 6-2	9 Bh 6-9	10 Bh 7-1	11 Bh 18-1	12 P 108-1	13 P 129-1	14 mh- 65/2	15 mh- 65/1	16 mh- 67/1	17 mh- 71/12	18 mh- 71/5	19 mh- 72/1	20 mh- 66/6	21 mh- 72/12	22 mh- 66/4	23 mh- 72/13
SiO_2	36.33	36.25	40.15	43.9	44.29	45.67	47.12	46.33	42.43	48.1	47.82	51.97	49.67	62.82	68.32	71.47	72.16	73.09	72.32	68.30	71.02	74.56	75.41
TiO_2	0.48	0.4	0.28	0.48	0.28	0.71	0.68	0.61	4.58	1.35	1.95	1.03	1.23	0.94	0.79	0.61	0.47	0.62	0.51	0.76	0.56	0.31	0.30
Al_2O_3	5.64	4.88	21.32	11.54	22.76	16.8	17.58	17.18	17.36	15.92	17.63	19.38	16.78	13.59	15.05	12.92	12.75	12.29	11.71	15.47	14.04	12.30	12.24
Fe_2O_3	5.77	8.25	2	1.19	2.29	1.99	2.33	3.08	5.72	5.78	4.46	1.89	2.7	2.75	0.81	1.73	1.52	1.54	2.79	0.79	2.06	1.77	1.70
FeO	5.37	3.45	3.29	4.74	1.2	3.52	4.89	3.34	7.84	4.82	4.84	5.05	6.36	2.26	2.87	2.20	2.39	2.12	2.51	2.30	2.30	1.66	1.78
MnO	0.17	0.17	0.06	0.09	0.07	0.12	0.11	0.11	0.17	0.12	0.22	0.14	0.21	0.05	0.10	0.07	0.03	0.07	0.04	0.07	0.07	0.02	0.04
MgO	31.16	31.15	12.66	19.43	7.1	9.9	8.26	4.09	5.23	9.55	7.62	5.92	8.11	0.97	1.05	0.32	0.46	0.89	0.16	0.50	0.05	0.08	0.14
CaO	3.95	3.2	12.86	13.74	17.83	15.73	13.65	17.24	10.87	8.91	10.63	9.16	9.83	7.07	3.31	3.24	2.67	2.62	3.48	3.30	2.58	1.68	1.56
Na_2O	0.41	0.09	1.51	0.98	1.28	1.92	2.42	2.7	3.77	4.86	4.32	4.49	4.23	6.03	5.43	5.19	6.15	4.66	4.55	6.40	6.09	6.45	6.21
K_2O	0.07	0.01	0.04	0.24	0.22	0.16	0.09	0.68	0.45	0.47	0.36	0.85	0.7	0.42	0.40	0.37	0.12	0.51	0.49	0.34	0.42	0.28	0.32
P_2O_5	0.01	0.02	0.01	0.02	–	0.01	0.01	–	0.02	0.13	0.14	0.11	0.18	0.07	0.08	0.04	0.03	0.00	0.00	0.05	0.01	0.00	0.00
LOI	10.3	11.66	5.27	2.9	1.79	3.21	2.9	3.1	2.3	1.2	1.35	1.92	1.32	2.00	2.22	1.99	1.15	1.92	1.63	2.15	0.90	0.90	0.66
Total	99.66	99.53	99.45	99.25	99.11	99.74	100.04	98.46	100.74	101.21	101.34	101.91	101.32	100.19	100.43	100.15	99.91	100.37	100.08	100.43	100.25	100.26	100.45
Rb	–	–	–	–	–	–	–	–	–	–	–	–	–	–	<10	<10	–	<10	–	<10	–	–	–
Ba	–	–	–	–	–	–	–	–	–	–	–	–	–	–	73	62	–	51	–	43	–	–	–
Nb	–	–	–	–	–	–	–	–	–	–	–	–	–	–	<10	<10	–	<10	–	<10	–	–	–
Sr	18	10	170	77	160	–	230	180	–	165	84	190	140	–	170	100	–	130	–	110	–	–	–
Zr	10	10	10	10	10	–	10	27	10	94	98	140	82	–	57	54	–	51	–	210	–	–	–
Y	11	10	11	10	10	–	14	12	14	26	24	51	37	–	8	12	–	<10	–	40	–	–	–
La	0.09	0.06	0.06	0.08	0.09	–	0.42	0.34	0.61	5.9	4.54	4.33	3.87	–	3.70	4.50	–	3.30	3.70	24.00	31.00	29.00	–
Ce	0.34	0.23	0.19	0.43	0.27	–	2.95	1.55	1.84	16.57	11.36	13.41	11.5	–	7.80	8.40	–	6.80	7.30	52.00	63.00	60.00	–
Nd	–	–	–	–	–	–	–	–	–	–	–	–	–	–	4.80	4.80	–	0.00	3.80	0.00	32.00	28.00	–
Sm	0.20	0.1	0.05	0.34	0.2	–	1.22	1	1.02	4.66	2.89	3.92	3.76	–	1.30	1.00	–	0.92	0.75	4.30	5.30	5.00	–
Eu	0.10	0.05	0.11	0.15	0.15	–	0.81	0.59	0.57	1.66	1.01	1.55	1.36	–	0.53	0.54	–	0.53	0.51	1.40	1.40	0.86	–
Tb	0.05	0.03	0.03	0.12	0.07	–	0.37	0.32	0.34	1.14	0.68	1.13	1.15	–	0.21	0.18	–	0.13	0.09	0.77	0.83	0.71	–
Yb	0.29	0.2	0.03	0.45	0.23	–	1.22	1.24	1.13	3.83	2.27	3.3	3.35	–	0.93	0.69	–	0.47	0.68	4.20	4.60	3.70	–
Lu	0.05	0.03	0.04	0.07	0.03	–	0.18	0.2	0.16	0.59	0.36	0.52	0.42	–	0.16	0.13	–	0.07	0.12	0.70	0.79	0.63	–

1 and 2, plagioclase wehrlite; 3, troctolite; 4, olivine gabbro; 5, leucogabbro; 6 and 7, coarse-grained gabbro; 8, gabbro–norite; 9, ferrogabbro; 10 and 11, diabase; 12 and 13, basalts; 14–19, tonalites, plagiogranites of the Khinantynup slice; 20–23, plagiogranites of the Elgeminay slice. Major elements determined by wet chemistry, trace elements by XRF, and REE by INAA.

Table 8. *Major (wt%) and trace (ppm) element contents of clinopyroxenes from plutonic ophiolitic rocks of the Ganychalan terrane*

Sample:	1 Bm 19-8	2 Bm 19-11	3 Bm 19-14	4 Bm 23-2	5 Bm 17-3	6 Bh 3-3	7 Bh 15-1	8 Bh 6-2	9 Bh 6-9
n:	2	4	3	6	2	2	2	2	4
SiO_2	51.42	51.56	52.34	52.44	52.98	52.05	52.12	51.77	48
TiO_2	0.49	0.37	0.38	0.39	0.25	0.84	0.68	0.66	2.02
Al_2O_3	3.65	3.16	2.86	3.01	2.21	2.97	2.25	3.55	6.77
Cr_2O_3	1.15	0.97	0.53	0.81	0.09	0.49	0.03	0.08	0.02
FeO	3.91	4.21	3.97	3.83	5.31	4.94	8.62	8.86	10.27
MnO	0.13	0.11	0.11	0.11	0.17	0.14	0.21	0.25	0.26
MgO	15.77	16.36	16.25	16.39	16.24	15.69	14.56	15.41	14.34
CaO	22.8	22.75	22.71	22.89	23.6	21.12	20.71	19.36	17.24
Na_2O	0.49	0.36	0.29	0.42	0.25	0.43	0.32	0.38	1.48
Total	99.8	99.85	99.46	100.26	101.07	98.64	99.45	100.23	100.36
MAG	87.79	87.35	87.91	88.4	84.5	84.99	75.06	75.61	71.5
n	1	2		2	2	1	3	1	1
Ti	3699	2015	–	2505	1381	2911	5054	6420	4332
Sr	1.73	0.92	–	1.06	0.72	1.06	1.22	1.39	2.11
Zr	21.12	4.82	–	6.88	2.89	11.42	24.2	21.35	48.6
La	0.33	0.21	–	0.31	0.39	0.4	0.56	1.46	1.34
Ce	1.74	0.81	–	1.3	0.88	1.55	2.93	2.28	5.6
Nd	3.31	1.38	–	1.6	0.93	2.58	5.41	4.73	8.79
Sm	1.74	0.73	–	0.95	0.45	1.26	2.96	2.48	3.84
Eu	0.48	0.35	–	0.32	0.24	0.39	0.87	0.9	1.65
Dy	3.99	1.98	–	2.04	1.35	2.63	6.3	5.79	8.05
Er	2.65	1.38	–	1.38	0.93	1.73	4.38	3.41	4.68
Y	14.81	6.98	–	7.16	5	9.06	23.08	19.23	24.14
Yb	2.49	1.15	–	1.02	0.74	1.36	3.56	2.94	3.91

Trace elements were determined by secondary ion mass spectrometry. MAG is the molecular ratio 100Mg/(Mg + Fe). Mineral compositions were analysed by electronic microprobe. *n*, number of spots analysed.

incompatible elements (La + Sm + Yb of 0.52 ppm). These features suggest comagmatic origin of the cumulates (olivine-bearing gabbroids and wehrlites) and leucogabbros, a conclusion that is further supported by the clinopyroxene composition, the Mg number being as high as 84.5, and the low incompatible element abundances (Table 7).

The coarse-grained gabbros, gabbronorites, and ferrogabbros, despite their petrographic diversity, make up a chemically uniform group (Table 7). They have low Mg number of 68–41.7 and elevated TiO_2, up to 4.5 wt%, as a result of a considerable proportion of titanomagnetite. The average REE (La + Sm + Yb) content in rocks within this group is *c.* 2.7 ppm, which is the highest value of all the plutonic complexes. These samples are LREE depleted (La/Yb = 0.3–0.5). Clinopyroxenes from coarse-grained gabbros and gabbronorites display moderate and uniform Mg number (75.6) and TiO_2 contents (0.6 wt%), and are low in Cr_2O_3 (0.03–0.08 wt%) and high in REE (Table 8). Clinopyroxenes from ferrogabbroic samples have the lowest Mg number of 71.5 and Cr_2O_3 content of 0.02 wt%, whereas their incompatible element concentrations are the highest.

Diabases and basalts are chemically uniform and constitute a moderately differentiated rock series. Alkalinity is somewhat elevated owing mainly to spilitization-induced high Na_2O content (Na_2O + K_2O of 3.15–5.62 wt%). Although the $FeO^*/(FeO^* + MgO)$ ratio shows meaningless variations, from 0.94 to 1.70, MgO content ranges from 5.73 to 9.13 wt%; TiO_2 from 1.00 to 1.89 wt%, and Al_2O_3 from 15.2 to 18.7 wt%. The REE total (La + Sm + Yb) ranges from 9.4 to 13.9 ppm. REE patterns are flat and slightly LREE enriched (La/Yb = 1.16–2.00). These characteristics are similar to N-MORB and similar to T-MORB (Fig. 18).

Tonalites in the Khinantynup slice have gneissic textures with relics of subhedral granular texture. Plagioclase crystals are partly bent and have undulatory extinction. Quartz forms lens-shaped grains with undulatory extinction or aggregates of small grains with sutured boundaries. Primary

mafic minerals, green hornblende and brown biotite, occur as relics in aggregates of secondary chlorite, sericite, and fine scaly green biotite. Plagiogranites also have gneissic texture, a lower amount of mafic minerals (1–2%), and as much as 30–40% quartz. Accessory minerals are zircon, sphene, and apatite.

Tonalites and plagiogranites from the Elgeminai slice contain quartz–albite granophyric intergrowths. They are composed of quartz, plagioclase, amphibole, biotite, zircon, apatite, magnetite, and epidote. In plagiogranites, quartz accounts for 30–45%, and minor K-feldspar (<1%) is present.

Plagiogranites from both slices fall dominantly in the trondhjemite field on the Ab–An–Or diagram (O'Connor 1969) (Fig. 19). They are low in Al_2O_3 (11.71–15.47 wt%), K_2O (0.12–0.51 wt%), and Rb and Nb (<10 ppm) (Table 7).

Chondrite-normalized REE patterns for tonalites and plagiogranites from the two slices differ considerably (Fig. 20, Table 5). Those from the Khinantynup slice have low REE totals, a slightly fractionated REE distribution (La_n/Yb_n = 2.66–4.7; La_n/Sm_n = 1.25–1.41), and positive Eu anomalies (Eu_n/Eu^* = 0.98–1.29) (Fig. 20). REE patterns from the Elgeminai tonalites and plagiogranites show higher REE totals, are partly more fractionated (La_n/Yb_n = 3.2–5.4; La_n/Sm_n = 1.21–1.29), and have negative Eu anomalies (Eu_n/Eu^* = 0.27–0.48).

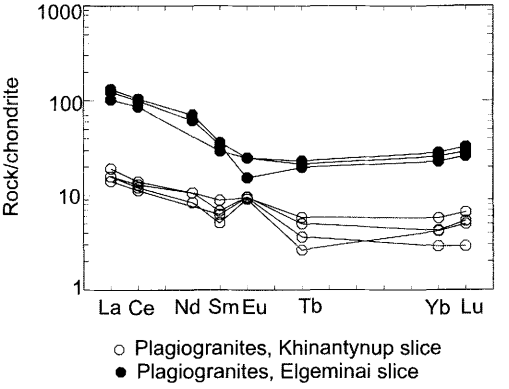

Fig. 20. Chondrite-normalized (Sun & McDonough 1989) REE patterns for plagiogranites and tonalites from the Khynantinup and Elgeminai slices, Ganychalan terrane ophiolites (data from Table 5).

Origin of gabbroic and volcanic rocks and plagiogranites of the Ganychalan terrane

The above compositional data suggest that the entire spectrum of ultramafic–mafic plutonic ophiolitic rocks from the Ganychalan terrane were produced by crystal fractionation of a basaltic melt. This is evidenced by (1) TiO_2, Zr, Y, and REE increasing consistently from olivine-bearing cumulates to ferrogabbros, while Mg number generally decreasing; (2) parallelism of the REE patterns. The overall degree of REE enrichment of the gabbros matches that of MOR gabbros (Fig. 18).

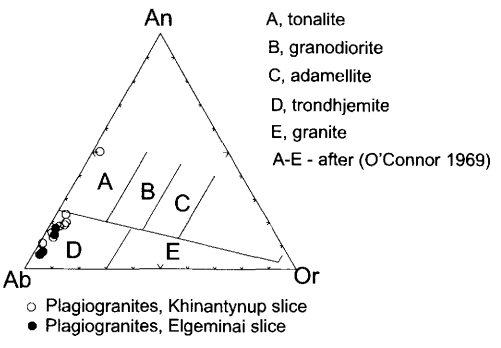

Fig. 19. Ab–An–Or diagram (O'Connor 1969) for plagiogranites and tonalites from the Khynantinup and Elgeminai slices, Ganychalan terrane ophiolites.

To decide if the Mrachnaya and Khinantynup plutonic rocks are complementary to the Elgiminay basalts, Ganelin & Peyve (2001) calculated compositions of hypothetical parental melts in equilibrium with clinopyroxenes from the plutonic rocks. Using melt–clinopyroxene partition coefficients from Hart & Dunn (1993), they showed that hypothetical parental melt compositions underwent varying degrees of fractionation (Fig. 21a and b). REE abundances from melts in equilibrium with clinopyroxenes from the Mrachnaya olivine-bearing rocks and the Khinantynup noncumulate gabbros display a moderate degree of fractionation consistent with the upper limit of the N-MORB compositional range or with a somewhat enriched type, similar to T-MORB (Fig. 21a). This type matches closely the diabases and pillow basalts from the Elgeminai slice.

The hypothetical melts in equilibrium with clinopyroxenes from coarse-grained gabbros, gabbronorites, and ferrogabbros from the upper part of the Khinantynup slice are very strongly fractionated, their REE enrichment being fivefold for clinopyroxenes from coarse-grained gabbro and gabbronorite and tenfold for clinopyroxene from ferrogabbro (Fig. 21b). Parental melt compositions similar to the calculated melts have been proposed by various workers for the upper gabbroic complexes of a variety of ophiolites and modern ocean

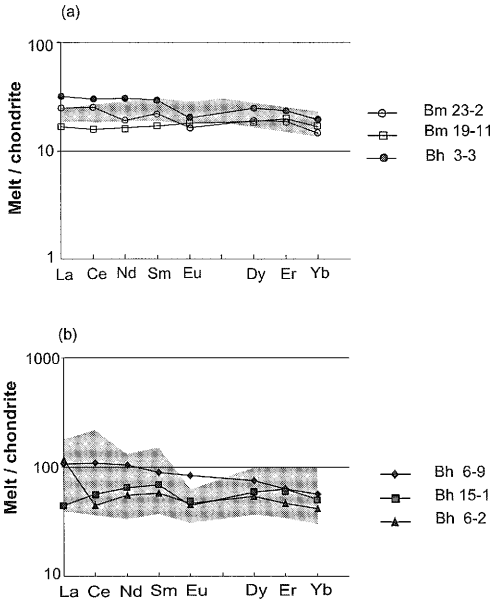

Fig. 21. Chondrite-normalized (Sun & McDonough 1989) REE patterns for hypothetical melts parental to clinopyroxenes from plutonic rocks of the Ganychalan terrane (rock names are given in Table 6). In (**a**), grey field indicates diabases and pillow basalts from the Elgeminai slices; in (**b**), grey field indicates melts in equilibrium with clinopyroxenes from the upper gabbro from ODP Site 894, Hess Deep (Gillis 1996).

crust assemblages (Pallister & Hopson 1981; Dick & Natland 1996; Kelemen *et al.* 1997; Tiepolo *et al.* 1997). All these workers attributed the considerable REE enrichment of liquids parental to high-level plutonic rocks to a strong, 40–50%, fractionation of primary N- and/or T-MORB-like melts of mantle derivation. Therefore, our data suggest that Ganychalan ophiolites are a geodynamically coherent assemblage generated in a MOR setting.

Based on the presence of high-Ti hornblende, Khanchuk *et al.* (1992) proposed that the Ganychalan terrane ophiolite originated in an oceanic island setting. Nekrasov *et al.* (2001) used Ti, Zr, and Y variations to discriminate several plutonic series in the Ganychalan terrane. According to Nekrasov *et al.* (2001), these series may have resulted from stepwise melting of an enriched mantle source, suggestive of an oceanic plateau setting for ophiolite petrogenesis. This is not inconsistent with the above data from the ophiolitic reference section; however, identifying individual geochemical series would require a large number of samples from various portions of the Ganychalan terrane to be analysed.

No petrogenetic model for the Khinantynup and Elgeminai tonalites and plagiogranites has been developed yet. The difference in REE totals and the character of chondrite-normalized REE patterns imply different origins for tonalites and plagiogranites of the two slices (Table 7, Fig. 20). Low REE contents in the tonalites and plagiogranites from the Khinantynup slice render them similar to their host coarse-grained gabbros and ferrogabbros (Figs 18 and 20), suggesting that these rocks might be fractionates of gabbroic magma, but positive Eu-anomaly in plagiogranites is at odds with this process. Unfortunately, we have no isotopic data on gabbros or plagiogranites to prove or disprove their kinship. Another possible explanation of different LREE enrichment degrees and REE totals of the Elgeminai and Khynantynup tonalites and plagiogranites is their origin from different mafic sources as a result of partial melting or different degrees of such melting.

Ophiolites of the Kuyul terrane

Geological setting

The Kuyul thrust pile (Sokolov 1992) brings together three terranes, the Upupkin, Ainyn, and Kuyul terranes, that are thrust over each other successively from NW to SE (Fig. 15). The Upupkin terrane is composed of Devonian shallow-water organic limestone, Upper Carboniferous to Lower Permian clastic rocks, and Permian and Triassic tuffaceous epiclastic deposits. The Upper Jurassic to Lower Cretaceous strata comprise turbidites deposited in the forearc of the Uda–Murgal arc (Sokolov *et al.* 1999). In places, these turbidites contain equant bodies of serpentinized ultramafic material enclosed in sedimentary serpentinites. According to Sokolov *et al.* (2000), these rocks strongly resemble the Mariana arc serpentinite diapirs (Fryer 1992; Lagabrielle *et al.* 1992).

The Ainyn terrane is composed of Upper Jurassic to Lower Cretaceous turbidites. The terrane is highly deformed and displays a broken formation, sedimentary mélange composed of terrigenous material (type I and type IV mélanges of Cowan (1985)) and numerous duplexes (Khudoley & Sokolov 1998). The depositional environment is interpreted as the landward slope of an accretionary prism (Khudoley & Sokolov 1998; Sokolov *et al.* 1999).

The Kuyul terrane is traceable for 140 km northeastward from the Mametchinsky Peninsula to the eastern side of the Talovka River in discrete outcrops 10–20 km wide. To the SE, the terrane is overlapped by Paleogene–Quaternary sedimentary rocks (Fig. 15b). The ophiolite is disrupted into a serpentinite mélange containing blocks of ultramafic, gabbroic, and metamorphic (greenschists, blueschists and amphibolites) rocks, as well as

basalts, cherts, limestones, and terrigenous rocks. Detailed mapping has identified a number of mélange slices distinguished by clast lithologies (Sokolov *et al.* 1996). The characteristic lithologies and geodynamic interpretations of tectonostratigraphic assemblages are listed in Table 9.

The most complete ophiolite fragment is the Gankuvayam sequence (Khanchuk *et al.* 1990), or slice (Sokolov *et al.* 1996). The Gankuvayam ophiolite is a dismembered suite, truncated at several levels by serpentinite mélange zones and folded into a synform fold. Khanchuk *et al.* (1990) have reconstructed the following ophiolite sequence (Fig. 22): (1) serpentinized harzburgite overlain by dunite, 470 m thick; (2) a gabbro–troctolite–wehrlite complex, 340 m thick; (3) plagiogranite, 40 m thick; (4) a dyke complex, compositionally differentiated from basaltic to dacitic, 400 m thick; (5) a pillow lava sequence ranging from basalt to dacite, 300 m thick.

The age of ophiolite is estimated on the basis of Bathonian to Early Tithonian radiolarians in cherts from interpillow spaces within basalts of the differentiated series (Grigoriev *et al.* 1995).

The Gankuvayam ophiolite has been interpreted to have originated from a variety of geodynamic settings, such as: (1) a Galapagos-type spreading centre (Khanchuk *et al.* 1990); (2) an intraoceanic island arc (Palandzhyan 1992); (3) a suprasubduction-zone setting (Sokolov *et al.* 1996). Resolving this issue called for follow-up studies on Gankuvayam ultramafic rocks from various localities in the Kuyul terrane, including the Mamet Peninsula. Results from this sampling exercise are presented below.

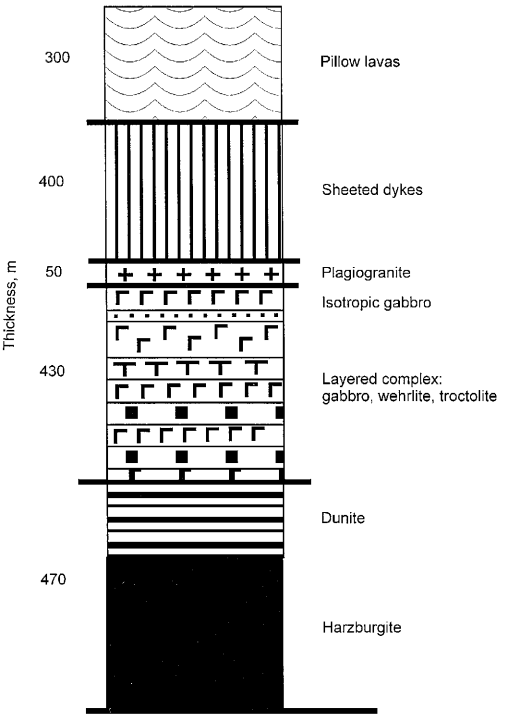

Fig. 22. Ophiolite stratigraphy from the Gankuvayam section.

Petrography and geochemistry of the ultramafic rocks

The ultramafic rocks are represented by tectonized residual peridotites and cumulative ultramafic rocks of the dunite–orthopyroxenite series. Overall, the massive ultramafic rocks are composed of serpentinized spinel peridotites (harzburgites and diopside harzburgites). Less frequently, dunites form lenses and bands in peridotites, clino- and orthopyroxenites, wehrlites, and websterites. The modal mineral composition of the ultramafic rocks and chemical composition of the main rock-forming minerals are shown in Figure 23.

Most of the ultramafic rocks are significantly altered. Their serpentinization degree is 60–

Table 9. *Tectonostratigraphic units of the Kuyul terrane*

Tectonic sheet	Rocks	Age	Geodynamic setting
Gankuvayam	Peridotite, cumulate complex, gabbro, plagiogranite, sheeted dykes, basalt–andesite–dacite complex	J_2–J_3^1	Suprasubduction zone
Veselaya	Basalt–limestone–chert, peridotite, cumulate, gabbro	P, Tr–J_2, J_3^1	Oceanic
Vstrechny	Basalt-chert	Tr_2–J_3^1	Oceanic
Unnavayam	Peridotite, cumulate complex, gabbro	Mz?	Oceanic
Talovka	Peridotite, basalt	?	Within-plate
Tylpyntyhlavaam	Sandstone, siltstone, mudstone, chert, olistostrome	J_3–K_1	Trench sediment
Udachny	Amphibolite, greenschist, blueschist	134, 122, 82 Ma (K/Ar method)	Subduction zone

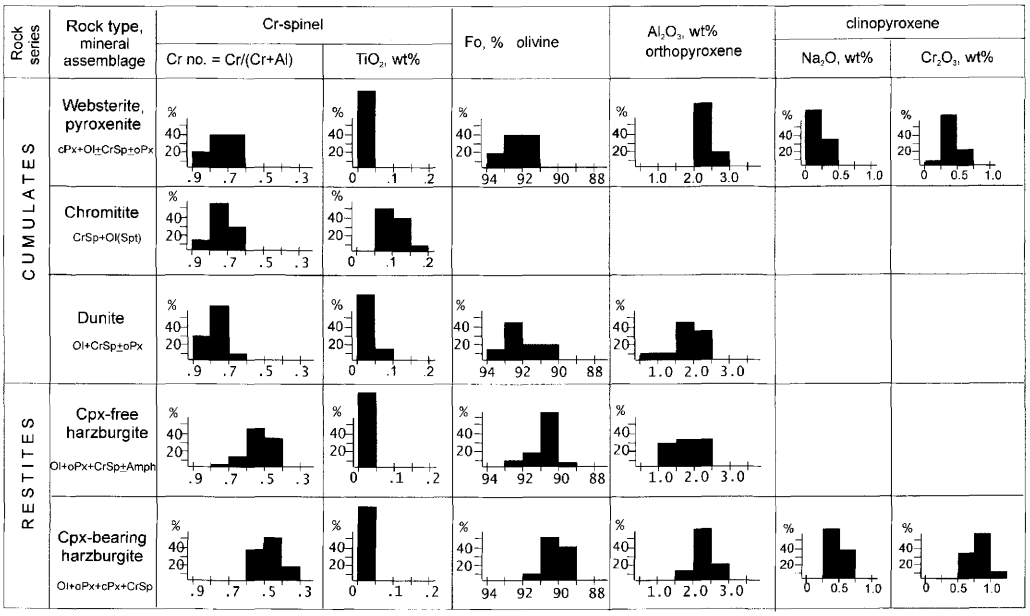

Fig. 23. Mineral composition features of ultramafic rocks from the Kuyul ophiolite terrane. Amph, amphibole; Cpx, clinopyroxene; Cr-Sp, chrome spinel; Ol, olivine; Opx, orthopyroxene; Spt, serpentine.

100%. Our study is therefore focused on Cr-spinel, whose chemistry best portrays the petrogenesis of the ultramafic rocks (e.g. Irvine 1967; Dick & Bullen 1984; Arai 1994), as it is resistant to serpentinization.

Representative analyses of Cr-spinels from various ultramafic rocks from the Gankuvayam sequence are shown in Table 10. The Cr number, used as a measure of depletion in ultramafic rocks, is highly variable and largely overlaps the range typical of Cr-spinel compositions from oceanic and island-arc peridotites (Fig. 24). The Cr number of Cr-spinel correlates negatively with the Mg number, which is typical of residual mantle peridotites (Dick & Bullen 1984; Barnes & Roeder 2001). Cr-spinel compositions from the harzburgites indicate strong depletion and suggest a residual origin for these rocks (Dick & Bullen 1984; Ishii *et al.* 1992; Arai 1994) (Fig. 24).

There are no systematic differences in Cr number between Cr-spinels from the dunites, orthopyroxenites, and chromitites. This invokes tight genetic links among these rocks, which could all be members of a dunite–orthopyroxenite–chromitite suite (e.g. Arai 1994). High Fe oxidation degrees in spinels from dunites and chromitites further support this conclusion.

Major element contents of the harzburgites vary in a narrow range (Table 9) and correspond to non-isochemically recrystallized residual mantle-derived peridotites (Bazylev *et al.* 1999). This is further supported by a good correlation (Fig. 24) between Cr_2O_3 and Al_2O_3 of the host ultramafic rocks and their accessory Cr-spinels. The harzburgites are appreciably depleted in Al_2O_3 and alkalis; remarkably, Al_2O_3 and Cr_2O_3 contents, immobile under metamorphic conditions, are closely similar to one another, which is typical of residual SSZ-type peridotites (e.g. Bazylev *et al.* 1993, 1999; Rampone *et al.* 1995; Parkinson & Pearce 1998; Pearce *et al.* 2000; Takazawa *et al.* 2000). The harzburgites are slightly enriched in TiO_2 as compared with typical restite peridotites (Barnes & Roeder 2001).

Trace element contents of the ultramafic rocks are given in Table 11 and Figure 25. Cu, Zn, Sc, V and Ga show a negative correlation with MgO, and Ni, Cr, and Co a positive correlation with MgO. A similar relationship exists for most mantle-derived peridotites, in agreement with models for partial melting of initial fertile ultramafic rocks (e.g. Niu 1997).

Peridotites of the Gankuvayam sequence are very strongly REE depleted (Fig. 25), harzburgites having no more than 0.2–0.5 times chondritic values (Fig. 25, Table 11). Chondrite-normalized REE patterns for the dominant ultramafic rocks, Di-free harzburgites, have asymmetric U-shaped forms ($(La/Sm)_N = 2.76 \pm 0.54$; $(Sm/Yb)_N = 1.15 \pm 0.19$) (Fig. 25). Similar REE patterns and

Table 10. *Representative microprobe analyses of Cr-spinels in ultramafic rocks from the Gankuvayam sequence*

Rock:	Di-free harzburgites					Di-bearing harzburgites			Dunites						Chromitites			Websterite		
Sample:	546			504		552			553			583			536			584		
	c	tz	r	c	r	c	tz	r	c	tz	r	c	tz	r	c	tz	r	c	tz	r
TiO_2	0.03	0.05	0.00	0.05	0.00	0.03	0.05	0.04	0.07	0.08	0.06	0.03	0.07	0.04	0.24	0.21	0.22	0.08	0.07	0.05
Al_2O_3	12.53	11.14	11.99	16.69	16.37	30.71	31.02	31.37	12.76	12.82	12.93	11.38	11.39	11.11	15.04	15.06	15.31	7.74	7.80	7.55
FeO	18.70	13.17	16.20	15.29	15.02	14.60	13.99	14.10	19.29	18.75	18.71	15.76	16.23	17.03	11.71	11.76	11.73	18.06	18.76	17.97
Fe_2O_3	1.34	0.67	2.33	1.02	1.35	1.04	0.78	0.55	0.98	0.56	0.19	1.28	0.59	0.02	3.27	2.91	3.17	1.29	0.78	1.25
MnO	0.33	0.24	0.33	0.24	0.27	0.24	0.18	0.19	0.36	0.37	0.33	0.30	0.33	0.31	0.22	0.22	0.25	0.36	0.35	0.35
MgO	9.90	13.26	11.45	12.55	12.44	14.29	14.54	14.63	9.48	9.72	9.75	11.65	11.41	10.79	14.73	14.72	14.7	10.16	9.70	10.17
NiO	0.05	0.15	0.00	0.00	0.01	0.12	0.12	0.11	0.03	0.02	0.00	0.04	0.08	0.05	0.13	0.16	0.15	0.09	0.00	0.05
ZnO	0.11	0.06	0.10	0.15	0.02	0.09	0.15	0.14	0.23	0.14	0.15	0.11	0.13	0.15	0.02	0.07	0.04	0.01	0.07	0.07
Cr_2O_3	57.50	60.93	58.04	54.20	53.55	38.41	37.64	37.94	57.10	57.20	57.35	59.62	60.25	60.62	54.33	54.84	54.11	64.23	64.41	64.50
Total	100.49	99.67	100.44	100.19	99.03	99.53	98.47	99.07	100.30	99.66	99.47	100.17	100.48	100.12	99.69	99.95	99.68	102.02	101.94	101.96
Cations recalculated per 32 oxygens																				
Ti	0.007	0.010	0.000	0.009	0.000	0.005	0.008	0.007	0.014	0.015	0.012	0.007	0.013	0.009	0.045	0.040	0.041	0.016	0.013	0.011
Al	3.851	3.391	3.657	4.962	4.926	8.583	8.720	8.758	3.937	3.967	4.006	3.484	3.482	3.425	4.462	4.457	4.537	2.391	2.418	2.334
Fe^{2+}	4.078	2.843	3.506	3.228	3.207	2.896	2.790	2.793	4.222	4.118	4.112	3.422	3.520	3.725	2.464	2.471	2.466	3.960	4.126	3.945
Fe^{3+}	0.263	0.131	0.454	0.193	0.259	0.186	0.141	0.098	0.194	0.110	0.038	0.251	0.115	0.004	0.620	0.549	0.600	0.255	0.154	0.247
Mn	0.074	0.053	0.072	0.052	0.058	0.049	0.037	0.037	0.080	0.083	0.073	0.067	0.073	0.069	0.047	0.046	0.053	0.081	0.078	0.079
Mg	3.847	5.102	4.416	4.722	4.733	5.051	5.169	5.164	3.698	3.805	3.820	4.510	4.410	4.204	5.526	5.512	5.511	3.969	3.805	3.980
Ni	0.011	0.031	0.000	0.000	0.003	0.022	0.023	0.021	0.006	0.005	0.000	0.008	0.017	0.010	0.026	0.033	0.031	0.020	0.000	0.010
Zn	0.022	0.012	0.020	0.027	0.005	0.017	0.026	0.025	0.045	0.027	0.030	0.021	0.025	0.029	0.004	0.013	0.008	0.002	0.015	0.014
Cr	11.855	12.437	11.878	10.813	10.810	7.201	7.097	7.107	11.816	11.876	11.916	12.237	12.355	12.533	10.812	10.889	10.761	13.311	13.394	13.384
Cations	24.007	24.009	24.003	24.005	24.000	24.008	24.011	24.010	24.011	24.007	24.006	24.064	24.009	24.008	24.006	24.010	24.008	24.004	24.002	24.005
Cr no.	0.75	0.79	0.76	0.69	0.69	0.46	0.45	0.45	0.75	0.75	0.75	0.78	0.78	0.79	0.71	0.71	0.70	0.85	0.85	0.85
Mg no.	0.49	0.64	0.56	0.59	0.60	0.64	0.65	0.65	0.47	0.48	0.48	0.57	0.56	0.53	0.69	0.69	0.69	0.50	0.48	0.50
Fe^3 no.	0.02	0.01	0.03	0.01	0.02	0.01	0.01	0.01	0.01	0.01	0.00	0.02	0.01	0.00	0.04	0.03	0.04	0.02	0.01	0.02

Samples 548 and 583 are from the Mametchinsky Peninsula, the rest are from the Gankunvayam sequence. Fe_2O_3 and FeO calculated from spinel stoichiometry. c, grain cores; r, rims; tz, transitional zones. Cr number = $Cr/(Cr + Al)$, Mg number = $Mg/(Mg + Fe^{2+})$, Fe^3number = $Fe^{3+}/(Fe^{3+} + Cr + Al)$. Analysed on CAMEBAX microprobe in the Institute of Volcanology, Petropavlovsk-Kamchatsky (analyst V. M. Chubarov).

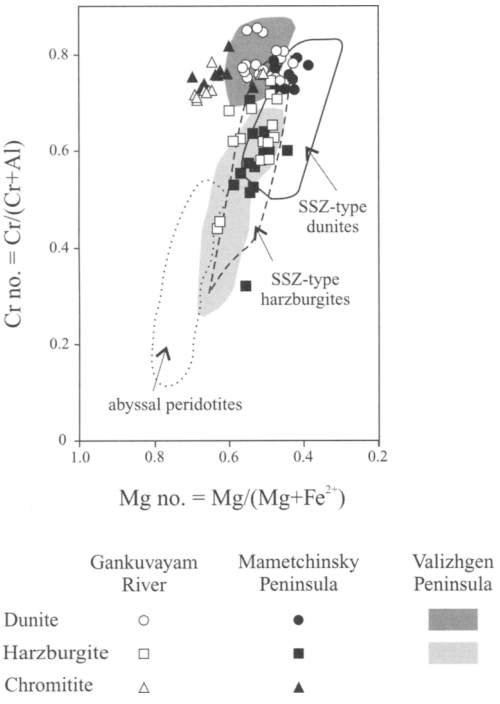

Fig. 24. Compositions of rock-forming and accessory Cr-spinels from ultramafic rocks of the Gankuvayam sequence. Fields of Cr-spinel compositions in abyssal peridotites (dotted line), SSZ-type harzburgites (dashed line), and SSZ-type dunites (continuous line) are shown. Compositional fields are after Dick & Bullen (1984) and Ishii *et al.* (1991).

extremely low REE contents are inherent in residual spinel peridotites of typical SSZ ophiolite complexes (e.g. Parkinson & Pearce 1998; Pearce *et al.* 2000).

Hence, the ultramafic compositions detailed above suggest an SSZ setting for their genesis. The initial ultramafic rocks underwent extensive partial melting and reaction with primitive island-arc melts, resulting in cumulate veins and chromite mineralization in the ultramafic rocks.

Petrography and geochemistry of the plagiogranites

Plagiogranites form a separate slice between the gabbroic rocks and sheeted dyke complex in the Gankuvayam thrust sheet (Fig. 22). Their lower contact with gabbro is sharp and faulted, whereas the upper part of the plagiogranite slice contains fragments of sheeted dykes. The plagiogranites are strongly tectonized and brecciated along both contacts.

The plagiogranites are divided into plagiogranites proper (65–75 wt% SiO_2) and quartz diorites and tonalites (62–65 wt% SiO_2). The latter are the least differentiated members, their volume being negligible.

The plagiogranites have subhedral granular to granophyric texture. They contain 30–40% modal quartz, 40–60% plagioclase, and 5–15% amphibole. Plagioclase, An_{25-35}, is euhedral (0.3–1.2 mm across), partly saussuritized, and often zoned. Quartz is anhedral. Amphibole forms green euhedral prisms. Accessory minerals include zircon, apatite, sphene, and magnetite. Secondary alteration minerals are epidote, chlorite, albite, and prehnite.

The tonalites and quartz diorites contain the same minerals but have lower percentages of quartz (20–25 modal %), higher percentages of plagioclase (55–70%) and amphibole (15–25%), and more calcic plagioclase.

On the Ab–An–Or diagram, the felsic rocks plot with tonalites and trondhjemites. Their low K_2O (0.1–0.8%) (Luchitskaya 1996) places them with oceanic plagiogranites (Coleman & Donato 1979). On Harker diagrams, plagiogranites, intermediate to felsic dykes, and gabbros from the upper part of gabbroic section form a coherent fractionation trend (Luchitskaya 1996).

Chondrite-normalized REE patterns of plagiogranites are slightly LREE enriched, with an almost horizontal HREE portion (La_n/Yb_n = 0.8–1.37) and a negative Eu anomaly (Eu_n/Eu^* = 0.45–0.90). The similarity of these rocks to those of the Samail ophiolite is evident (Fig. 26). The similarity of REE patterns for plagiogranites, dacites, andesites, and basalts from the sheeted dyke complex suggests that the rocks are cogenetic (Fig. 27).

On spidergrams of Pearce *et al.* (1984), the plagiogranites are slightly enriched in Rb and depleted in HFSE with respect to ORG (Luchitskaya 1996). Their ORG-normalized patterns are similar to those of ocean-ridge granites as given by Pearce *et al.* (1984) (Troodos plagiogranites) and volcanic-arc granites (granites of Lower Intrusive complex, Oman (Luchitskaya 1996)). On an Nb–Y diagram (Pearce *et al.* 1984), plagiogranites plot in the ORG field (Luchitskaya 1996).

Origin of the ophiolite

The harzburgites of the Gankuvayam unit are restites, and the lower gabbro–wehrlite complex represents basal cumulates formed in a magma chamber at the crust–mantle interface, with gabbronorites and plagiogranites forming coeval intrusions. The initial ultramafic rocks underwent extensive partial melting and reaction with primi-

Table 11. *Major (wt%) and trace (ppm) element contents of ultramafic rocks of the Gankuvayam sequence*

Sample:	571	504	546	581	515	583/1	548	552	547	583	553
SiO_2	36.96	37.64	36.56	37.50	38.44	36.72	38.14	36.08	31.20	32.56	31.98
TiO_2	0.04	0.06	0.03	0.04	0.04	0.04	0.06	0.05	0.02	0.01	0.01
Al_2O_3	1.12	1.92	1.03	1.42	2.24	0.81	1.72	2.34	1.03	1.23	1.12
Cr_2O_3	0.31	0.27	0.24	0.32	0.23	0.25	0.21	0.27	0.37	0.31	0.34
Fe_2O_3	4.11	3.11	3.95	3.77	3.99	3.86	3.28	5.84	4.82	4.11	6.33
FeO	3.75	4.45	3.05	3.43	1.22	3.13	4.08	3.41	3.59	2.70	0.91
MnO	0.12	0.11	0.10	0.11	0.12	0.11	0.11	0.11	0.11	0.10	0.11
MgO	39.59	37.82	38.22	37.50	37.09	37.74	36.85	36.06	41.37	41.13	41.29
CaO	0.90	1.01	0.83	0.90	0.96	0.71	1.35	1.23	0.45	0.56	0.41
Na_2O	0.05	0.09	0.04	0.06	0.04	0.04	0.06	0.10	0.05	0.07	0.03
K_2O	0.01	0.03	0.03	0.03	0.01	0.01	0.03	0.02	0.02	0.01	0.01
H_2O^-	0.83	0.70	0.91	1.47	1.45	1.61	1.06	1.20	1.26	1.81	1.06
LOI	11.56	12.05	13.96	12.55	13.40	14.07	12.55	14.20	15.26	14.67	15.61
Total	99.35	99.26	98.95	99.10	99.23	99.10	99.50	100.91	99.55	99.27	99.21
V	26.0	17.4	4.3	21.5	14.2		24.5	31.2	17.0	12.6	13.5
Cr	2104	1842	1632	2204	1586		1429	1867	2531	2118	2345
Ni	1445	1532	1985	1025	893		787	950	1565	1485	1782
Rb	0.25	0.84	0.35	0.61	0.68		0.25	0.32	0.14	0.41	0.39
Sr	25	29	74	51	26		84	95	24	18	16
Y	1.4	0.9	0.8	1.0	3.1		4.5	3.2	0.5	0.9	1.0
Zr	5.1	2.7	7.1	1.5	3.2		4.1	12.1	8.2	6.3	14.1
Nb	1.2	0.8	0.7	2.6	3.7		4.2	0.5	2.1	2.6	0.6
Ba	12.5	19.5	24.1	14.2	16.2		31.2	24.1	8.2	15.4	22.0
La	0.06	0.04	0.06	0.04	0.05		0.10	0.06	0.16	0.13	0.10
Ce	0.09	0.06	0.12	0.10	0.08		0.18	0.16	0.26	0.21	0.21
Pr	0.01	0.01	0.02	0.02	0.02		0.03	0.03	0.05	0.06	0.05
Nd	0.03	0.03	0.03	0.03	0.03		0.04	0.05	0.05	0.05	0.04
Sm	0.01	0.01	0.01	0.01	0.01		0.01	0.01	0.02	0.03	0.02
Eu	0.00	0.00	0.00	0.00	0.00		0.00	0.01	0.01	0.01	0.01
Gd	0.01	0.01	0.01	0.01	0.02		0.01	0.01	0.01	0.01	0.00
Tb	0.00	0.00	0.00	0.00	0.00		0.00	0.00	0.01	0.01	0.01
Dy	0.01	0.01	0.01	0.01	0.01		0.02	0.03	0.03	0.04	0.04
Ho	0.00	0.00	0.00	0.00	0.00		0.01	0.01	0.01	0.01	0.01
Er	0.01	0.01	0.01	0.01	0.01		0.01	0.01	0.02	0.02	0.02
Tm	0.00	0.00	0.00	0.00	0.00		0.00	0.00	0.01	0.01	0.01
Yb	0.01	0.01	0.01	0.01	0.01		0.01	0.01	0.02	0.21	0.17
Lu	0.00	0.00	0.00	0.00	0.00		0.00	0.00	0.01	0.01	0.01
Th	0.10	0.12	0.41	0.10	0.24		0.14	0.32	0.14	0.41	0.42

571–583/1, Di-free harzburgites; 548 and 552, Di-bearing harzburgites; 547–553, dunites. Major elements analysed by XRF in the Karpinsky Geological Institute, St. Petersburg; trace elements by ICP-MS in the Institute of Geochemistry, Irkutsk (G. A. Samdimirova, analyst).

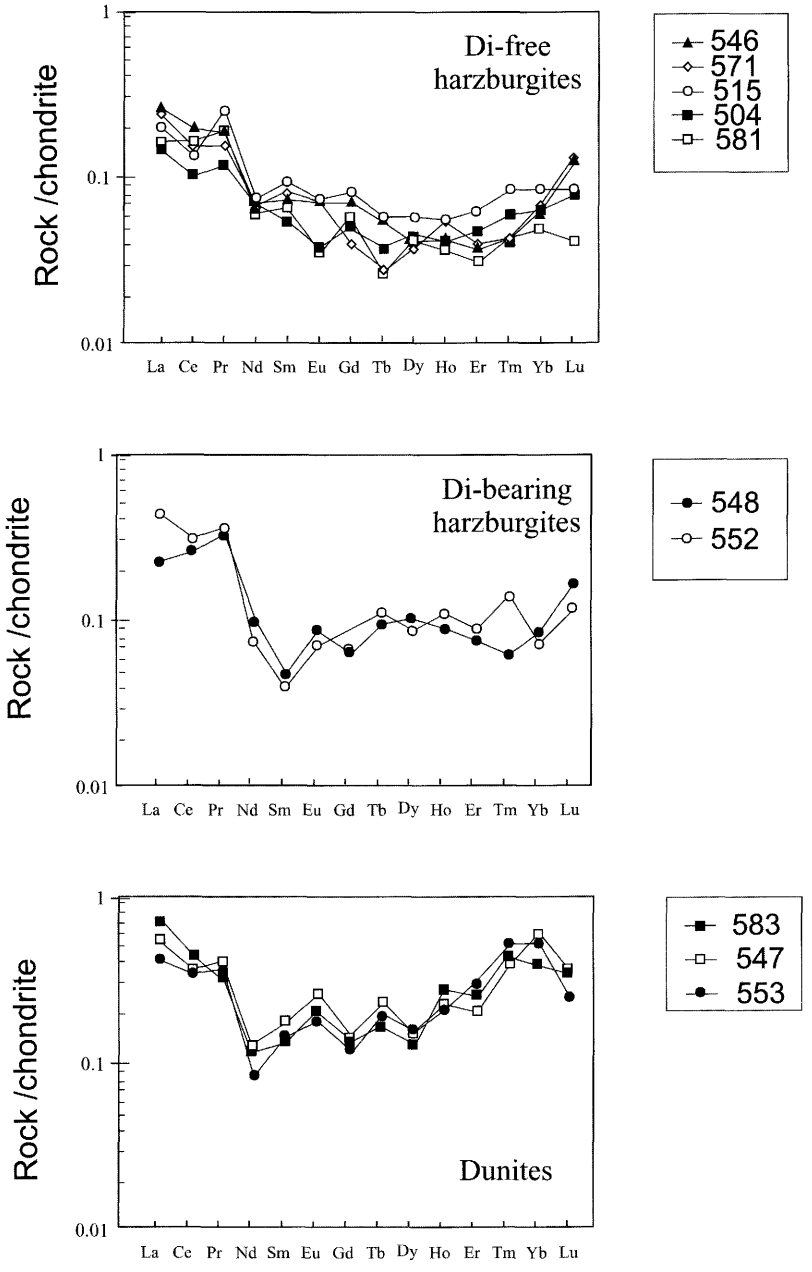

Fig. 25. Chondrite-normalized (Anders & Grevesse 1989) REE patterns for the Gankuvayam sequence ultramafic rocks.

tive island-arc melts, resulting in cumulate veins and chromite mineralization in the ultramafic rocks.

The plagiogranites may have formed by fractional crystallization of a basic magma combined with some filter-pressing (squeezing of remaining interstitial acid melt) mechanism. They are believed to have formed in the upper part of the ophiolite crustal section above a subduction zone (for details, see Luchitskaya (1996, 2001)).

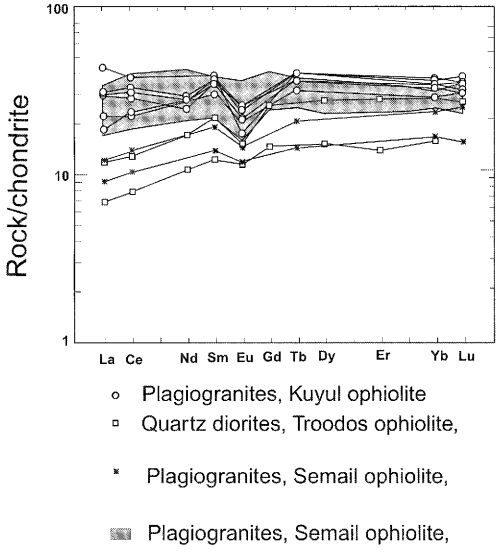

Fig. 26. Chondrite-normalized (Sun & McDonough 1989) REE patterns for plagiogranites from the Kuyul terrane, Troodos ophiolites (Kay & Senechal 1976) and Samail ophiolites (Pallister & Knight 1981; Coleman & Donato 1979).

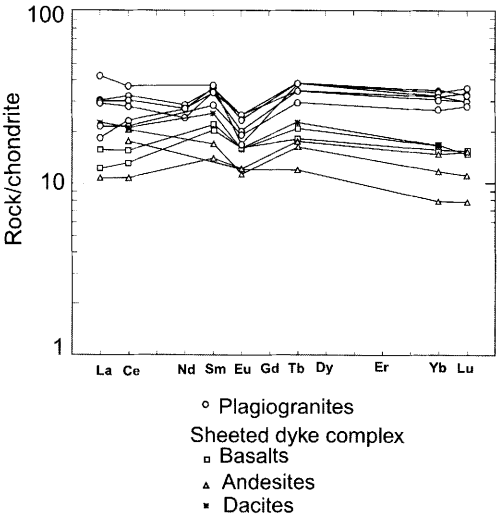

Fig. 27. Chondrite-normalized (Sun & McDonough 1989) REE patterns for plagiogranites, and basalts, andesites and dacites from the sheeted dyke complex from the Kuyul ophiolite terrane.

It thus follows that the additional studies in ultramafic compositions and geochemical data on the plagiogranites further corroborate the inference (Palandzhyan 1992; Sokolov *et al.* 1996) that the Gankuvayam ophiolite originated in an SSZ setting.

Study of volcanic (Gankuvayam type) and chert–volcanic (Kingiveyem type) assemblages indicates that the Kuyul terrane comprises tectonically juxtaposed assemblages of distinctive ages and origins (Grigoriev *et al.* 1995) (Table 9). Gankuvayam extrusive rocks and dykes are composed of calc-alkaline basalt to dacite (Grigoriev *et al.* 1995; Sokolov *et al.* 1996).

The Kingiveyem type of stratigraphy (Table 9, Veselaya and Vstrechny slices) includes chert–basalt–limestone and chert–basalt associations of Late Triassic to early Tithonian age. Chemically, the basalts are N-MORB-like (Khanchuk *et al.* 1990; Grigoriev *et al.* 1995). In addition, blocks of WPB, in association with limestones of Permian age (Grigoriev *et al.* 1995), occur in the serpentinite mélange.

N-MORB and WPB hosted in mélange and tectonic juxtaposition of geodynamically contrasting assemblages (Grigoriev *et al.* 1995; Sokolov *et al.* 1996) suggest that the Kuyul mélange may yet yield less depleted ultramafic rocks and gabbros of oceanic provenance.

Ophiolites of the Ust–Belaya segment

Tectonic setting

The Ust–Belaya terrane consists of a complex package of allochthonous units, thrust over the Middle Jurassic to Valanginian terrigenous, chert, and volcanic deposits of the Algan terrane (Palandzhyan & Dmitrenko 1996; Nekrasov *et al.* 2001) (Fig. 28a). The base of the overlap assemblage is composed of late Albian to early Senonian marine terrigenous deposits (Markov *et al.* 1982; Filatova 1988; Sokolov 1992), which represent sediment fill of a forearc basin in front of the Okhotsk–Chukotka continental-margin volcanic belt. Eocene to Oligocene strata comprise on-land volcanic deposits of the western Kamchatka–Koryak continental-margin volcanic belt, and its coeval terrigenous deposits.

The allochthonous package (Fig. 28b) is divided into three large nappes (Palandzhyan 2000). The Lower, or Utyosiki, thrust sheet incorporates slices of island-arc volcanic and clastic deposits of postulated Late Palaeozoic and Mesozoic age. Foliated serpentinites occur between some slices. The thrust unit has a total thickness of 1.6 km.

The Middle, Otrozhnaya, nappe consists of two thrust units. The lower unit consists of: (1) a Middle Palaeozoic ophiolite assemblage, comprising heavily deformed serpentinized harzburgites, lherzolites, and dunites overlain by a deformed slice *c.* 1 km thick of amphibolized gabbro; (2) a

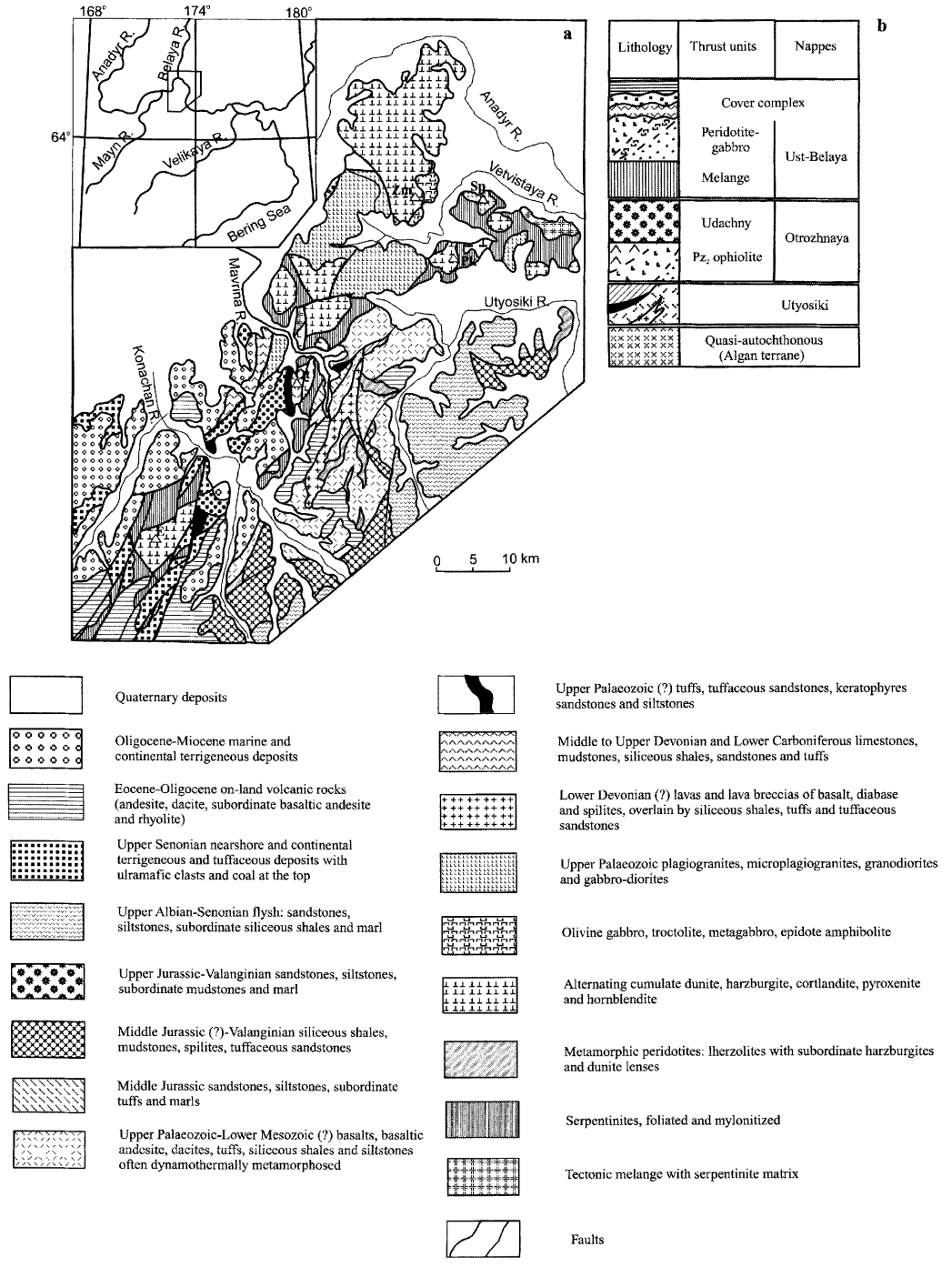

Fig. 28. (**a**) Geological map of the Ust–Belaya terrane (after S. A. Palandzhyan); (**b**) succession of the nappe units. In (**a**): △, mountain peak (E, Eldernyr; Ot, Otrozhnaya; Zm, Zmeyevik; Pk, Porfiritovyi Kamen; Sp, Sprut). (**b**) For symbols, see (**a**).

sequence, some 0.7 km thick, of MORB-like basaltic rocks; (3) cherty and tuffaceous clastic rocks with Mid- to Late Devonian faunas; (4) Early Carboniferous terrigenous rocks with serpentinite, diabase, and chert clasts and Cr-spinel grains. The gabbros and basalts are cut by diabase and porphyritic microplagiogranite dykes. The microplagiogranite dykes have whole-rock K–Ar ages of 218–178 Ma (Palandzhyan 1997).

The second thrust unit, Udachny, consists of *c.* 1.1 km thick Upper Jurassic to Valanginian flysch, interpreted to have been deposited in a forearc basin in front of the Uda–Murgal arc, and containing fragments of tuffaceous terrigenous material of Mid-Jurassic age, and carbonate and terrigenous sequences of Mid–Late Devonian and Early Carboniferous age.

The upper, Ust–Belaya nappe, over 5 km in thickness, is mainly composed of peridotites and gabbros. At the base of the nappe is a serpentinite mélange up to 0.5 km thick. Blocks in the mélange are composed not only of the overlying rocks (lherzolite, harzburgite, cumulate ultrabasic rocks, gabbro, basalt, siliceous–terrigenous rocks, organic limestone of Mid- and Late Devonian ages), but also of rocks lacking from all three nappes mentioned above, such as depleted harzburgite, high-Cr chromitite, schist, garnet amphibolite, and plagiogranite.

Petrography and geochemistry of the ophiolite

The peridotites show a variety of metamorphic fabrics, including protogranular, which is commonly preserved in lherzolites. Porphyroclastic and mosaic fabrics and mylonites are typical in the shear zones and at the base of the mantle suite. The peridotites are abundant in antigorite, a distinctive feature of the ultramafic rocks of the Ust–Belaya terrane, whereas in the other ultramafic massifs lizardite and chrysotile are abundant.

Stratigraphically higher, in the eastern part of Ust–Belaya unit, lherzolite gives way to Cpx-bearing harzburgites and dunites and then to a thinly banded (1–3 cm) sequence of alternating dunite, cortlandite (two-pyroxene hornblende peridotite), wehrlite, pyroxenite, and hornblendite, intruded by microgabbroic dykes (Table 12, Fig. 29a).

According to Nekrasov *et al.* (2001), the least depleted lherzolites of the Ust–Belaya massif are compositionally close to pyrolite. Major element compositions of coexisting minerals from the lherzolites and harzburgites are given in Fig. 30 and Table 13. Although the compositional range is wide, most peridotites are slightly to moderately depleted, as indicated by pyroxene and Cr-spinel

Table 12. *Major element contents (wt%) of ultramafic and mafic ophiolitic rocks of the Ust–Belaya terrane*

n:	1	2	3	4	5	6	7	8	9	10	11	12	13	14	15	16	17	18	19	20	21	22	23
Sample:	496/1	523/1	525/1	461/1	581/1	451/2	584/1	588/1	588/2	466/4	471/3	593/1	549/1	588/3	589/2	61	450	450/1	21	463/1	463/2	463/3	561/2
SiO_2	37.79	42.10	37.09	41.12	40.57	40.63	40.41	38.46	36.62	44.40	46.02	46.97	50.69	44.58	44.64	47.00	44.80	47.00	43.92	50.17	47.25	52.44	50.06
TiO_2	0.21	0.17	0.15	0.11	0.10	0.06	0.04	–	–	0.13	0.25	0.10	0.18	1.09	1.24	0.27	0.14	0.14	0.09	1.05	1.09	1.14	1.16
Al_2O_3	3.08	3.33	1.22	3.50	3.57	2.30	1.60	6.71	6.34	22.44	18.27	24.49	23.61	14.71	14.28	17.87	21.71	24.83	23.38	14.27	14.69	14.64	13.69
Cr_2O_3	0.46	0.42	0.36	0.39	0.31	0.55	0.42	n.d.	0.39	0.04	0.10	0.07	n.d.	n.d.	n.d.	n.d.	n.d.	n.d.	n.d.	n.d.	n.d.	n.d.	n.d.
Fe_2O_3	1.60	1.81	2.81	2.99	3.11	2.23	3.32	2.84	3.29	0.16	1.27	0.92	2.50*	14.05*	15.10*	1.74	1.07	1.05	1.72	13.88*	14.70*	13.91*	14.99*
FeO	6.23	5.18	5.65	5.42	5.04	6.04	5.14	7.32	6.80	3.64	5.25	1.89	n.d.	n.d.	n.d.	4.40	3.59	2.28	3.01	n.d.	n.d.	n.d.	n.d.
MnO	0.07	0.05	0.31	0.11	0.03	0.12	0.10	0.23	0.13	0.03	0.05	0.03	0.05	0.22	0.24	0.13	0.07	0.06	0.07	0.21	0.22	0.20	0.20
MgO	37.04	38.79	40.73	37.20	38.97	40.94	40.56	36.54	36.64	13.40	12.70	8.55	4.44	8.20	9.38	10.21	11.57	7.41	10.15	5.20	5.65	4.70	4.27
CaO	2.37	2.57	1.02	2.45	2.50	1.27	1.31	5.32	5.70	11.00	11.25	13.50	14.43	10.45	9.11	12.90	11.76	12.42	10.01	9.48	10.09	8.20	8.73
Na_2O	0.25	0.10	0.10	0.38	0.27	0.10	0.10	0.41	0.05	1.76	2.00	1.67	3.07	2.21	2.11	1.98	1.74	2.51	2.43	4.27	3.17	4.02	5.79
K_2O	0.10	0.10	0.06	0.10	0.10	0.10	0.10	0.01	n.d.	0.10	0.23	0.18	0.39	0.71	0.78	0.18	0.07	0.07	0.49	0.44	1.48	1.01	0.42
P_2O_5	0.12	0.11	0.11	0.03	0.09	0.03	0.03	n.d.	n.d.	0.08	0.10	0.11	0.01	0.11	0.12	0.01	0.01	0.01	0.01	0.04	0.03	0.12	0.05
H_2O	0.06	0.89	0.29	0.29	n.d.	0.22	0.24	n.d.	0.12	n.d.	n.d.	n.d.	n.d.	n.d.	n.d.	0.43	0.66	0.49	0.74	n.d.	n.d.	n.d.	n.d.
LOI	10.34	4.51	9.93	5.86	5.57	6.03	6.66	1.69	3.26	3.29	2.04	1.61	1.53	3.80	3.07	2.54	2.97	2.23	3.82	0.98	1.61	1.20	0.63
Total	99.62	100.21	99.83	99.85	100.23	100.53	100.03	99.53	99.34	100.47	99.53	100.09	100.90	100.13	100.07	99.66	100.16	100.50	99.84	99.99	99.98	101.58	99.99

1–3, Eldenyr massif (1 and 2, lherzolites; 3, Di harzburgites); 4–9, Ust–Belaya massif (4 and 5, lherzolites; 6 and 7, Di harzburgites; 8 and 9, kortlandites); 10–15, gabbroids of Ust–Belaya massif (10–12, olivine gabbro and troctolite; 13, metagabbro; 14 and 15, microgabbro from dykes in cumulates); 16–19, olivine gabbro, Otrozhny complex; 20–23, amphibolites, blocks in mélange. n.d., not determined.
*Total Fe as Fe_2O_3.

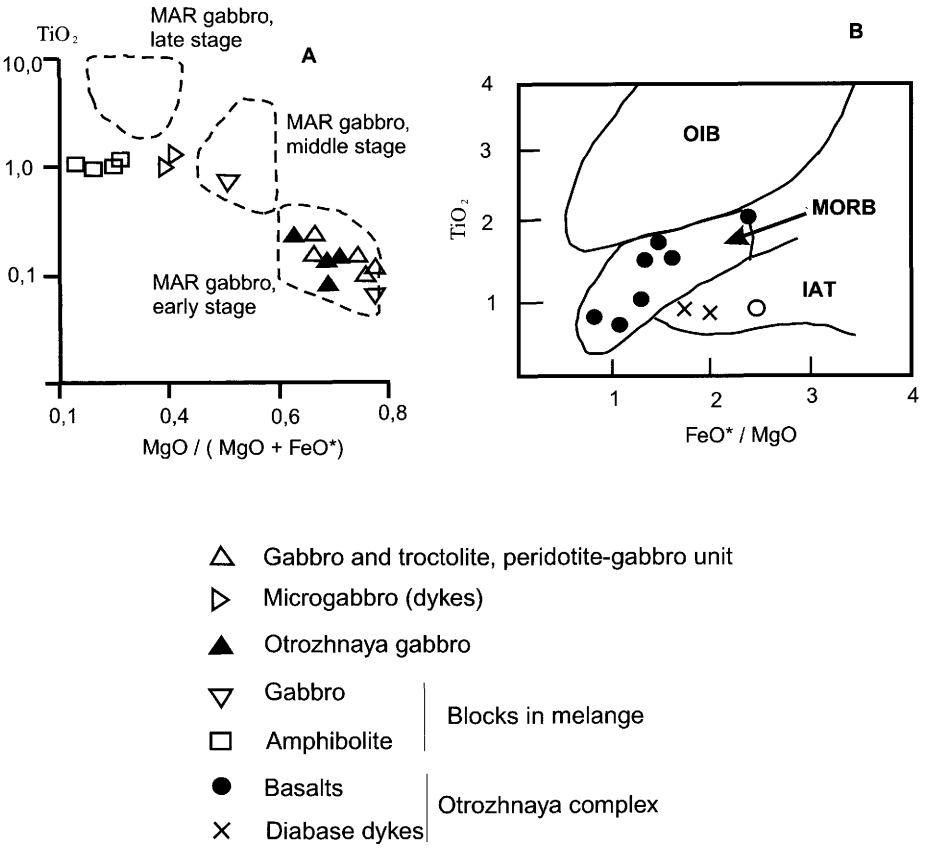

Fig. 29. Plots for mafic rocks showing (**a**) TiO_2 v. MgO/(MgO + FeO*) and (**b**) TiO_2 v. FeO*/MgO, wt% in whole rock. Compositional fields in (**a**) are after Miyashiro & Shido (1980); those in (**b**) are after (Glassely 1974).

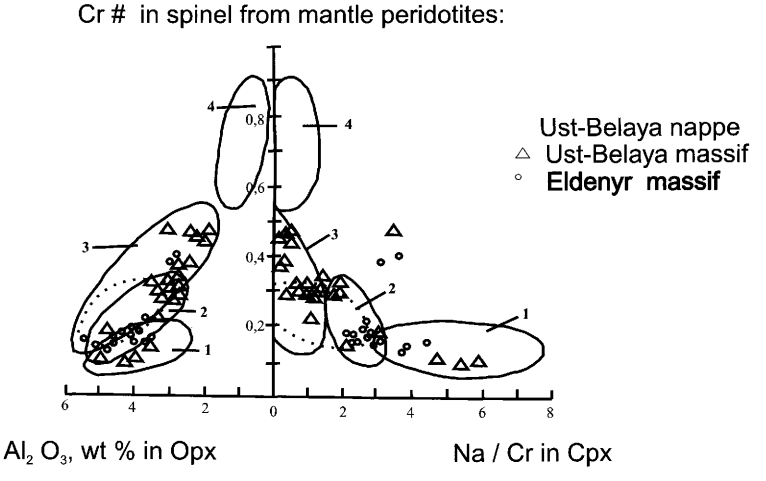

Fig. 30. Plot of Cr/(Cr + Al) in Cr-spinel v. Al_2O_3 in Opx and Na/Cr (crystallochemical formula units) in Cpx for metamorphic peridotites. Fields of mantle peridotite compositions from different geodynamic settings, after Kornprobst *et al.* (1981), Bonatti & Michael (1989) and Palandzhyan (1992). 1, Subcontinental; 2, passive margin; 3, mid-ocean ridge (dotted contours delineate extremely slow-spreading MOR peridotites), 4, suprasubduction zone.

Table 13. *Major element contents (wt%) of coexisting minerals from ophiolitic peridotites of the Ust–Belaya terrane*

Sample:	532/1, LZ				520/1, LZ				523/1, LZ				520/2, LZ				454/3, LZ				584/1, DHZ		
Mineral:	Ol	Spl	Opx	Cpx	Ol	Spl	Opx	Cpx	Ol	Spl	Opx	Cpx	Ol	Spl	Opx	Cpx	Ol	Spl	Opx	Cpx	Ol	Spl	Cpx
n:	4	7	2	3	3	5	2	3	5	6	5	5	3	6	4	3	6	6	7	4	2	5	3
SiO_2	40.90	n.d.	55.43	52.69	40.48	n.d.	54.79	52.89	40.16	n.d.	54.83	51.94	40.51	n.d.	55.06	53.64	39.79	n.d.	54.72	52.73	40.98	n.d.	53.18
TiO_2	–	0.10	0.05	0.09	0.02	0.04	0.07	0.12	0.01	0.02	0.04	0.12	0.01	0.05	0.03	0.12	0.01	0.01	0.02	0.11	–	0.02	0.02
Al_2O_3	–	51.48	4.05	4.45	0.03	52.69	3.67	4.87	–	51.10	3.97	5.09	–	48.00	3.72	5.06	–	53.74	3.57	4.53	–	41.14	3.34
Cr_2O_3	–	15.98	0.53	0.83	–	14.71	0.31	0.81	0.04	16.97	0.52	1.06	0.03	19.63	0.64	1.28	–	13.66	0.36	0.81	0.08	26.84	0.95
Fe_2O_3	n.d.	1.87	n.d.	n.d.	n.d.	1.85	n.d.	n.d.	n.d.	1.85	n.d.	n.d.	n.d.	2.18	n.d.	n.d.	n.d.	1.96	n.d.	n.d.	n.d.	2.66	n.d.
FeO*	9.15	11.24	6.28	2.19	9.00	11.02	6.37	2.07	8.56	11.19	5.83	1.97	8.75	11.61	5.59	1.97	9.06	11.86	6.31	2.15	9.13	13.12	1.79
MnO	0.17	0.13	0.10	0.10	0.11	0.12	0.15	0.08	0.15	0.11	0.13	0.10	0.16	0.14	0.14	0.11	0.11	0.13	0.13	0.08	0.16	0.16	0.10
MgO	49.38	18.63	33.37	16.31	50.60	18.84	33.90	15.75	50.58	18.72	34.19	15.75	50.93	18.07	34.37	15.16	50.23	18.53	34.37	16.17	50.15	16.44	16.55
NiO	0.37	0.29	0.12	0.07	0.40	0.28	0.02	0.06	0.38	0.24	0.05	0.04	0.36	0.23	0.11	0.02	0.29	0.27	0.05	0.02	0.35	0.20	0.01
CaO	–	n.d.	0.82	22.16	0.01	n.d.	0.50	22.94	0.01	n.d.	0.48	22.50	0.01	n.d.	0.55	22.01	0.01	n.d.	0.29	22.62	–	n.d.	24.20
Na_2O	n.d.	n.d.	–	0.76	n.d.	n.d.	0.03	0.95	n.d.	n.d.	0.02	1.11	n.d.	n.d.	0.01	1.37	n.d.	n.d.	0.04	0.69	n.d.	n.d.	0.29
Total	99.97	99.72	100.76	99.66	100.65	99.55	99.82	100.54	99.89	100.20	100.06	99.69	100.76	99.91	100.23	100.75	99.50	100.16	99.87	99.93	100.85	100.59	100.45
Cr	–	0.338	0.014	0.024	–	0.309	0.009	0.023	–	0.358	0.014	0.031	–	0.421	0.017	0.036	–	0.286	0.010	0.023	–	0.592	0.027
Al	–	1.621	0.164	0.191	–	1.652	0.150	0.207	–	1.605	0.162	0.219	–	1.533	0.143	0.214	–	1.674	0.146	0.194	–	1.352	0.142
Na	–	–	–	0.054	–	–	–	0.066	–	–	–	0.078	–	–	–	0.095	–	–	–	0.049	–	–	0.020
Cr*	–	17.23	7.87	11.10	–	15.77	5.66	11.00	–	16.55	8.79	12.25	–	21.53	10.63	14.40	–	14.57	6.36	10.70	–	30.44	15.98
F†	9.39	25.28	9.55	7.00	9.06	24.71	9.54	6.86	8.67	25.11	8.73	6.56	8.81	26.49	8.36	6.78	9.18	26.36	9.34	6.94	9.27	30.93	5.72

LZ, lherzolite; DHZ, diopside harzburgite; Ol, olivine; Spl, chromian spinel; Opx, orthopyroxene; Cpx, clinopyroxene; *n*, number of analysed grains (mean values are shown for several analyses for each mineral); n.d., not determined. FeO*, total Fe as FeO. In chromian spinel, FeO and Fe_2O_3 were calculated using the compound electroneutrality principle. 454/3, 584/1, Ust–Belaya massif; others, Eldernyr massif. All analyses from cores of mineral grains.

*$Cr = 100 \times Cr/(Cr + Al)$.

†$F = 100 \times Fe/(Fe + Mg)$.

compositions being similar to peridotites of modern passive margins and ultra slow-spreading centres. The least depleted lherzolites of the Ust–Belaya nappe, based on their mineral composition, are similar to subcontinental lherzolites (Fig. 30). Nekrasov *et al.* (2001) showed that the Ust–Belaya lherzolites have nearly chondritic REE contents with a slight negative Eu anomaly.

These data suggest that the rocks of the lherzolite unit of the Ust–Belaya terrane are oceanic lithospheric fragments of the marginal part of a large oceanic basin (Palandzhyan 1992). Nekrasov *et al.* (2001), on the other hand, proposed that the lherzolites resemble xenoliths of mantle rocks of the Ontong–Java Plateau.

The lherzolite–gabbro contact, exposed over a considerable length, is marked by a thin (0.1–0.2 km) transition zone, composed of dunite, wehrlite, and Pl-bearing dunite. The gabbroic complex is composed chiefly of banded olivine gabbro and troctolite with lens-like bodies of Pl-bearing ultramafic rocks in the lower part. Most of the banded gabbro is metamorphosed to amphibolite. Petrographic observations in gabbros with primary banded fabrics surviving among gabbro–amphibolites show that plagioclase crystallized before clinopyroxene and the rocks lack orthopyroxene, which places the cumulates with the A-1 type as described by Ohnenstetter (1985). These characteristics suggest that the ophiolite may have originated in a mid-ocean ridge or in a continental-margin basin, rather than in an SSZ setting.

Basalts in the Otrozhnaya nappe are similar to MORB-type tholeiites both in terms of major oxides (Fig. 29b) and trace elements, particularly REE, Zr, Y, and Nb (for details, see Nekrasov *et al.* 2001).

Origin of the ophiolite

Thrust faulting in the Ust–Belaya terrane has juxtaposed two ophiolite associations. The Lower to Middle(?) Devonian ophiolites, which make up the Ust–Belaya and Otrozhnaya nappes, have slightly depleted peridotites, primitive crustal magmatic lithologies, and MORB-like volcanic rocks. Major and trace element composition of restite peridotites and gabbros confirm oceanic affinity for these ophiolites (Palandzhyan 1992; Nekrasov *et al.* 2001).

The serpentinite mélange contains fragments of an SSZ-type ophiolite association that includes strongly depleted peridotite, high-Cr chromitites, and differentiated volcanic rocks. These ophiolites are tentatively dated as Late Palaeozoic to Early Mesozoic based on whole-rock K–Ar ages: 262 Ma from a dacite, 164 and 178 Ma from amphibolites, and 172, 186, and 218–178 Ma from plagiogranites (Palandzhyan 1997).

Discussion

The above summary illustrates the diversity of structural settings, ages, compositions, and origins of ophiolites in the West Koryak fold system (Fig. 31, Table 14). They are all parts of a continental-margin assemblage that was added to the North Asian continent at the end of the Early Cretaceous (Sokolov 1992; Parfenov *et al.* 1993; Khudoley & Sokolov 1998). The ophiolites are all deformed and unconformably overlain by upper Albian strata.

The ophiolites come in two age groups, Palaeozoic and Mesozoic. Palaeozoic ophiolites of the Ganychalan and Ust–Belaya terranes are oceanic in type. They can be viewed as being fragments of the Panthalassa Ocean.

Counterparts to Ganychalan ophiolites may be those of the Livengood terrane, Central Alaska. Exotic, possibly North American, provenance has been proposed for the Ordovician deposits overlying ophiolites of the Ganychalan terrane (Khanchuk *et al.* 1992; Sokolov *et al.* 1997). Other workers (Nekrasov *et al.* 2001), by contrast, believe that the Ganychalan and Ust–Belaya ophiolites were formed in an oceanic plateau near the Asian continent.

Correlating the Ust–Belaya ophiolites will be possible only after their age has been properly constrained. Currently, they are dated to the Devonian based on the Mid–Late Devonian age of their overlapping sediments (u_1 in Fig. 31). However, radiometric datings from the peridotites and gabbros of their structurally overlying MORB-like basalts are lacking. Not inconceivably, the ophiolites are older, Early Palaeozoic in age, representing fragments of the same oceanic plate as the Ganychalan ophiolites. Provided that their Devonian age is validated, they could be correlated with the Brooks Range ophiolites of North Alaska, which are interpreted as fragments of the Angachuyam Ocean (Nokleberg *et al.* 1994, 2001; Wirth *et al.* 1994).

The serpentinite mélange of the Ust–Belaya nappe (u_2 in Fig. 31) hosts occasional blocks of island-arc-derived lithologies: strongly depleted peridotites, plagiogranites, and differentiated volcanic rocks. The previous K/Ar measurements suggest Late Palaeozoic and Early Mesozoic age for the island-arc assemblage. This is in keeping with the reconstructions for the Koni–Taigonos island arc, which once marked the convergent boundary between the North Asian continent and NW Pacific (Parfenov 1984; Sokolov 1992; Sokolov *et al.* 1999; Parfenov *et al.* 1993). However,

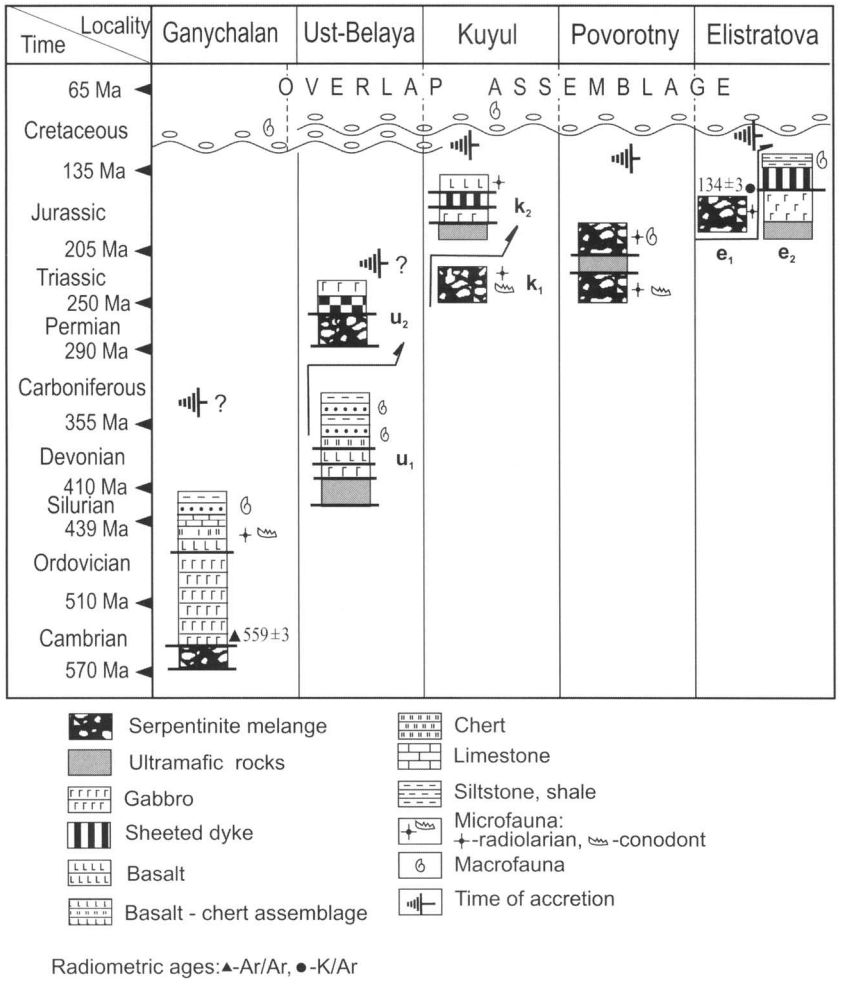

Fig. 31. Temporal and spatial distribution of the ophiolites. u_1, Otrozhnaya nappe; u_2, Ust–Belaya nappe; k_1, Unnavayam unit; k_2, Gankuvayam unit; e_1, Northern unit; e_2, Southern unit.

the K/Ar age determination ought to be validated by new measurements using other isotope systems.

Mesozoic ophiolites are dominated by those of SSZ origin (Fig. 31, Table 14). The most complete fragment of an ophiolite suite has been reported from the Gankuvayam unit (k_2 in Fig. 31) of the Kuyul terrane (Khanchuk *et al.* 1990; Sokolov *et al.* 1996) and in the Yelistratov Peninsula (e_2 in Fig. 31), where relics survive of a magma chamber composed of ultramafic–mafic cumulates and gabbro (Ishiwatari *et al.* 1998; Saito *et al.* 1999).

In addition, among Mesozoic ophiolites one finds rock fragments of oceanic provenance. These include the Unnavayam unit (k_1 in Fig. 31) of the Kuyul terrane (Grigoriev *et al.* 1995; Sokolov *et al.* 1996) and the Southern ultramafic body from the Yelistratov ophiolite (Ishiwatari *et al.* 1998; Saito *et al.* 1999). Previously, serpentinite mélanges occurring in the Cape Povorotny accretionary prism were believed to contain both oceanic lherzolites and SSZ harzburgites (Palandzhyan & Dmitrenko 1999; Sokolov *et al.* 1999), but more recent geochemical data (Bazylev *et al.* 2001), including those presented in this paper, suggest an SSZ origin for these rocks. On the other hand, because the accretionary pile contains some basalt–chert associations of oceanic origin and ensimatic volcanic rocks, as well as oceanic and SSZ gabbro, it is still possible that more detailed study may detect oceanic ultramafic rocks there as well.

The fact that SSZ assemblages are lacking in Early Palaeozoic ophiolites and, by contrast, are

Table 14. *Age, composition, structural location and geodynamic setting of NE Asia ophiolites*

Ophiolites	Composition (from bottom to top)	Age	Structural location	Geodynamic setting
1. Ganychalan terrane	*Mrachnaya slice*: serpentinite mélange with blocks of plagioclase wehrlite, pyroxenite, troctolite, olivine gabbro *Khynantynup slice*: layered gabbro, isotropic gabbro, gabbronorite, ferrogabbro, gabbro–diabase, diabase, plagiogranite *Ilgeminai slice*: basalt, tuff, chert	Early Palaeozoic	Forearc basement	Fragment of oceanic crust
2. Ust–Belaya terrane	*Otrozhnaya nappe:* serpentinized harzburgite, lherzolite, dunite, amphibolitized gabbro; MORB-like basaltic rocks; cherty and tuffaceous clastic rocks *Ust–Belaya, nappe*: serpentinite mélange; peridotite and gabbro	Late Palaeozoic	Forearc basement	Fragment of oceanic crust
3. Beregovoi terrane				
3.1. Cape Povorotny	Serpentinite mélange with blocks of ultramafic rocks (lherzolite, harzburgite), gabbro, sheeted dykes, plagiogranite, amphibolite, greenschist, island-arc volcanic and sedimentary rocks, oceanic basalt and chert	Mesozoic	Accretionary prism	Suprasubduction
3.2. Elistratov Peninsula	*Northern unit:*serpentinite mélange with blocks of harzburgite, dunite, sheeted dykes, metabasalts, radiolarite; *Southern unit:*harzburgite, cumulate complex, gabbro, sheeted dyke complex differentiated from basalt to dacite	Mesozoic	Forearc basement	Suprasubduction
4. Kuyul terrane	*Unnavayam unit:* serpentinite mélange with blocks of harzburgite, cumulates, basalt and chert Gankuvayam unit: harzburgite, dunite, cumulate complex (gabbro, wehrlite, troctolite), isotropic gabbro; plagiogranite, differentiated complexes from basalt to dacite: sheeted dykes and pillow lavas	Mesozoic	Accretionary prism	Oceanic (Unnavayam unit) and suprasubduction (Gankuvayam unit)

widespread in Mesozoic ophiolites might be critical to the general evolution of the Palaeo-Pacific ocean. This inference, however, should be tested against a more representative dataset covering other Circum-Pacific regions as well.

Ophiolites and their associated metamorphic, volcanic, and sedimentary rocks of Palaeozoic–Early Cretaceous age (including early Albian) show evidence of at least three deformation phases: D_1, D_2, and D_3 (Khudoley & Sokolov 1998). Fabrics and structures related to D_1 are clearly pronounced in the Ganychalan terrane. Khudoley & Sokolov (1998) proposed an Early Carboniferous age for the D_1 event. Rb/Sr ages obtained from Ganychalan greenschists (Vinogradov *et al.* 1995) imply that D_1 deformations were accompanied by some greenschist metamorphism at 327 ± 5 Ma. We interpret this deformational event as resulting from amalgamation of previously separated blocks, now represented by the Ilpenei, Mrachnaya, Khinantynup, and Elgeminai thrust sheets in the unique Ganychalan composite terrane.

The D_2 deformation event is well documented by palaeontological data (Khudoley & Sokolov 1998). The youngest rocks affected by D_2 folds and faults contain early Albian faunas, whereas the oldest unconformably overlying undeformed units contain late Albian faunas (Sokolov 1992). Based on regional geological considerations and terrane analysis, the latest Jurassic–Early Cretaceous tectonism is usually interpreted as the main stage of accretion of Pacific-related terranes to the Asian continental margin (Sokolov 1992; Parfenov *et al.* 1993; Nokleberg *et al.* 1994).

D_3 faults cross-cut all terranes and their overlap sequence, including Paleogene rocks (Bondarenko & Sokolov 1996; Khudoley & Sokolov 1998). The D_3 deformation event is interpreted as being related to major sinistral strike-slip displacement.

These deformation events reflect various phases of evolution of the continental margin of NE Asia and can be readily correlated with principal tectonic events in the north Circum-Pacific region. Thus, D_1 stage and island-arc volcanism in the Taigonos and Penzhina segments were related to evolution of the Palaeozoic convergent boundary of Asia and the NW Pacific (Zonenshain *et al.* 1990; Sokolov 1992; Parfenov *et al.* 1993). Strain analysis shows that the direction of maximum extension is parallel to the regional trend (Khudoley & Sokolov 1998) and is typical of accretionary belts of the Pacific Rim (Toriumi 1985). The event produced D_2 structures throughout all the terranes and correlates well with synchronous tectonic processes in southern Alaska (Nokleberg *et al.* 1994). The D_3 event is approximately synchronous with Late Cretaceous to Eocene dextral strike-slip displacements and transpression in Alaska and the northern Cordillera and is typical of post-accretionary tectonics (Coney *et al.* 1980; Gabrielse *et al.* 1991).

The degree of disruption of the ophiolites differs from locality to locality. Deformation is strongest and serpentinite mélanges are present in Cape Povorotny and Kuyul terrane ophiolites. The latter retains only one fragment (Gankuvayam unit), interpretable as a dismembered ophiolite. Ust–Belaya terrane and Yelistratova Peninsula ophiolites, alongside serpentinite mélange, preserve large intact fragments of gabbro, cumulates, and sheeted dykes. Ganychalan terrane ophiolites are dismembered, with serpentinite mélange zones being here encountered only locally, mainly in the base of the ophiolitic allochthon.

Therefore, the degree of disruption is least, strangely enough, in the older, Early Palaeozoic ophiolites of the Ganychalan terrane. This may be due to three circumstances: (1) the mode of ophiolite incorporation into continental margin; (2) dissimilarity of formative geodynamic settings of the ophiolites; (3) post-accretionary history of the accreted terranes. The first factor is favoured by the fact that overlap sediments are lacking from Mesozoic and available in Palaeozoic ophiolites. Ganychalan and Ust–Belaya ophiolites have preserved depositional contacts with strata of terrigenous provenance (Fig. 31). These were accumulated on top of the ophiolites as the oceanic plate converged with and resided near the continental margin. The age of sedimentary cover constrains the lower time limit for ophiolite accretion. In Mesozoic ophiolites, stratigraphic contacts survive only in post-accretionary deposits. Also, Cape Povorotny and the Kuyul terrane show extensive strike-slip motions (Bondarenko & Sokolov 1996; Khudoley & Sokolov 1998), probably suggestive of oblique subduction during the docking of Mesozoic ophiolite assemblages. Palaeozoic accreted terranes are made chiefly of oceanic ophiolites, and Mesozoic terranes of SSZ ophiolites, which lends support to the second factor. The third factor being in operation is evidenced by strike-slip offsets related to D_3 deformation (see below).

Not only do the ophiolites have different origins, but they also have different accretionary histories. Palaeozoic ophiolites of the Ganychalan and Ust–Belaya accreted terranes docked onto the Koni–Taigonos island arc, which marked the convergent boundary of the Asian continent and NW Pacific in Late Palaeozoic to Early Mesozoic times. The SSZ ophiolites from the serpentinite mélange of the Ust–Belaya nappe may be relics of the Koni–Taigonos island arc, whose fragments have recently been reported from the Penzhina District (Sokolov *et al.* 1999) and from the

Pekulney Range (Morozov 2001). No fragments of an ancient accretionary prism have been identified to date. They may have survived and might still be detected among Palaeozoic deposits of the Beregovoi terrane (Carboniferous flysch) in the Taigonos Peninsula and in the Upupkin terrane (Permian and Triassic tuffaceous–terrigenous and clastic deposits). At the same time, subduction-related glaucophane–greenschist metamorphic rocks of Carboniferous age are well developed in the Ganychalan terrane (Ilpenei unit) of Penzhina District (Dobretsov 1974; Silantyev *et al.* 1994).

The exact timing of accretion and original location of the Ganychalan and Ust–Belaya terranes remain unknown. In this context, Ganychalan ophiolites should be classed with 'suspect terranes' as described by Coney *et al.* (1980). The Carboniferous and Permian deposits within the Koni–Taigonos arc and in terrigenous sequences associated with the ophiolites were clearly formed at high latitudes, because they contain boreal faunas and Angaran floras (Sokolov 1992). In addition, Carboniferous strata in the Ust–Belaya terrane contain ophiolitic detritus (Markov *et al.* 1982; Palandzhyan 2000), suggesting that this terrane was previously amalgamated with or even accreted onto the Eurasian plate.

No reliable age data for the Yelistratov Peninsula ophiolites are available. They are overlain by Berriasian strata, deposited in the forearc of the Uda–Murgal island arc. Serpentinite mélange contains occasional blocks of basalt and radiolarite of Mid- to Late Jurassic age. Conceivably, they could be Mesozoic in age, like the Cape Povorotny and Kuyul ophiolites. However, the Yelistratov ophiolite was accreted to the Uda–Murgal arc somewhat earlier than the Cape Povorotny ophiolite. The latter is overlain by Valanginian–Hauterivian strata of the Vitayetglia unit (Fig. 5), which were deposited in a forearc basin associated with the Uda–Murgal island arc and contain ophiolitic detritus (Sokolov *et al.* 1999).

It is not yet possible to constrain the timing of accretion of the Kuyul ophiolites. These ophiolites form part of the accretionary wedge (Ainyn terrane) exposed in the Penzhina segment of the Uda–Murgal island-arc system. The first ophiolitic clasts to appear in the overlap sequence and which are clearly derived from the Kuyul terrane are dated as late Albian. On the other hand, ophiolite fragments have been reported from Hauterivian strata of the Ainyn and Upupkin terranes as well (Nekrasov 1976; Markov *et al.* 1982; Palandzhyan 1992). However, our own studies (Grigoriev *et al.* 1995; Sokolov *et al.* 1996) have not confirmed the presence of Mesozoic ophiolitic clasts in the Ainyn terrane, and serpentinite conglomerates and sandstones in the Matchinsky Peninsula are unfossiliferous. These coarse clastic rocks may be late Albian in age (K. A. Krylov, pers. comm.). Fragments of the more ancient Ganychalan ophiolite have been reported from Hauterivian strata of the Upupkin terrane (Sokolov *et al.* 2000).

In Late Jurassic to Early Cretaceous time, a new convergent boundary took shape, with a younger Uda–Murgal island-arc system stretching along it (Sokolov *et al.* 1999). Along this boundary the Pacific plates (Izanagi and Farallon) were subducting with the result that ophiolites of Cape Povorotny, the Yelistratov Peninsula, and the Kuyul terrane were emplaced in the forearc. Accretionary prisms of Cape Povorotny and the Penzhina District contain both oceanic rock assemblages and fragments of ensimatic arcs, with outboard chert–basalt associations of Cape Povorotny, from the Izanagi plate (Bazhenov *et al.* 1999).

The original positions of the ensimatic island-arc complexes and their relationships with the convergent boundary of the North Asian continent remain as yet unclear. In unravelling these issues, the greatest promise seems to be offered by the Yelistratov Peninsula ophiolites, because they are extremely well exposed and their stratigraphy is relatively coherent, such that primary intrusive contacts of SSZ gabbro with its surrounding oceanic upper-mantle rocks are preserved intact today (Ishiwatari *et al.* 1998; Saito *et al.* 1999).

The accretionary prisms of Cape Povorotny and Ainyn terrane contain terrigenous mélanges (Khudoley & Sokolov 1998; Sokolov *et al.* 1999). By and large, these mélanges are very similar to those described from the Shimanto Belt of southeastern Japan (Kano *et al.* 1991) and from southern Alaska (Fisher & Byrne 1987).

The existence of two island-arc systems of different ages (Koni–Taigonos and Uda–Murgal) has determined the evolution of the NE Asian continental margin. Sequential growth of the North Asian continent (Fig. 2) is evidenced by ophiolites becoming increasingly younger oceanward, a pattern typical of Circum-Pacific ophiolites (Ishiwatari 1994). This is especially readily apparent in the Penzhina segment, where Mesozoic ophiolites of the Kuyul accreted terrane occur SE of the Early Palaeozoic ophiolites of the Ganychalan terrane. In association with ophiolites one finds glaucophane schists, also younging oceanward. In the Ganychalan terrane, subduction-related metamorphic schists are dated at 327 ± 5 Ma, and in the Kuyul terrane, at 139 ± 6 Ma (Rb/Sr method, four isochron points) with an initial Rb/Sr ratio of 0.711 (Vinogradov *et al.* 1995), and 92 ± 10 Ma (Rb/Sr method, two isochron points) with an initial Rb/Sr ratio of 0.7324 (Vinogradov *et al.* 1995).

The long-lived convergent boundary between the North Asian continent and the NW Pacific, initiated in the Late Palaeozoic, is evidenced by the ages of SSZ ophiolites, glaucophane and greenschist rocks, and island-arc assemblages. This reconstruction places additional constraints on migration of the Omolon and Okhotsk microcontinents. Previous notions (Parfenov 1984; Zonenshain *et al.* 1990) on Pacific provenance of the microcontinents and their arrival from southern latitudes require revision. On the other hand, palaeomagnetic and palaeobiogeographical data imply that both Palaeozoic and Mesozoic ophiolites and their associated chert and basalt assemblages are rather far travelled (Heiphetz *et al.* 1994; Bazhenov *et al.* 1999; Harbert *et al.* 2003). In this respect, Pacific ophiolites differ significantly from their Tethyan counterparts.

Conclusions

Lithostratigraphic, petrographic, mineralogical, geochemical, and temporal characteristics of the ophiolites and associated volcanic rocks of the West Koryak fold system are extremely variable and suggest a spectrum of formative tectonic settings: ocean basin, back-arc basin, volcanic arc, and within plate. West Koryak ophiolites are very diversified, as in other orogenic belts (e.g. the Brooks Range, Klamath Mountains, Japan).

Ages of reliably dated ophiolites of the West Koryak fold system are consistent with temporal distribution of ophiolites in worldwide orogenic belts. According to Ishiwatari (1994), distribution of Phanerozoic ophiolites shows two peaks, Ordovician and Jurassic–Cretaceous. The oceanward and downward younging of the ophiolites through accretionary piles is very readily demonstrable in the Penzhina segment. Such a pattern has been reported from Japan (Ishiwatari 1994) and the Klamath Mountains (Coleman 1986), and it is characteristic of accretionary continental margins.

In most accreted terranes (Ust–Belaya, Kuyul, Beregovoi), ophiolites of contrasting ages and geodynamic types are tectonically juxtaposed. Thus, both SSZ and oceanic (MOR, BABB) ophiolites are present in the Ust–Belaya and Kuyul terranes, where they form individual thrust sheets.

The ophiolites have distinctive tectonic positions. The Palaeozoic ophiolites occur as nappes in the Ganychalan and Ust–Belaya terranes, and Mesozoic ophiolites and mélanges occur among accretionary piles of the Beregovoi and Kuyul terranes. Some of them (Ganychalan, Yelistratov, Ust–Belaya) are incorporated in pre-arc basement of the Uda–Murgal island-arc system, whereas others (Cape Povorotny, Kuyul) are part of accretionary prisms of the same system.

The above considerations support the model for ophiolite generation in a large ocean basin with active margins (e.g. the Pacific Ocean), followed by their tectonic juxtaposition within a single orogenic belt (West Koryak fold system).

Thanks are due to our reviewers P. T. Robinson, R. Hebert, and C. Buchan. We thank Y. Dilek for his fruitful criticism and invaluable suggestions. This work was supported by the Russian Foundation for Basic Research (project nos 02-05-64217, 01-05-64469, 00-05-64165) and by INTAS (project no. 96-1880).

References

Amri, I., Benoit, M. & Ceuleneer, G. 1996. Tectonic setting for the genesis of oceanic plagiogranites: evidence from a paleo-spreading structure in the Oman ophiolite. *Earth and Planetary Science Letters*, **139**, 177–194.

Anders, E. & Grevesse, N. 1989. Abundances of the elements: meteoritic and solar. *Geochimica et Cosmochimica Acta*, **53**, 197–214.

Arai, S. 1992. Chemistry of chromian spinel in volcanic rocks as a potential guide to magma chemistry. *Mineralogical Magazine*, **56**, 173–184.

Arai, S. 1994. Characterization of spinel peridotites by olivine–spinel compositional relationships: review and interpretation. *Chemical Geology*, **113**, 191–204.

Barnes, S.J. & Roeder, P.L. 2001. The range of spinel compositions in terrestrial mafic and ultramafic rocks. *Journal of Petrology*, **42**, 2279–2302.

Batanova, V.G. & Sobolev, A.V. 2000. Compositional heterogeneity in subduction-related mantle peridotites, Troodos massif, Cyprus. *Geology*, **28**, 55–58.

Bazhenov, M.L., Aleksuytin, M.V., Bondarenko, G.Ye. & Sokolov, S.D. 1999. Mesozoic paleomagnetism of the Taigonos Peninsula, the Sea of Okhotsk: implications to kinematics of the continental and oceanic plates. *Earth and Planetary Science Letters*, **173**, 113–127.

Bazylev, B.A. & Silantyev, S.A. 2000. Geodynamic interpretation of the subsolidus recrystallization of mantle spinel peridotites: 1. Mid-oceanic ridges. *Petrology*, **8**, 201–213.

Bazylev, B.A., Magakyan, R., Silantyev, S.A., Ignatenko, K.I., Romashova, T.V. & Xenophontos, C. 1993. Petrology of peridotites from the Mamvonia complex, Southwestern Cyprus. *Petrology*, **1**, 302–330.

Bazylev, B.A., Zakariadze, G.S., Zhelyazkova-Panayotova, M.D., Kolcheva, K., Oberkhänsli, R. & Solov'eva, N.V. 1999. Petrology of ultramafic rocks from the ophiolite association in the crystalline basement of the Rhodope massif. *Petrology*, **7**, 191–212.

Bazylev, B.A., Silantyev, S.A. & Ganelin, A.V. 2000. Different ultramafic types at Povorotny Cape ophiolite mélange, Taigonos Peninsula, NE Russia.

Geosciences 2000. Confererence abstracts, University of Manchester, 25.

BAZYLEV, B.A., PALANDZHYAN, S.A., GANELIN, A.V., SILANTYEV, S.A., ISHIWATARI, A. & DMITRENKO, G.G. 2001. Petrology of peridotites from the ophiolite mélange in Cape Povorotny, Taigonos peninsula, NE Russia: mantle processes beneath a subduction zone. *Petrology*, **9**, 142–160.

BELYI, V.F. & AKININ, V.V. 1985. *Geological Structure and Ophiolites in Yelistratov Peninsula, Volumes 1 and 2*. NE Scientific Centre of the USSR Academy of Science, Magadan (in Russian).

BIZIMIS, M., SALTERS, V.J.M. & BONATTI, E. 2000. Trace and REE content of clinopyroxenes from supra-subduction zone peridotites. Implications for melting and enrichment processes in island arcs. *Chemical Geology*, **165**, 67–85.

BOGDANOV, N.A. & TIL'MAN, S.M. 1992. *Tectonics and Geodynamics of Northeast Russia*. Institute of the Lithosphere, Moscow (in Russian).

BONATTI, E. & MICHAEL, P.E. 1989. Mantle peridotites from continental rifts to ocean basins to subduction zones. *Earth and Planetary Science Letters*, **91**, 297–311.

BONDARENKO, G.E. & SOKOLOV, S.D. 1996. Strike-slips in the structure of southwestern part of Taigonos Peninsula. *Pacific Geology*, **2**, 99–106.

COLEMAN, R.G. 1984. The diversity of ophiolites. *Geologie en Mijnbouw.*, **63**, 267–283.

COLEMAN, R.G. 1986. Ophiolites and accretion of the North American Cordilliera. *Bulletin de la Société Geologique de France*, **6**, 961–968.

COLEMAN, R.G. & DONATO, M.M. 1979. Once more about oceanic plagiogranites. *In:* BARKER, F. (ed.) *Trondhjemites, Dacites and Related Rocks*. Mir, Moscow, 118–130.

CONEY, P.J., JONES, D.L. & MONGER, J.W.H. 1980. Cordilleran suspect terranes. *Nature*, **288**, 329–333.

COWAN, D.S. 1985. Structural style in Mesozoic and Cenozoic mélanges in the western Cordillera of North America. *Geological Society of America Bulletin*, **96**, 451–462.

COX, J., SEARLE, M. & PEDERSEN, R. 1999. The petrogenesis of leucogranite dykes intruding the northern Semail ophiolite, United Arab Emirates: field relationships, geochemistry and Sr/Nd isotope systematics. *Contributions to Mineralogy and Petrology*, **137**, 267–287.

DICK, H.J.B. 1989. Abyssal peridotites, very slow spreading ridges and ocean ridge magmatism. *In:* SAUNDERS, A.D. & NORRY, M.J. (eds) *Magmatism in the Ocean Basins*. Geological Society, London, Special Publications, **42**, 71–105.

DICK, H.J.B. & BULLEN, T. 1984. Chromian spinel as a petrogenetic indicator in abyssal and alpine-type peridotites and spatially associated lavas. *Contributions to Mineralogy and Petrology*, **86**, 54–76.

DICK, H.J.B. & NATLAND, J.H. 1996. Late-stage melt evolution and transport in the East Pacific Rise. *In:* GILLIS, M.C., ALLAN, K.M. & MEYER, P.S. (eds) *Proceedings of the Ocean Drilling Program, Scientific Results, 147*. Ocean Drilling Program, College Station, TX, 103–134.

DILEK, Y., MOORES, E.M., ELTHON, D. & NICOLAS, A. 1999. Ophiolites and oceanic crust: new insights from field studies and Ocean Drilling Program. *GSA Today*, **9**, 30–32.

DOBRETSOV, N.L. 1974. *Glaucophane Schist and Eclogite–Glaucophane Schist Complexes of the USSR*. Nauka, Novosibirsk (in Russian).

ELTHON, D. 1991. Geochemical evidence for formation of the Bay of Islands ophiolite above a subduction zone. *Nature*, **354**, 141–143.

FILATOVA, N.I. 1988. *Perioceanic Volcanic Belts*. Nedra, Moscow (in Russian).

FISHER, D.M. & BYRNE, T. 1987. Structural evolution of underthrusted sediments, Kodiak Islands, Alaska. *Tectonics*, **6**, 775–793.

FRYER, P. 1992. A synthesis of leg 125 drilling of serpentinite seamounts on Mariana and Izu–Bonin forearcs. *In:* FRYER, P. *ET AL.* (eds) *Proceedings of the Ocean Drilling Program, Scientific Results, 125*. Ocean Drilling Program, College Station, TX, 593–614.

FUJITA, K. & NEWBERRY, T. 1982. Tectonic evolution of Northeastern Siberia and adjacent regions. *Tectonophysics*, **89**, 337–357.

GABRIELSE, H., MONGER, J.W.H., YORATH, C.J. & DODDS, C. 1991. Transcurrent faults. *In:* GABRIELSE, H. & YORATH, C.J. (eds) *Geology of the Cordilleran Orogen in Canada*. Geological Society of America, The Geology of North America, **G-2**, 651–660.

GANELIN, A.V. & PEYVE, A.A. 2001. Geodynamic setting of formation of the Ganychalan terrane ophiolite (Koryakya Upland). *In:* KARPOV, A.G. (ed.) *Petrology and Metallogeny of Basic–Ultrabasic Complexes of Kamchatka*. Scientific World, Moscow, 215–230 (in Russian).

GILLIS, C.M. 1996. Rare-earth element constraints on the origin of amphibole in gabbroic rocks from site 894, Hess Deep. *In:* GILLIS, M.C., ALLAN, K.M. & MEYER, P.S. (eds) *Proceedings of the Ocean Drilling Program, Scientific Results, 147*. Ocean Drilling Program, College Station, TX, 135–155.

GLASSLEY, W. 1974. Geochemistry and tectonics of Crescent volcanic rocks, Olympic Peninsula, Washington. *Geological Society of America Bulletin*, **85**, 785–794.

GRIGORIEV, V.N., SOKOLOV, S.D., KRYLOV, K.A., GOLOZUBOV, V.V. & PRALNIKOVA, I.E. 1995. Geodynamic types of the Triassic–Jurassic volcanic–siliceous complexes in the Kuyul terrane (Koryak Upland). *Geotectonics*, **29**, 248–258 (in Russian).

HARBERT, W., SOKOLOV, S., KRYLOV, K., ALEXUTIN, M., GRIGORIEV, V. & HEIPHETZ, A. 2003. Reconnisance paleomagnetism of Late Triassic blocks, Kuyul region, northern Kamchatka Peninsula, Russia. *Tectonophysics*, **361**, 215–227.

HART, S.R. & DUNN, T. 1993. Experimental cpx/melt partitioning of 24 trace elements. *Contributions to Mineralogy and Petrology*, **113**, 1–8.

HEIPHETZ, A., HARBERT, W. & LAYER, P. 1994. Preliminary reconnaissance paleomagnetism of some Late Mesozoic ophiolites, Kuyul region, Koryak superterrane, Russia. *In:* THURSTON, D.K. & FUJITA, K. (eds) *Proceedings of the International Conference on Artic Margisn MMS 94-0040.*

US Department of Interior Minerals Management Service Alaska Outer Continental Shelf Region, Anchorage, 229–234.

IRVINE, T.N. 1967. Chromium spinels as a petrogenetic indicator. II. Petrologic applications. *Canadian Journal of Earth Sciences*, **4**, 71–103.

ISHII, T., ROBINSON, P.T., MAEKAWA, H. & FISKE, R. *ET AL.* 1992. Petrological studies of peridotites from diapiric serpentinite seamounts in the Izu–Ogasawara–Mariana forearc. *In:* FRYER, P. (ed.) *Proceeding of the Ocean Drilling Program, Scientific Results, 125*. Ocean Drilling Program, College Station, TX, 445–486.

ISHIWATARI, A. 1994. Circum-Pacific Phanerozoic multiple ophiolite belts. *In:* ISHIWATARI, A., MALPAS, J. & ISHIZUKA, H. (eds) *Proceedings of the 29th International Congress. Part D. Circum-Pacific Ophiolite*. Utrecht, Netherland: VSP, 7–28.

ISHIWATARI, A., SOKOLOV, S.D., SAITO, D., TSUJIMORI, T. & MIYASHITA, S. 1998. Geology and petrology of Yelistratov ophiolite in Taigonos Peninsula, Northeastern Russia: an island-arc ophiolite intruded into oceanic mantle. *In:* HANSKI, E. & VUOLLO, J. (eds) *International Ophiolite Symposium and Field Excursion—Generation and Emplacement of Ophiolites through Time*. Geological Survey of Finland, Special Papers, **26**, 29–30.

JAQUES, A.L. & GREEN, D.H. 1980. Anhydrous melting of peridotite at 0–15 kbar pressure and the genesis of tholeiitic basalts. *Contributions to Mineralogy and Petrology*, **73**(3), 287–310.

KANO, K.I., NAKAJI, M. & TAKEUCHI, S. 1991. Asymmetrical melange fabrics as possible indicators of the convergent direction of plates: a case study from Shimanto Belt of the Akaishi Mountains, central Japan. *Tectonophysics*, **185**, 375–388.

KAY, R.W. & SENECHAL, R.G. 1976. The rare earth geochemistry of the Troodos ophiolite complex. *Journal of Geophysical Research*, **81**(5), 964–970.

KELEMEN, P.B., KOGA, K. & SHIMIZU, N. 1997. Geochemistry of gabbro sills in the crust–mantle transition zone of the Oman ophiolite: implications for the origin of the oceanic lower crust. *Earth and Planetary Science Letters*, **146**, 475–488.

KHANCHUK, A.I., GRIGORYEV, V.N. & GOLOZUBOV, V.V. *ET AL.* 1990. *Kuyul Ophiolite Terrane*. Academy of Science Publications, Vladivostok (in Russian).

KHANCHUK, A.I., GOLOZUBOV, V.V., PANCHENKO, A.V., IGNATIEV, A.V. & CHUDAEV, O.V. 1992. Ganychalan terrane of the Koryak Upland. *Pacific Geology*, **3**, 82–93 (in Russian).

KHUDOLEY, A.K. & SOKOLOV, S.D. 1998. Structural evolution of the northeastern Asian continental margin: an example from the western Koryak fold-and-thrust belt (northeast Russia). *Geological Magazine*, **135**, 311–330.

KORNPROBST, J., OHNENSTETTER, D. & OHNENSTETTER, M. 1981. Na and Cr contents in clinopyroxenes from peridotites: a possible discriminant between 'sub-continental' and 'sub-oceanic' mantle. *Earth and Planetary Science Letters*, **53**, 241–254.

LAGABRIELLE, Y., KARPOFF, A.M. & COTTON, J. 1992. Mineralogical and geochemical analyses of sedimentary serpentinite from conical seamount (hole 778A): implications for the evolution of serpentinite seamount. *In:* FRYER, P., PEARCE, J.A., STOCKING, L.B., *ET AL.* (eds) *Proceedings of the Ocean Drilling Program, Scientific results, 125*. Ocean Drilling Program, College Station, TX, 325–342.

LANGMUIR, C.H., KLEIN, E. & PLANK, T. 1992. Petrological systematics of Mid-Ocean ridge basalts: constraints on melt generation beneath ocean ridges. *In:* LANGMUIR, C.H. *ET AL.* (eds) *Mantle Flow and Melt Generation at Mid-Ocean Ridges*. Geophysical Monograph, American Geophysical Union, **71**, 183–280.

LUCHITSKAYA, M.V. 1996. Plagiogranites of the Kuyul ophiolite massif, Northeastern Russia. *Ofioliti*, **21**, 131–138.

LUCHITSKAYA, M.V. 2001. Tonalite–Trondhjemite Complexes of Koryakya–Kamchatka Region (Geology, Geodynamics). *Transactions of the Geological Institute of the Russian Academy of Sciences, Moscow, GEOS*, **123**.

LYCHAGIN, P.P., BYALOBZHESSKY, S.G., KOLYASNIKOV, YU.A., KORAGO, YE.A. & LIKMAN, V.B. 1991. The magmatic history of the South Anyui folded zone. *In:* SIDOROV, A.A. & MILOV, A.P. (eds) *Geology of Continent–Ocean Transition Zone in Northeast Asia*. SVKNII RAN, Magadan, 140–157 (in Russian).

MARKOV, M.S., NEKRASOV, G.E. & PALANDJYAN, S.A. 1982. Ophiolites and melanocratic basement of the Koryak Upland. *In:* PUSHCHAROVSKY, Y.M. & TIL'MAN, S.M. (eds) *Essays of Tectonics of the Koryak Upland*. Nauka, Moscow, 30–70.

MIYASHIRO, A. & SHIDO, F. 1980. Differentiation of gabbros in the Mid-Atlantic Ridge near 24°N. *Journal of Geochemistry*, **14**, 145–154.

MOROZOV, O.L. 2001. Geology and Structure of Central Chukotka. *Transactions of the Geological Institute of the Russian Academy of Sciences, Moscow, GEOS*, 200 (in Russian).

NEKRASOV, G.E. 1976. *Tectonics and Magmatism of Taigonos and Northwestern Kamchatka*. Nauka, Moscow (in Russian).

NEKRASOV, G.E., ZABOROVSKAYA, N.B. & LYAPUNOV, S.M. 2001. Pre-Late Paleozoic ophiolites of the western part of the Koyak Upland: fragments of an oceanic plateau. *Geotectonics*, **2**, 41–63 (in Russian).

NIU, Y. 1997. Mantle melting and melt extraction processes beneath ocean ridges: evidence from abyssal peridotites. *Journal of Petrology*, **38**, 1047–1074.

NOKLEBERG, W.J., PARFENOV, L.M. & MONGER, J.W.H. *ET AL.* 1994. *Circum-North Pacific Tectono-Stratigraphic Terrane Map*. US Geological Survey Open-File Report, **94-714**.

NOKLEBERG, W.J., PARFENOV, L.M. & MONGER, J.W.H. *ET AL.* 2001. *Phanerozoic Tectonic Evolution of the Circum-North Pacific*. US Geological Survey Professional Paper IG2G.

O'CONNOR, J.T. 1969. A classification for quartz-rich igneous rocks based on feldspar ratios. US Geological Survey, Professional Papers, **525-B**, 79–84.

OHNENSTETTER, M. 1985. Classification pétrographique

et structurale des ophiolites, de la dynamique des zones transition croûte–manteau. Incidence sur la nature et la disposition des corps de chromite associés. *Comptes Rendus de l'Académie des Sciences, Série II*, **301**(20), 1413–1418.

OZAWA, K. & SHIMIZU, N. 1995. Open-system melting in the upper-mantle—constraints from the Hayachine–Miyamori Ophiolite, Northeastern Japan. *Journal of Geophysical Research*, **100**, 22315–22335.

OXMAN, V.S., PARFENOV, L.M. & PROKOPIEV, A.V. *ET AL.* 1995. The Chersky Range ophiolite belt, Northeast Russia. *Journal of Geology*, **103**, 539–556.

PALANDZHYAN, S.A. 1992. *Classification of Mantle Peridotites by Geodynamic Settings of their Formation*. SVKNII DVO RAN, Magadan (in Russian).

PALANDZHYAN, S.A. 1997. Granitoids of the Ophiolite Belts of Koryak Foldbelt. *In:* BYALOBZHESSKY, S.G. (ed.) *Magmatism and Mineralization of Northeast Russia*. SVKNII DVO RAN, Magadan, 204–224 (in Russian).

PALANDZHYAN, S.A. 2000. Ophiolites of the Ust–Belaya terrane: a Middle Paleozoic oceanic-type association in the West Koryak fold-and-thrust belt. *In: Magmatism and Metamorphism in the Northeast Asia*. North East Interdisciplinary Research Institute, Magadan, 180–184 (in Russian).

PALANDZHYAN, S.A. & DMITRENKO, G.G. 1996. *Ophiolitic Complexes and Associated Rocks in the Ust–Belaya Mountains and Algan Ridge, Russian Far East*. US Geological Survey, Open-File Report, **OF 92-20-1**.

PALANDZHYAN, S.A. & DMITRENKO, G.G. 1999. Peridotites of the Taigonos Pribrezhny Belt: chemical compositions of minerals as indicators of geodynamic conditions of ophiolites formation. *In:* KARYAKIN, YU.V. (ed.) *Tectonics, Geodynamics and Magmatic and Metamorphic Processes. Proceedings of 32nd Tectonic Conference*. GEOS, Moscow, 53–57 (in Russian).

PALLISTER, J.S. & HOPSON, S.A. 1981. Samail Ophiolite plutonic suite: field relations, phase variation, cryptic variation and layering, and a model of spreading ridge magma chamber. *Journal of Geophysical Research*, **86**, 2593–2644.

PALLISTER, J.S. & KNIGHT, R.J. 1981. Rare-earth element geochemistry of the Semail ophiolite near Ibra, Oman. *Journal of Geophysical Research*, **86**, 2673–2697.

PARFENOV, L.M. 1984. *Continental Margins and Island Arcs in the Mesozoides of Northeastern Asia*. Nauka, Novosibirsk (in Russian).

PARFENOV, L.M., NATAPOV, L.M., SOKOLOV, S.D. & TSUKANOV, N.V. 1993. Terrane analysis and accretion in northeast Asia. *Island Arc*, **2**, 35–54.

PARKINSON, I.J. & PEARCE, J.A. 1998. Peridotites from the Izu–Bonin–Mariana forearc (ODP Leg 125): evidence for mantle melting and melt–mantle interaction in a suprasubduction zone setting. *Journal of Petrology*, **39**, 1577–1618.

PEARCE, J.A. 1992. An element recycling. *Nature*, **360**, 629–630.

PEARCE, J.A. & NORRY, M.J. 1979. Petrogenetic implications of Ti, Zr, Y, and Nb variations in volcanic rocks. *Contributions to Mineralogy and Petrology*, **69**, 33–47.

PEARCE, J.A., HARRIS, N.B.W. & TINDLE, A.G. 1984. Trace element discrimination diagrams for the tectonic interpretation of granitic rocks. *Journal of Petrology*, **25**, 956–983.

PEARCE, J.A., BARKER, P.F., EDWARDS, S.J., PARKINSON, I.J. & LEAT, P.T. 2000. Geochemistry and tectonic significance of peridotites from the South Sandwich arc–basin system, South Atlantic. *Contributions to Mineralogy and Petrology*, **139**, 36–53.

PEDERSEN, R.B., MALPAS, J. & FALLOON, T. 1996. Petrology and geochemistry of gabbroic and related rocks from Site 894, Hess Deep. *In:* MÉVEL, C., ALLAN, J.F. & MEYER, P.S. (eds) *Proceedings of the Ocean Drilling Program, Scientific Results, 147*. Ocean Drilling Program, College Station, TX, 3–19.

PEYVE, A.A. 1984. *Structure and Structural Position of the Koryaksky Range Ophiolites*. Nauka, Moscow (in Russian).

PUSHCHAROVSKY, YU.M., SOKOLOV, S.D., TILMAN, S.M. & KRYLOV, K.A. 1992. Tectonics and geodynamics of northwestern rim of the Pacific Ocean. *In:* BORUKAEV, CH.B. & VRUBLEVSKY, A.A. (eds) *Issues of Tectonics and Mineral and Energy Resources of Northwestern Pacific*. DVO ITIG AN USSR, Khabarovsk, **1**, 128–137 (in Russian).

RAMPONE, E., HOFMANN, A.W., PICCARDO, G.B., VANNUCCI, R., BOTTAZZI, P. & OTTOLINI, L. 1995. Petrology, mineral and isotope geochemistry of the External Liguride peridotites (Northern Apennines, Italy). *Journal of Petrology*, **36**, 81–105.

RIKHTER, YA.A. 1997. New data on the gabbro–tonalite assemblage of the Mid-Atlantic ridge equatorial segment. *Doklady Russian Academy of Sciences*, **355**, 506–508 (in Russian).

ROSENKRANTZ, A.A. (ed.) 1986. *Geological Map of USSR. New Series. Scale 1:1 000 000. Sheets P-58, 59*. Mingeo USSR, VSEGEI, Leningrad.

SAITO, D., ISHIWATARI, A., TSUJIMORI, T., MIYASHITA, S. & SOKOLOV, S.D. 1999. Yelistratov ophiolite in Taigonos peninsula, Far-East Russia: an island arc ophiolite intruding into oceanic mantle. *Memoirs of Geological Society of Japan*, **52**, 303–316 (in Japanese with English abstract).

SAUNDERS, A.D. & TARNEY, J. 1984. Geochemical characteristics of basaltic volcanism within back-arc basin. *In:* KOKELAAR, B.P. & HOWELLS, M.F. (eds) *Marginal Basin Geology: Volcanic and Associated Sedimentary and Tectonic Processes in Modern and Ancient Marginal Basins*. Geological Society, London, Special Publications, **16**, 59–76.

SAUNDERS, A.D., TARNEY, J. & WEAVER, S.D. 1980. Transverse geochemical variations across the Antarctic Peninsula: implications for the genesis of calc-alkaline magmas. *Earth and Planetary Science Letters*, **46**, 344–360.

SAUNDERS, A.D., NORRY, M.J. & TARNEY, J. 1991. Fluid influence on the trace element compositions of subduction zone magmas. *Philosophical Transactions of the Royal Society of London*, **335**, 377–392.

SEARLE, M.P. & COX, J.S. 1999. Tectonic setting, origin and obduction of the Oman ophiolite. *Geological*

Society of America Bulletin, **111**, 104–122.

SHAPIRO, M.N. & GANELIN V.G. 1988. Paleogeodynamic interrelations in the large blocks of the Mesozoic of the North-Eastern USSR. *Geotectonics*, **5**, 94–104 (in Russian).

SHERVAIS, J.W. 1982. Ti–V plots and the petrogenesis of modern and ophiolitic lavas. *Earth and Planetary Science Letters*, **59**, 101–118.

SHERVAIS, J.W. 2001. Birth, death, and resurrection: the life cycle of suprasubduction zone ophiolites. *Geochemistry, Geophysics, Geosystems*, **2**, 200GC 000080.

SILANTYEV, S.A., SOKOLOV, S.D. & POLUNIN, G.V. 1994. New data on the composition of metamorphic rocks of the Talovka River basin (Penzhina region, Northern Russia). *Geotectonics*, **2**, 169–176.

SILANTYEV, S.A., SOKOLOV, S.D., BONDARENKO, G.YE, MOROZOV, O.L., BAZYLEV, B.A., PALANDZHYAN, S.A. & GANELIN, A.V. 2000. Geodynamic setting of the high-grade amphibolites and associated igneous rocks from the accretionary complex of Povorotny Cape, Taigonos Peninsula, Northeastern Russia. *Tectonophysics*, **325**, 107–132.

SOBOLEV, A.V. & BATANOVA, V.G. 1995. Mantle lherzolites of the Troodos ophiolite complex, Cyprus: clinopyroxene geochemistry. *Petrology*, **3**, 440–448.

SOKOLOV, S.D. 1992. Accretionary tectonics of the Koryak–Chukotka Segment of the Pacific belt. *Transactions of Geological Institute, Russian Academy of Sciences*, 182 (in Russian).

SOKOLOV, S.D., GRIGORIEV, V.N., PEYVE, A.A., BATANOVA, V.G., KRYLOV, K.A., LUCHITSKAYA, M.V. & ALEKSUTIN, M.V. 1996. The structural and compositional regulation in serpentinite mélanges. *Geotectonics*, **1**, 3–16.

SOKOLOV, S.D., GRIGORIEV, V.N., ARISTOV, V.A., PEYVE, A.A. & SHTERENBERG, L.E. 1997. Ordovician deposits of the Ganychalan terrane. *Stratigrafiya i Geologicheskaya Korrelyatsiya*, **5**, 73–84 (in Russian).

SOKOLOV, S.D., BONDARENKO, G.YE., MOROZOV, O.L. & GRIGORIYEV, V.N. 1999. Transition zone of the Asian continent–Northwestern Pacific in Late Jurassic and Early Cretaceous. *In:* GAVRILOV, YU. O. & KURENKOV, S.A. (ed.) *Theoretic and Regional Problems of Geodynamics*. Nauka, Moscow, 30–84 (in Russian).

SOKOLOV, S.D., LAGABRIELLE, Y., GERARD, J.-K. & BAZYLEV, B.A. 2000. Geodynamic setting of ultramafic bodies of Mt. Dlinnaya (Penzhina region, Northeast Russia). *Byulleten' Moskovskogo Obshchestva Ispytateley Prirody, Seria Geologicheskaya*, **75**, 51–55 (in Russian).

SUN, S.-S. & MCDONOUGH, W.F. 1989. Chemical and isotopic systematics of oceanic basalts: implications for mantle composition and processes. *In:* SAUNDERS, A.D. & NORRY, M.J. (eds) *Magmatism in the Ocean Basins*. Geological Society, London, Special Publications, **42**, 313–345.

TAKAZAWA, E., FREY, F.A., SHIMIZU, N. & OBATA, M. 2000. Whole rock compositional variations in an upper mantle peridotite (Horoman, Hokkaido, Japan): are they consistent with a partial melting process? *Geochimica et Cosmochimica Acta*, **64**, 695–716.

TIEPOLO, M., TRIBUZIO, R. & VANNUCCI, R. 1997. Mg- and Fe-gabbroids from Northern Apennine ophiolites: parental liquids and igneous differentiation process. *Ofioliti*, **22**, 57–69.

TORIUMI, M. 1985. Two types of ductile deformation/regional metamorphic belts. *Tectonophysics*, **113**, 307–326.

VINOGRADOV, V.I., YURKOVA, R.M., SOKOLOV, S.D., BUYAKAYTE, M.I. & VORONIN, B.I. 1995. Rb–Sr dating of dynamometamorphosed rocks from the Penzhinskiy Ridge, Kamchatka. *Geotectonics*, **28**, 424–430.

WIRTH, K.R., BIRD, J.M. & WESSELS, J.N. 1994. The diversity of accreted oceanic lithosphere in the Brooks Range, Alaska. *In:* ISHIWATARI, A., MALPAS, J. & ISHIZUKA, H. (eds) *Proceeding of the 29th International Congress. Part D. Circum-Pacific Ophiolite*. VSP, Utrecht, 89–108.

ZABOROVSKAYA, N.B. 1978. *Inner Zone of the Okhotsk–Chukotka Belt, Taigonos*. Nauka, Moscow (in Russian).

ZONENSHAIN, L.P., KUZMIN, M.I. & NATAPOV, L.M. 1990. *Tectonics of Lithospheric Plates of the USSR Territory, Book 2*. Nedra, Moscow (in Russian).